

**UCSF**

**UC San Francisco Electronic Theses and Dissertations**

**Title**

Development of a modular, convergent synthetic platform for minimal macrolide antibiotic pharmacophores

**Permalink**

<https://escholarship.org/uc/item/9dc568hc>

**Author**

Edmondson, Quinn

**Publication Date**

2024

Peer reviewed|Thesis/dissertation

Development of a modular, convergent synthetic platform for minimal macrolide antibiotic pharmacophores

by  
Quinn Edmondson

DISSERTATION

Submitted in partial satisfaction of the requirements for degree of  
DOCTOR OF PHILOSOPHY

in

Chemistry and Chemical Biology

in the

GRADUATE DIVISION

of the

UNIVERSITY OF CALIFORNIA, SAN FRANCISCO

Approved:

Signed by:

*Ian B Seiple*

0F55EF21BB3D419...

Ian B Seiple

Chair

DocuSigned by:

*Danica Galonic Fujimori*

DocuSigned by:  
4D6...

Danica Galonic Fujimori

*Adam R. Renslo*

FBDB6299FCD244B...

Adam R. Renslo

---

Committee Members



**“We don’t have NMR eyes.” – Ian B. Seiple**

**This thesis is dedicated to John A. Detrio**

**Thank you for being the scientist in my life, always answering my questions, and  
encouraging me to ask more.**

## Acknowledgements

First and foremost, I would like to thank Ian Seiple. The level of care and patience you extended to everyone in your lab is something too few students that pursue a doctorate receive. Your enthusiasm and optimism, even in the face of devastating results, inspired me to wake up every morning (sometimes on the couch in your office) remembering why I chose this project, why I chose to study total synthesis, and why I even like science. There were very few times it was easy – a global pandemic altering the course of history, you got married and started a family, the multiple NMR magnet quenches and hardware failure, and then your great opportunity to move the lab to a new institution. Through all of this, you made time to help me troubleshoot even the smallest things I was struggling with. You have been the best possible mentor I could have asked for, and I truly would not have changed this experience for anything.

I want to thank all current and former members of the Seiple lab. Jon, you showed me how to do chemistry when I started with very little synthetic experience and taught me the best techniques to maximize the success of my science. Qi, Lingchao, and Yanmin, I learned so much from you guys in such a short period of time. Minh, you always knew how to find the most efficient way to get work done and were so fun to chat with about our out-of-the-box ideas. Yoshito, Jesus, Leo, Javarcia, Isabel, and Seul Ki, you all have been so fun to work with and helped shape the wonderful culture of the lab that make work not feel like work. Andrew, you always made my day in lab hyping each other up, asking ourselves what the mechanism was to every reaction we saw, being quick to make each other laugh and cheer each other up. You are an icon and having worked with you made me a better scientist. Arthur, you are one of my best friends. I look forward to coming in lab every day because I have a funny thing to show you, or an ‘after 5pm’ joke to tell you, or to commiserate about grad school and science together. I jokingly had “What would Arthur do?”

written above my hood because I felt bad asking you so many questions, but to this day I always think what you would do when I encounter problems in lab. Behind Ian, I learned the most chemistry from you.

I also want to extend my gratitude to all other UCSF mentors and colleagues I have had over the course of my graduate career. This includes Adam Renslo, Danica Galonic Fujimori, Ryan Gonciarz, Ziyang Zhang, Fatima Ugur, Kaitlyn Tsai, Doug Wassarman, Taia Wu, Roberto Efraín Díaz, Mark Kelly, Paul Klauser, Matt Callahan, Neha Prasad, Julia Molla, Arezou Razavi, Brian Kam, Peter Lee, Anna, and Rosa.

Thank you to my mentors from my time at UC Santa Cruz: Scott Lokey, Josh Schwochert, Cameron Pye, Victoria Klein, Walter Bray, Carrie Partch, Matthew Naylor, and Shero Lao. Were it not for you all, I would not have decided that I wanted to pursue research and go to graduate school.

I would not have been able to finish this journey without the friends I am so lucky to be surrounded by in my life. Ed, Anson, Lance, Taryn (and Maxine), Sophie, Sam, Catfish, Bebe, Roshan, Demir, Millie, Morgan, Kyra, Ben, Anne, Drew, Mel, Wes, Jake, Annie, Kata, Tom, Evelyn, Larry, Letitia, Taylor, Kate, Angelo, Eva, Scott, Tony, Heather, Sam, Katrina, Julian, Michael Vincent, Mason, John, Aaron, Adam, Cole, Ben, Wyatt, and Otis.

I also want to thank my family. Mom, Dad, Hailey, John, Fran, Dorothy, Poppy, Allie, Nick, Christine, Monica, Phil, Shea, Bryn, Greg, and Sue. The love and support you have shared with me my whole life brought me to where I am at today. I cherish our weekly video calls to solve a crossword together. A tradition I hope we continue.

Lastly, I want to thank my fiancé Sami. You have kept me grounded in my darkest times and basked with me in my brightest moments. Your light in my life brought me to where I am now. I love you.

## Contributions

The chapters in this dissertation were performed under the guidance of Dr. Ian Seiple, with the collaboration and feedback of many Seiple lab members. My committee members Dr. Adam Renslo and Dr. Danica Galonic Fujimori also provided scientific guidance that helped make this work successful. Other collaborators that were crucial in moving this work forward are Nick Settineri (Lawrence Berkeley National Lab Advanced Light Source ; Molecular Foundry, Office of Science, Office of Basic Energy Sciences, U.S. Department of Energy, Contract No. DE-AC02-05CH11231) for obtaining X-ray crystal structures. Jasmine Keyes performed some of the large-scale synthesis of relevant intermediates. Dr. David Sherman provided an authentic sample of narbomycin.

Chapter 1 contains the initial work in our attempts to synthesize the macrolide antibiotic narbomycin by incorporating a dioxinone moiety for the purposes of a thermolytic acyl ketene-type cyclization. It outlines our failure to establish the correct C4/C5 stereochemical configuration, and in doing so, develop a stereoselective methodology for *anti* vinylogous Mukaiyama aldol products.

Chapter 2 contains the majority of my results and outlines a successful synthetic route to narbomycin using an unprecedented thermal macrocyclization method, in which an oxazolidinone chiral auxiliary undergoes direct intramolecular displacement.

Quinn Edmondson provided the experimentation and manuscript preparation for most of the following dissertation, which is a substantive contribution comparable to other dissertations in Chemistry & Chemical Biology. Ian Seiple directed and supervised the research and provided guidance feedback throughout.



# Development of a modular, convergent synthetic platform for minimal macrolide antibiotic pharmacophores

Quinn Edmondson

## Abstract

Macrolide antibiotics are structurally diverse polyketide natural products produced by bacteria that exhibit antimicrobial activity through inhibition of bacterial protein synthesis. Macrolides and their semisynthetic derivatives are critical for the treatment of infectious disease, many of which are first-line therapeutics. Ketolides are a subclass of the macrolides which bear a ketone at the C3 position of the macrocycle. While predominantly semisynthetic, there are some ketolide natural products, like narbomycin, that have marked structural simplicity compared to other macrolides yet maintain good antibiotic activity. Here we report a modular, convergent platform for the synthesis of narbomycin, which we propose to be a minimal pharmacophore for macrolide antibiotics. This platform enables the facile incorporation of structural modifications to this minimal pharmacophore to generate novel unnatural products that can increase potency and overcome clinically relevant resistance mechanisms.

In chapter 1, I describe our first attempts to synthesize narbomycin through a critical macrocyclization step using the thermolytic properties of a dioxinone moiety. A vinylogous Mukaiyama aldol was used to incorporate this dioxinone and set the C4/C5 stereochemical configuration. Despite screening for reaction conditions, the desired *syn* aldol products were unable to be obtained, but a method for stereoselective access to *anti* vinylogous Mukaiyama dioxinone aldol products was developed. Some mechanistic rationale for our findings is discussed.

In chapter 2, I describe the successful total synthesis of narbomycin. This route uses a robust Liebeskind-Srogl coupling to join two halves of the molecule together and employs an unprecedented macrocyclization strategy that likely proceeds *via* direct intramolecular displacement of an oxazolidinone chiral auxiliary. I also outline some of the challenges faced in the final steps of the synthesis associated with the reduction of an exocyclic alkene. X-ray crystallographic data acquired and processed by Nick Settineri from the LBNL Advanced Light Source aided in the determination of stereochemistry and informed our synthetic efforts.

## Table of Contents

<b>List of Figures</b> .....	xi
<b>List of Tables</b> .....	xii
<b>List of Abbreviations</b> .....	xiii
<b>Chapter 1. Failed attempts at narbomycin total synthesis and a novel <i>anti</i>-aldol transformation</b> .....	1
1.1 Introduction.....	2
1.2 Synthetic route using a dioxinone cyclization strategy .....	3
1.3 Mechanistic considerations.....	5
1.4 General Experimental Procedures .....	8
1.5 References.....	37
<b>Chapter 2. Total synthesis of narbomycin using an unprecedented macrocyclization</b> .....	40
2.1 Revised synthetic route to narbomycin: the right and left halves.....	41
2.2 Couping the halves and macrocyclization .....	43
2.3 Optimization of the C8 reduction and the total synthesis of narbomycin .....	45
2.4 Conclusion and outlook .....	48
2.5 General Experimental Procedures .....	49
2.6 References.....	108

## List of Figures

Figure 1.1 Natural and semisynthetic ketolide antibiotics.....	2
Figure 1.2 Failed attempts to set the C4/C5 stereochemistry in a C6-deoxy system.....	4
Figure 1.3a X-ray crystal structure of <b>9b</b> and <b>9c</b> .....	5
Figure 1.3b X-ray crystal structure of a late-stage <i>epi</i> -C5 narbomycin-like macrocycle.....	5
Figure 1.4a Proposed Felkin-Ahn model transition states for C5 stereochemistry .....	6
Figure 1.4b Putative open transition states of the vinylogous Mukaiyama aldol .....	6
Figure 2.1 Synthesis of the right half.....	41
Figure 2.2 Synthesis of the left half.....	42
Figure 2.3 Coupling of the halves and macrocyclization .....	43
Figure 2.4 Representative list of attempted conditions for the selective reduction of C8 olefin..	45
Figure 2.5 Completion of the total synthesis of narbomycin.....	47
Figure 2.6 First series of analogues .....	48

## List of Tables

Table 1.1 Crystal data and structure refinement for QEdmondson02A_UCSF .....	15
Table 1.2 Atomic coordinates for qedmondson02a_ucsf.....	16
Table 1.3 Bond lengths and angles for qedmondson02a_ucsf.....	17
Table 1.4 Anisotropic displacement parameters for qedmondson02a_ucsf.....	21
Table 1.5 Hydrogen coordinates for qedmondson02a_ucsf.....	22
Table 1.6 Torsion angles for qedmondson02a_ucsf.....	24
Table 1.7 Crystal data and structure refinement for QEdmondson03_UCSF.....	26
Table 1.8 Atomic coordinates for qedmondson03_ucsf .....	27
Table 1.9 Bond lengths and angles for qedmondson03_ucsf.....	28
Table 1.10 Anisotropic displacement parameters for qedmondson03_ucsf. ....	32
Table 1.11 Hydrogen coordinates for qedmondson03_ucsf.....	33
Table 1.12 Torsion angles for qedmondson03_ucsf.....	34
Table 2.1 Crystal data and structure refinement for QEdmondson04_UCSF.....	91
Table 2.2 Atomic coordinates for qedmondson04_ucsf .....	92
Table 2.3 Bond lengths and angles for qedmondson04_ucsf.....	93
Table 2.4 Anisotropic displacement parameters for qedmondson04_ucsf. ....	102
Table 2.5 Hydrogen coordinates for qedmondson04_ucsf. ....	103
Table 2.6 Torsion angles for qedmondson04_ucsf.....	105

## List of Abbreviations

Bn – benzyl

Bz – benzoyl

dba – dibenzylideneacetone

DCE – 1,2-dichloroethane

DIC – diisopropylcarbodiimide

DMAP – 4-dimethylaminopyridine

DMSO – dimethylsulfoxide

HMDS – hexamethyldisilazane

MHAT – metal-hydrogen atom transfer

NMR – nuclear magnetic resonance

Nu – nucleophile

OTf – trifluoromethanesulfonate

p-TolSH – para-toluenethiol

Py – pyridine

TBS – tert-butyldimethylsilyl

TBDPS – tert-butyldiphenylsilyl

TFA – trifluoroacetic acid

THF – tetrahydrofuran

TMS – trimethylsilyl

**Chapter 1. Failed attempts at narbomycin total synthesis and a  
novel *anti*-aldol transformation**

## 1.1 Introduction

Macrolides are a structural class of antibiotics that target the nascent polypeptide exit tunnel (NPET) in the 50S subunit of the prokaryotic ribosome to inhibit protein synthesis by interfering with the elongation of the growing polypeptide chain via ternary interactions with the ribosome and specific peptide sequence motifs.<sup>1,2</sup> Macrolide natural products, produced by *Streptomyces* bacteria, are structurally diverse polyketides—the macrolactone cores ranging from 12- to 16-membered rings, a variety of side-chain functionalities and oxidation patterns, and at least one pendant sugar.<sup>3</sup> Since their initial discovery and isolation, macrolides, especially erythromycin and its semisynthetic derivatives (e.g., clarithromycin, azithromycin), have seen widespread use and immense success as therapeutics against infectious disease.<sup>4</sup>

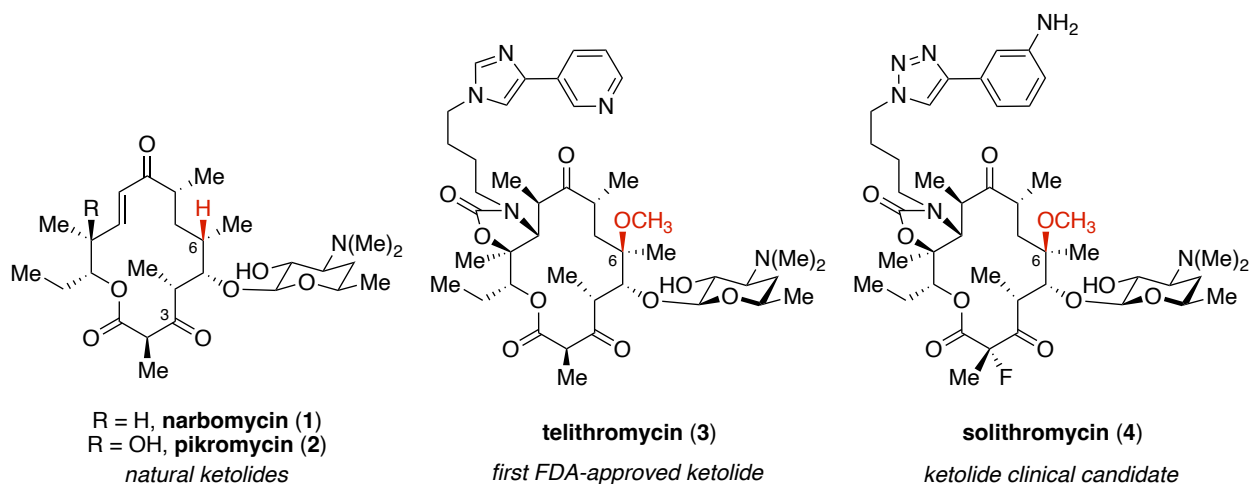


**Figure 1.1.** Natural and semisynthetic ketolide antibiotics

One subclass of macrolides are the ketolides (Figure 1), in which the C3 position along the macrocycle is a ketone instead of a glycosidated alcohol. This motif is observed in natural product ketolides like narbomycin<sup>5</sup> (1, Figure 1.1) and pikromycin<sup>6</sup> (2), as well as in the FDA-approved telithromycin (3) and clinical candidate solithromycin (4), both of which were historically produced semisynthetically from erythromycin<sup>7</sup>. Despite their lack of structural complexity, natural product ketolides like pikromycin and narbomycin still maintain modest antibiotic activity<sup>8</sup>



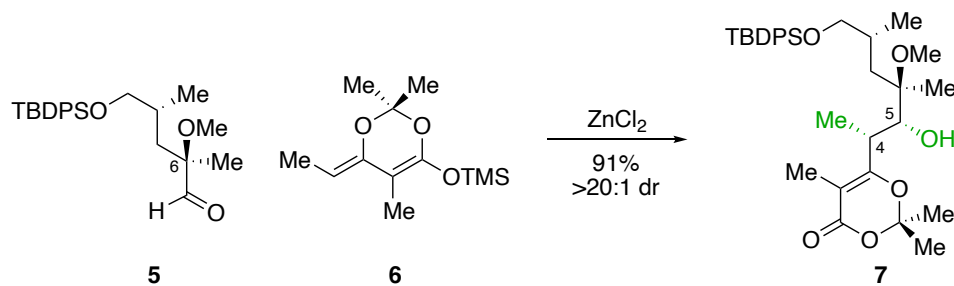
and are known to evade activation of some clinically significant antibiotic resistance mechanisms.<sup>9</sup> These simple 14-membered macrolides can be thought of as minimal pharmacophores (i.e., the steric and electronic ensemble needed to elicit a particular pharmacological effect) for macrolide antibiotics. We hypothesized that a short, modular synthesis of narbomycin, a minimal pharmacophore, would enable a systematic, structure-guided interrogation of the varied functionality found in different macrolide natural products, as well as fully synthetic derivatives that would be inaccessible to biosynthetic machinery. The products of such a route would inform the design of future generations of macrolide antibiotics aimed at overcoming clinically relevant resistance mechanisms.

## 1.2 Synthetic route using a dioxinone cyclization strategy

The first total synthesis of narbomycin by Kang employed an olefin metathesis approach to cyclize the macrocycle, having earlier constructed the macrolactone ester under Yamaguchi conditions, and used enzymatic desymmetrization to concomitantly establish the C6 and C8 stereocenters, overall completing the synthesis in 21 steps (longest linear sequence)<sup>10</sup>. We initially envisioned a shorter synthesis inspired by Myers' synthetic platform for ketolide antibiotics like solithromycin<sup>11</sup>. This approach would use a robust cyclization strategy developed by Boeckman that utilizes a 1,3-dioxin-4-one function (herein referred to as a dioxinone), which, upon heating, undergoes a retro-[4+2] to liberate acetone and produce an electrophilic acyl-ketene that is intercepted by the secondary alcohol at the opposite end of the linear intermediate.<sup>12,13</sup>

Myers incorporated this dioxinone by a vinylogous Mukaiyama aldol reaction between **5** and **6**<sup>14</sup> (Figure 1.2), at the same time setting the *syn* configuration of the C4 and C5 stereocenters. A key

Myers 2016



This work

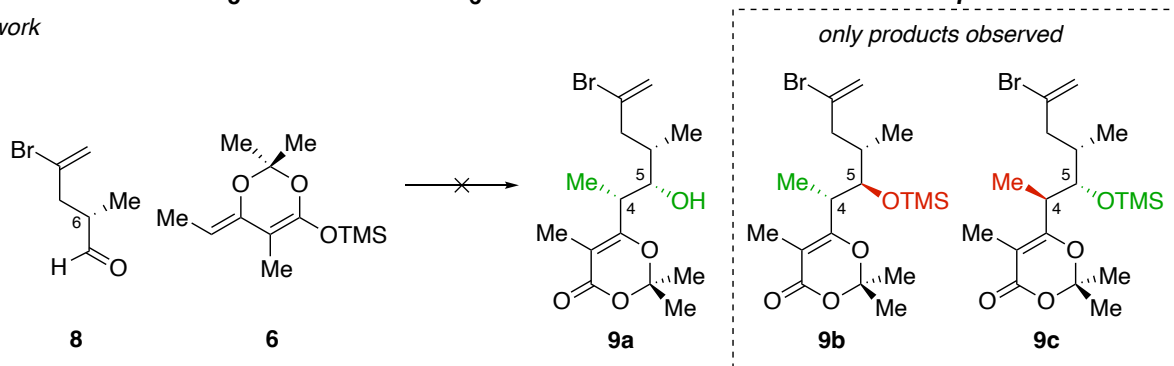


**Figure 1.2,** Failed attempts to set the C4/C5 stereochemistry in a C6-deoxy system.

feature of this transformation is the presence of the methoxy substituent at the C6 position on **5**. It was hypothesized that this coordinating functionality and the use of divalent Lewis acids helped to impart facial selectivity, *via* chelation control, in the approach of the aldehyde to the silyl ketene acetal **5**, yielding **7** with high diastereoselectivity.<sup>11</sup> However, the analogous C6 position of narbomycin is a proton instead of a methoxy substituent. Initial attempts at this transformation to couple aldehyde **8** and **6** using Myers' conditions failed to produce any aldol product. A screen of achiral Lewis acids gave promising results with high yields, but were inseparable mixtures of two diastereomers, of which we were uncertain of the configurations of the newly formed stereocenters. Further screening using chiral oxazaborolidine Lewis acids<sup>15,16</sup> yielded more stereoselective silyl ether aldol products (dr >9:1). This enabled selective transformation of both of the diastereomeric products seen in the aldol using achiral Lewis acids, depending on the enantiomer of chiral Lewis acid employed. The diastereomerically pure aldol products could be crystallized and their structures determined by X-ray crystallography. The X-ray structure

indicated exclusively *anti* aldol products under all tested conditions (**9b** and **9c**, Figure 1.3a). These results were further confirmed when the intermediates were taken forward in parallel to produce cyclic intermediates. One of these products was able to be crystallized and its structure determined by X-ray crystallography (Figure 1.3b).

### 1.3 Mechanistic considerations

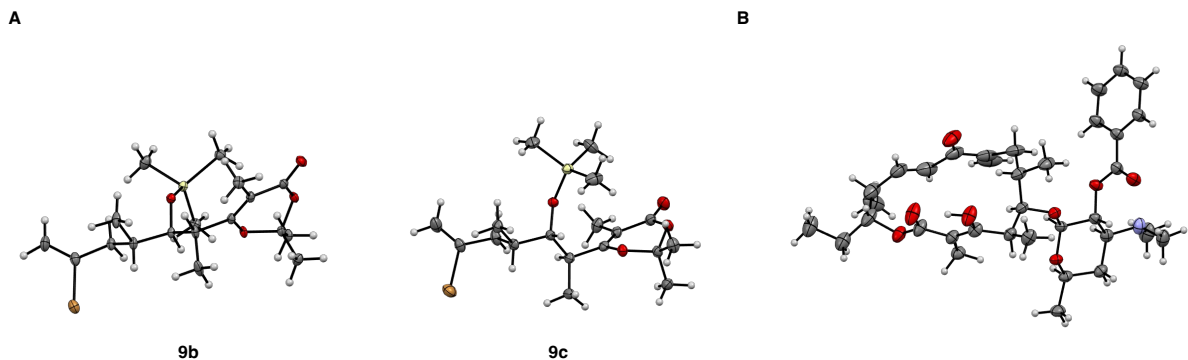


**Figure 1.3.** a) X-ray crystal structure of **9b** and **9c**. b) X-ray crystal structure of a late-stage *epi*-C5 narbomycin-like macrocycle.

There are a few points to consider when mechanistically rationalizing the outcome of this vinylogous Mukaiyama aldol. The C5 stereocenter may be explained with Felkin-Anh model of additions into carbonyls<sup>17,18</sup> (Figure 1.4A), with the nucleophilic addition preferentially occurring when the smallest substituent, in this case a proton, is in a gauche orientation relative to the aldehyde and the largest substituent is orthogonal to the aldehyde. However, as we have seen, this intrinsic selectivity can be overcome by controlling the available face of the aldehyde for nucleophilic attack by use of a chiral Lewis acid to yield either Felkin or anti-Felkin products. The C4 stereocenter may be explained by an open transition state, anti-periplanar approach of the silyl ketene acetal nucleophile. Theoretically, the nucleophile can approach the aldehyde in one of two ways (Figure 1.4B). In the first, the C2 methyl group is less sterically bulky than the ethyl

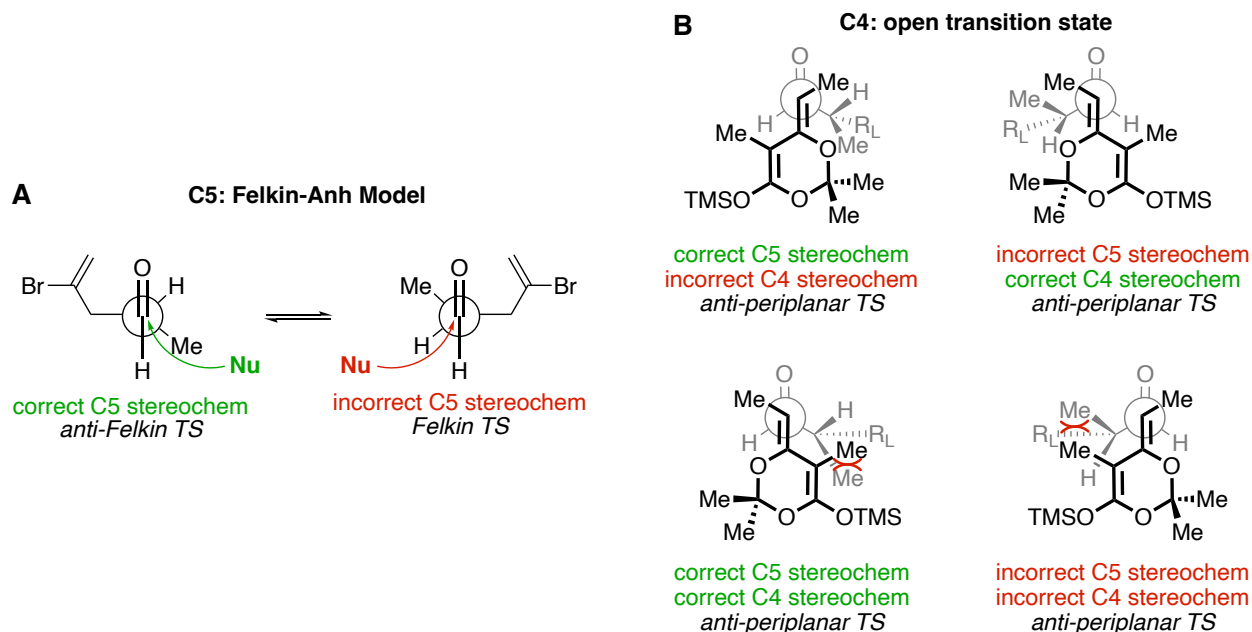


**Figure 1.4**, a) proposed Felkin-Ahn model transition states for C5 stereochemistry. b) putative open transition states that would produce the four possible stereoisomers from the vinylogous Mukaiyama aldol.

substituent, so that when the nucleophile approaches at the Bürgi-Dunitz angle ( $\sim 107^\circ$ ) the C2 methyl would preferentially be situated towards the larger carbonyl substituent, while the ethyl would be situated towards the smaller carbonyl substituent, in this case a proton. In the second, the inverse would happen, where the C2 methyl has enough steric bulk such that the nucleophile would orient itself with said methyl situated towards the smaller carbonyl substituent, the proton. Factoring in the bond rotation about the aldehyde carbon and the  $\alpha$ -carbon bearing a methyl group, as in the aforementioned Felkin model, there are four possible stereochemical outcomes (Figure 1.4B). Only anti aldol products are observed, indicating that the C2 methyl sterically clashes with the larger carbonyl substituent and is thus the determining factor for how the nucleophile approaches the aldehyde. An analogous explanation can be made for a syn-clinal approach of the nucleophile (not pictured).

It is important to note the above explanation is merely an exercise in rationalizing the products observed, and not intended to inform future Mukaiyama aldol reactions. Firstly, there are very few adequate models and systems that can predict the stereochemical outcomes of vinylogous Mukaiyama aldols<sup>19,20</sup> (e.g., the Kobayashi aldol<sup>21</sup>). Secondly, there are very few examples in the literature in which fully substituted dioxinones, as opposed to acetate-like dioxinone nucleophiles, are used as substrates for these types of transformations. Only this work and the Myers work<sup>11</sup> use these highly substituted dioxinone nucleophiles. Given the drastically different outcomes, and limited substrate scope, more thorough methodological investigations would benefit the field of polyketide synthesis.

Even with a synthetic method to selectively establish the correct C4 stereochemistry, attempts to invert the incorrect C5 alcohol stereocenter *via* Mitsunobu reaction were fruitless. Alternate methods to establish the C4 and C5 stereocenters in a more linear method using a series of Evans aldols and then convert that intermediate to a dioxinone<sup>22</sup> also failed. With an apparent impasse reached, we decided to turn to an alternate synthetic strategy in our efforts to synthesize narbomycin, in which the C4/5 configuration can be correctly set while maintaining a modular, convergent synthetic platform.

## 1.4 General Experimental Procedures

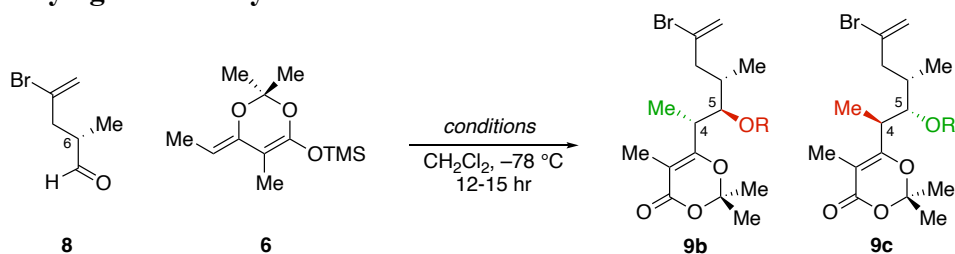
All reactions were performed in flame- or oven-dried glassware fitted with rubber septa under a positive pressure of nitrogen or argon, unless otherwise noted. All reaction mixtures were stirred throughout the course of each procedure using Teflon-coated magnetic stir bars. Air- and moisture-sensitive liquids were transferred via syringe or stainless-steel cannula. Solutions were concentrated by rotary evaporation below 35 °C. Analytical thin-layer chromatography (TLC) was performed using glass plates pre-coated with silica gel (0.25-mm, 60-Å pore size, 230–400 mesh, SILICYCLE INC) impregnated with a fluorescent indicator (254 nm). TLC plates were visualized by exposure to ultraviolet light (UV), and then were stained by submersion in a basic aqueous solution of potassium permanganate or with an acidic ethanolic solution of anisaldehyde, followed by brief heating.

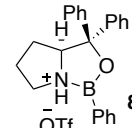
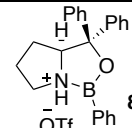
**Materials:** CH<sub>2</sub>Cl<sub>2</sub>, THF, ethyl ether, and acetonitrile to be used in anhydrous reaction mixtures were dried by passage through activated alumina columns immediately prior to use. Hexanes used were ≥85% n-hexane. Other commercial solvents and reagents were used as received, unless otherwise noted.

**Instrumentation:** Unless otherwise noted, proton nuclear magnetic resonance (<sup>1</sup>H NMR) spectra and carbon nuclear magnetic resonance (<sup>13</sup>C NMR) spectra were recorded on a 400 MHz Bruker Avance III HD 2-channel NMR spectrometer at 23 °C or a 500 MHz Bruker DRX 4-channel NMR spectrometer at 23 °C. Proton chemical shifts are expressed in parts per million (ppm, δ scale) and are referenced to residual protium in the NMR solvent (CHCl<sub>3</sub>: δ 7.26). Carbon chemical shifts are expressed in parts per million (ppm, δ scale) and are referenced to the carbon resonance of the NMR solvent (CDCl<sub>3</sub>: δ 77.0). Data are represented as follows: chemical shift, multiplicity (s = singlet, d = doublet, t = triplet, q = quartet, dd = doublet of doublets, dt = doublet of triplets, sxt =

sextet, m = multiplet, br = broad, app = apparent), integration, and coupling constant (J) in hertz (Hz). High-resolution mass spectra were obtained at the QB3/Chemistry Mass Spectrometry Facility at University of California, Berkeley using a Thermo LTQ-FT mass spectrometer.

## Dioxinone vinylogous Mukaiyama aldol screen



entry	R	Lewis acid	yield (%)	dr (9b:9c)	entry	R	Lewis acid	yield (%)	dr (9b:9c)
1	H	ZnCl <sub>2</sub> (1 equiv)	0	-	8	TMS	 (50 mol %)	55	9:1
2	H	TiCl <sub>4</sub> (1 equiv)	97	2:1	9	TMS	 (50 mol %)	39	1:9
3	H	TiCl <sub>4</sub> (2 equiv)	42	4:1					
4	H	BF <sub>3</sub> ·Et <sub>2</sub> O (1 equiv)	20	1.1:1					
5	H	SnCl <sub>4</sub> (1 equiv)	57	2:1					
6	H	Et <sub>2</sub> AlCl (1 equiv)	11	2:1					
7	H	Yb(OTf) <sub>3</sub> (1 equiv)	2	1.5:1					

## Silyl ether aldol product 9b

A 10-mL round-bottom flask was charged with phenylboronic acid (17 mg, 0.14 mmol, 0.50 equiv) and (R)-diphenyl(pyrrolidin-2-yl)methanol (36 mg, 0.14 mmol, 0.50 equiv). The vessel was equipped with a Dean-Stark apparatus with reflux condenser and the system was evacuated and flushed with nitrogen (3 times). PhMe was added, and the resulting clear solution was brought to reflux by means of a 145 °C oil bath. After 17 h, the mixture was allowed to cool to 23 °C and was concentrated under reduced pressure. The resulting white solid was dried at ≤1 Torr for 1 h. The vessel was flushed with nitrogen, and CH<sub>2</sub>Cl<sub>2</sub> (1 mL) was added. The resulting colorless solution was cooled to -78 °C, and trifluoromethanesulfonic acid (13 μL, 0.14 mmol, 0.50 equiv) was added dropwise by means of glass syringe (CAUTION: TfOH rapidly corrodes most plastic syringes!). Some of the TfOH froze upon contact with the solution. After 30 min, the solids had dissolved, and a mixture of **8** (50 mg, 0.28 mmol, 1.00 equiv; *vide infra*) and **6**<sup>14</sup> (75 mg, 1.10 Eq, 0.31 mmol)



in CH<sub>2</sub>Cl<sub>2</sub> (2 mL) was added dropwise. The mixture was stirred at –78 °C for 16 h before being quenched with saturated aqueous NaHCO<sub>3</sub> (3 mL). The vessel was removed from the cooling bath and was allowed to warm to ambient temperature (approximately 20 °C) while it was rapidly stirred. The biphasic mixture was transferred to a separatory funnel and the layers were separated. The aqueous layer was extracted with CH<sub>2</sub>Cl<sub>2</sub> (2 × 5 mL). The combined organic layers were washed with water (10 mL) and brine (10 mL). The washed organic solution was dried over sodium sulfate, filtered, and concentrated to reveal a viscous pale-yellow oil. <sup>1</sup>H NMR analysis of the crude indicated a 9:1 mixture of product diastereomers. The crude mixture was purified by flash chromatography (silica gel, eluent: 0-30% EtOAc/hexanes) to yield **9b** (46 mg, 39%) as a white crystalline solid. Product could be crystallized from pentanes at –20 °C.

**TLC** (25% EtOAc/hexanes): R<sub>f</sub> = 0.55 (UV, *p*-anisaldehyde).

**<sup>1</sup>H NMR** (400 MHz, CDCl<sub>3</sub>) δ 5.60 (s, 1H), 5.44 (s, 1H), 3.78 (dd, J = 9.8, 1.7 Hz, 1H), 2.96 – 2.84 (m, 1H), 2.52 (dd, J = 14.1, 3.3 Hz, 1H), 2.23 (dd, J = 14.2, 10.2 Hz, 1H), 2.11 – 2.01 (m, 1H), 1.82 (s, 3H), 1.70 (s, 3H), 1.62 (s, 3H), 1.03 (d, J = 6.9 Hz, 3H), 0.94 (d, J = 6.8 Hz, 3H), 0.06 (s, 9H).

**<sup>13</sup>C NMR** (100 MHz, CDCl<sub>3</sub>) δ 167.1, 162.9, 134.2, 118.4, 104.9, 101.9, 41.4, 39.4, 32.8, 27.6, 22.8, 17.7, 13.9, 10.2, 0.7.

**HRMS** (ESI-TOF) m/z calcd for C<sub>18</sub>H<sub>32</sub>BrO<sub>4</sub>Si [M + H]<sup>+</sup> 419.1253, found 419.1247

### **Silyl ether aldol product 9c**

The procedure is identical to the synthesis of **9b**, instead using (*S*)-diphenyl(pyrrolidin-2-yl)methanol to generate the chiral oxazaborolidine Lewis acid catalyst. **9c** (65 mg, 55%) was isolated as a crystalline white solid. Product could be crystallized from hexanes at ambient temperature.

**TLC** (25% EtOAc/hexanes):  $R_f = 0.55$  (UV, *p*-anisaldehyde).

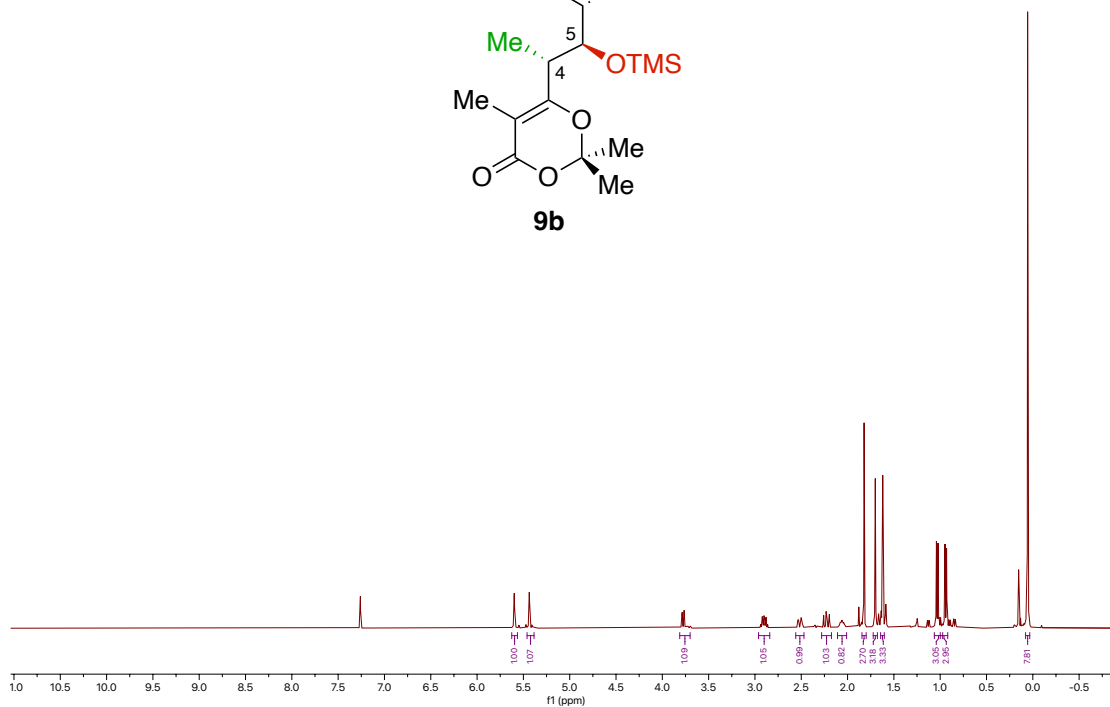
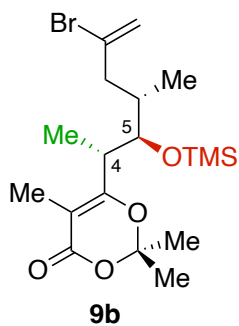
**$^1\text{H NMR}$**  (400 MHz,  $\text{CDCl}_3$ )  $\delta$  5.58 (s, 1H), 5.47 (d,  $J = 1.6$  Hz, 1H), 3.75 (dd,  $J = 9.6, 1.6$  Hz, 1H), 2.96 – 2.84 (m, 1H), 2.42 – 2.25 (m, 2H), 2.05 (dddd,  $J = 8.5, 7.1, 5.5, 1.7$  Hz, 1H), 1.83 (s, 3H), 1.70 (s, 3H), 1.62 (s, 3H), 1.00 (d,  $J = 6.9$  Hz, 3H), 0.84 (d,  $J = 6.7$  Hz, 3H), 0.05 (s, 9H).

**$^{13}\text{C NMR}$**  (100 MHz,  $\text{CDCl}_3$ )  $\delta$  167.1, 162.9, 133.7, 118.3, 105.0, 102.0, 76.0, 47.1, 39.7, 33.3, 27.7, 22.7, 14.0, 10.6, 10.2, 0.8

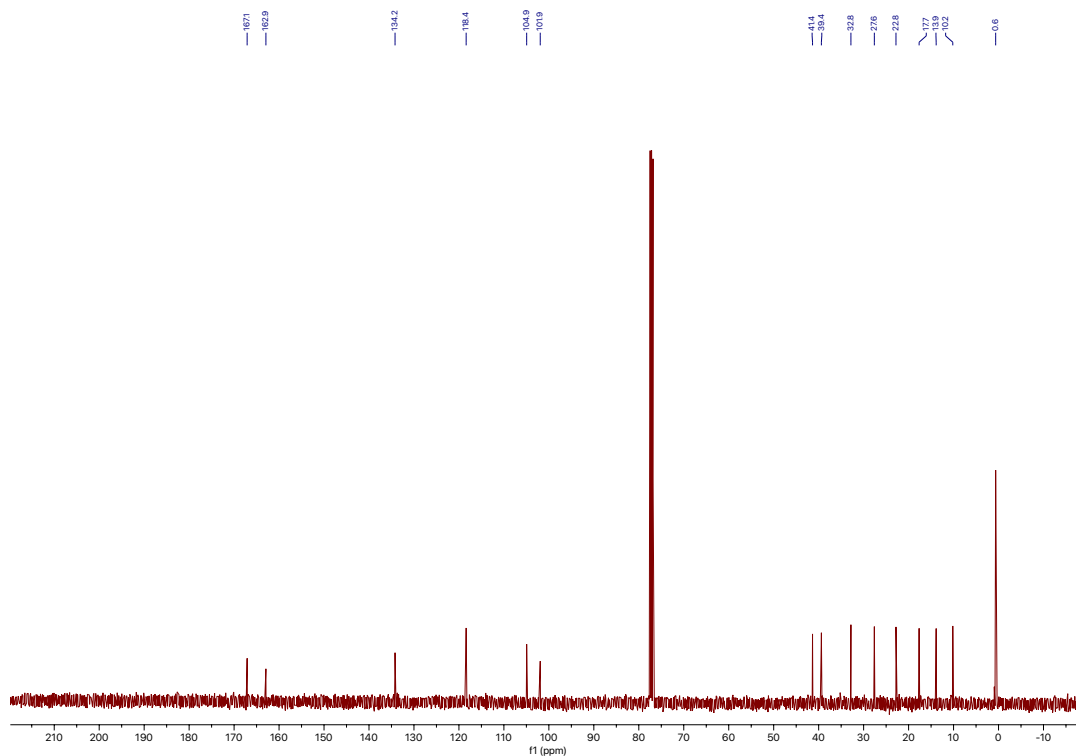
**HRMS** (ESI-TOF)  $m/z$  calcd for  $\text{C}_{18}\text{H}_{32}\text{BrO}_4\text{Si}$   $[\text{M} + \text{H}]^+$  419.1253, found 419.1246

# $^1\text{H}$ NMR and $^{13}\text{C}$ NMR Spectra for Compounds

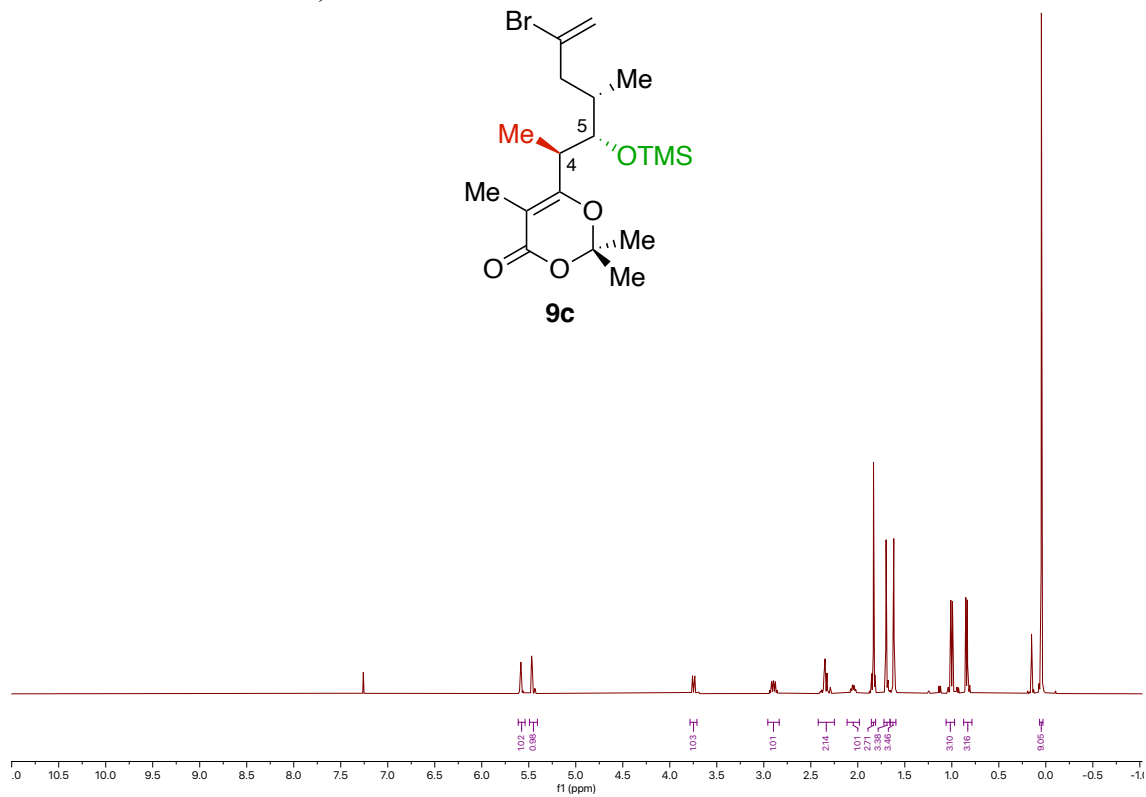
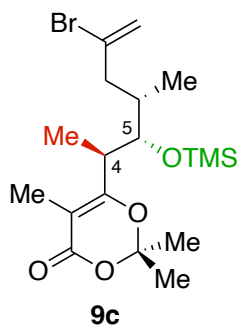
( $^1\text{H}$  NMR,  $\text{CDCl}_3$ , 400 MHz)



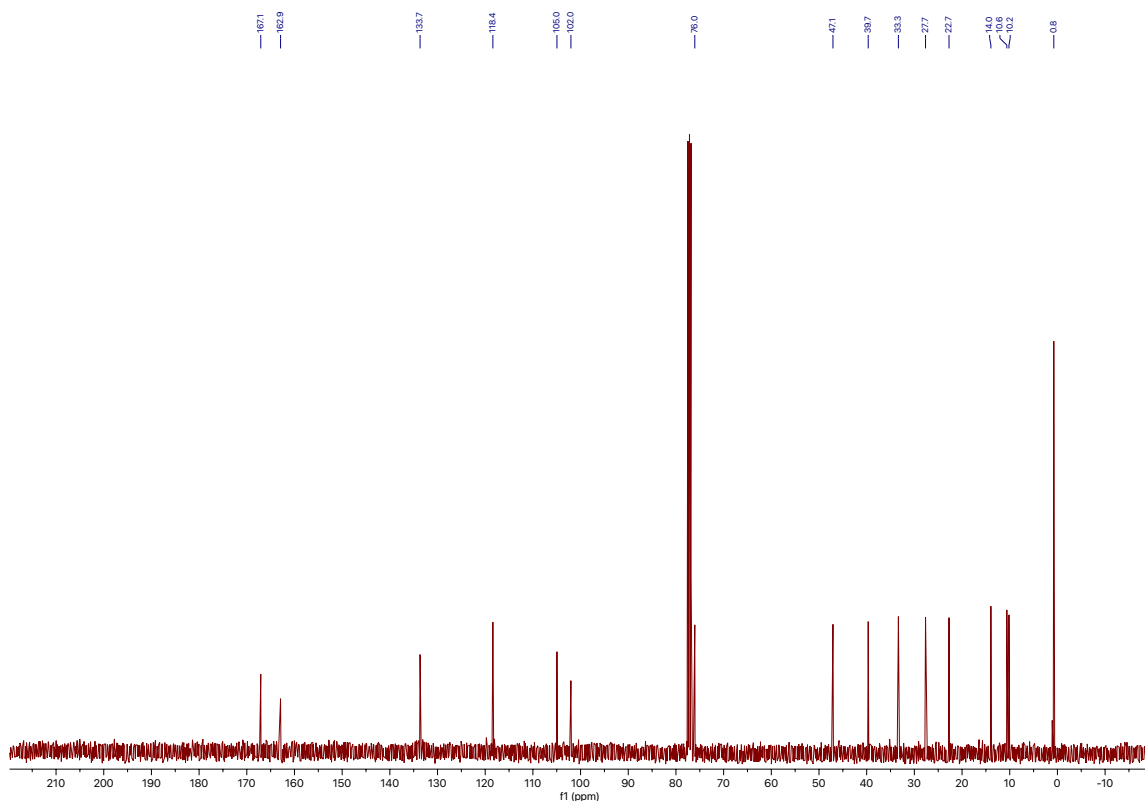
( $^{13}\text{C}$  NMR,  $\text{CDCl}_3$ , 100 MHz)



(<sup>1</sup>H NMR, CDCl<sub>3</sub>, 400 MHz)



(<sup>13</sup>C NMR, CDCl<sub>3</sub>, 100 MHz)



## X-Ray Crystallographic Information

Compound **9b**: CCDC 2402906

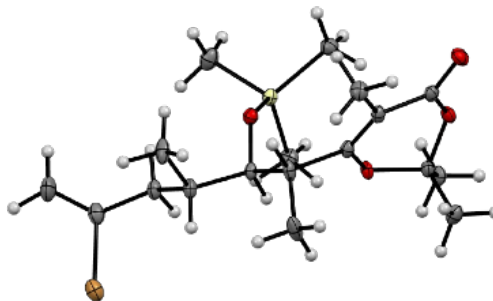
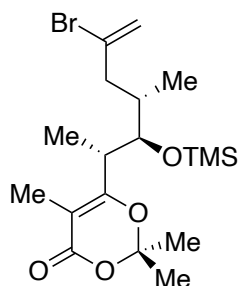


Table 1.1 Crystal data and structure refinement for QEdmondson02A\_UCSF.

Identification code	QEdmondson02A_UCSF	
Empirical formula	C <sub>18</sub> H <sub>31</sub> Br O <sub>4</sub> Si	
Formula weight	419.43	
Temperature	100(2) K	
Wavelength	1.54184 Å	
Crystal system	Orthorhombic	
Space group	P 21 21 21	
Unit cell dimensions	a = 6.39930(10) Å	α = 90°.
	b = 12.3792(2) Å	β = 90°.
	c = 26.2195(3) Å	γ = 90°.
Volume	2077.06(5) Å <sup>3</sup>	
Z	4	
Density (calculated)	1.341 Mg/m <sup>3</sup>	
Absorption coefficient	3.394 mm <sup>-1</sup>	
F(000)	880	
Crystal size	0.310 x 0.210 x 0.180 mm <sup>3</sup>	
Theta range for data collection	3.371 to 74.502°.	
Index ranges	-7 ≤ h ≤ 7, -15 ≤ k ≤ 15, -32 ≤ l ≤ 29	
Reflections collected	21344	
Independent reflections	4215 [R(int) = 0.0293]	
Completeness to theta = 74.000°	99.4 %	
Absorption correction	Semi-empirical from equivalents	
Max. and min. transmission	1.00000 and 0.51649	
Refinement method	Full-matrix least-squares on F <sup>2</sup>	
Data / restraints / parameters	4215 / 0 / 225	

Goodness-of-fit on F <sup>2</sup>	1.069
Final R indices [I>2sigma(I)]	R1 = 0.0210, wR2 = 0.0562
R indices (all data)	R1 = 0.0210, wR2 = 0.0562
Absolute structure parameter	-0.010(6)
Extinction coefficient	n/a
Largest diff. peak and hole	0.312 and -0.294 e.Å <sup>-3</sup>

Table 1.2 Atomic coordinates ( x 10<sup>4</sup>) and equivalent isotropic displacement parameters (Å<sup>2</sup>x 10<sup>3</sup>) for qedmondson02a\_ucs. U(eq) is defined as one third of the trace of the orthogonalized U<sup>ij</sup> tensor.

	x	y	z	U(eq)
Br(1)	7584(1)	4685(1)	4301(1)	23(1)
Si(1)	687(1)	6260(1)	5971(1)	14(1)
O(1)	1930(2)	4816(1)	7607(1)	16(1)
O(2)	-43(3)	3392(1)	7779(1)	21(1)
O(3)	3781(3)	4949(1)	6835(1)	14(1)
O(4)	1483(2)	5034(1)	5809(1)	15(1)
C(1)	3870(3)	5143(2)	7377(1)	15(1)
C(2)	4027(4)	6347(2)	7447(1)	19(1)
C(3)	5685(4)	4534(2)	7609(1)	21(1)
C(4)	1202(3)	3802(2)	7491(1)	15(1)
C(5)	1884(3)	3344(2)	7005(1)	15(1)
C(6)	1083(4)	2233(2)	6872(1)	20(1)
C(7)	3041(3)	3967(2)	6691(1)	14(1)
C(8)	3721(4)	3659(2)	6161(1)	16(1)
C(9)	5947(5)	3202(2)	6187(1)	26(1)
C(10)	3559(3)	4617(2)	5789(1)	13(1)
C(11)	2916(4)	7196(2)	6086(1)	19(1)
C(12)	-925(4)	6771(2)	5431(1)	25(1)
C(13)	-1021(4)	6144(2)	6541(1)	19(1)
C(14)	4086(4)	4294(2)	5235(1)	16(1)
C(15)	2718(5)	3386(2)	5030(1)	24(1)
C(16)	3935(4)	5295(2)	4889(1)	17(1)
C(17)	4703(4)	5128(2)	4355(1)	21(1)
C(18)	3648(5)	5278(2)	3928(1)	30(1)

Table 1.3 Bond lengths [Å] and angles [°] for qedmondson02a\_ucsf.

---

Br(1)-C(17)	1.929(3)
Si(1)-O(4)	1.6561(16)
Si(1)-C(13)	1.858(2)
Si(1)-C(11)	1.862(2)
Si(1)-C(12)	1.863(3)
O(1)-C(4)	1.372(3)
O(1)-C(1)	1.438(3)
O(2)-C(4)	1.209(3)
O(3)-C(7)	1.358(3)
O(3)-C(1)	1.443(2)
O(4)-C(10)	1.426(3)
C(1)-C(2)	1.505(3)
C(1)-C(3)	1.513(3)
C(2)-H(2A)	0.9800
C(2)-H(2B)	0.9800
C(2)-H(2C)	0.9800
C(3)-H(3A)	0.9800
C(3)-H(3B)	0.9800
C(3)-H(3C)	0.9800
C(4)-C(5)	1.461(3)
C(5)-C(7)	1.349(3)
C(5)-C(6)	1.509(3)
C(6)-H(6A)	0.9800
C(6)-H(6B)	0.9800
C(6)-H(6C)	0.9800
C(7)-C(8)	1.506(3)
C(8)-C(9)	1.535(3)
C(8)-C(10)	1.538(3)
C(8)-H(8)	1.0000
C(9)-H(9A)	0.9800
C(9)-H(9B)	0.9800
C(9)-H(9C)	0.9800
C(10)-C(14)	1.543(3)

Table 1.3 (continued) Bond lengths [ $\text{\AA}$ ] and angles [ $^\circ$ ] for qedmondson02a\_ucsf.

---

C(10)-H(10)	1.0000
C(11)-H(11A)	0.9800
C(11)-H(11B)	0.9800
C(11)-H(11C)	0.9800
C(12)-H(12A)	0.9800
C(12)-H(12B)	0.9800
C(12)-H(12C)	0.9800
C(13)-H(13A)	0.9800
C(13)-H(13B)	0.9800
C(13)-H(13C)	0.9800
C(14)-C(15)	1.524(3)
C(14)-C(16)	1.539(3)
C(14)-H(14)	1.0000
C(15)-H(15A)	0.9800
C(15)-H(15B)	0.9800
C(15)-H(15C)	0.9800
C(16)-C(17)	1.499(3)
C(16)-H(16A)	0.9900
C(16)-H(16B)	0.9900
C(17)-C(18)	1.320(3)
C(18)-H(18A)	0.9500
C(18)-H(18B)	0.9500
O(4)-Si(1)-C(13)	108.41(10)
O(4)-Si(1)-C(11)	112.06(10)
C(13)-Si(1)-C(11)	111.64(11)
O(4)-Si(1)-C(12)	106.67(10)
C(13)-Si(1)-C(12)	108.23(12)
C(11)-Si(1)-C(12)	109.64(11)
C(4)-O(1)-C(1)	117.28(17)
C(7)-O(3)-C(1)	115.88(16)
C(10)-O(4)-Si(1)	128.90(13)
O(1)-C(1)-O(3)	109.36(17)
O(1)-C(1)-C(2)	106.65(18)



Table 1.3 (continued) Bond lengths [Å] and angles [°] for qedmondson02a\_ucsf.

---

O(3)-C(1)-C(2)	106.70(18)
O(1)-C(1)-C(3)	110.71(18)
O(3)-C(1)-C(3)	110.06(18)
C(2)-C(1)-C(3)	113.18(19)
C(1)-C(2)-H(2A)	109.5
C(1)-C(2)-H(2B)	109.5
H(2A)-C(2)-H(2B)	109.5
C(1)-C(2)-H(2C)	109.5
H(2A)-C(2)-H(2C)	109.5
H(2B)-C(2)-H(2C)	109.5
C(1)-C(3)-H(3A)	109.5
C(1)-C(3)-H(3B)	109.5
H(3A)-C(3)-H(3B)	109.5
C(1)-C(3)-H(3C)	109.5
H(3A)-C(3)-H(3C)	109.5
H(3B)-C(3)-H(3C)	109.5
O(2)-C(4)-O(1)	118.0(2)
O(2)-C(4)-C(5)	125.3(2)
O(1)-C(4)-C(5)	116.48(19)
C(7)-C(5)-C(4)	118.3(2)
C(7)-C(5)-C(6)	124.5(2)
C(4)-C(5)-C(6)	117.0(2)
C(5)-C(6)-H(6A)	109.5
C(5)-C(6)-H(6B)	109.5
H(6A)-C(6)-H(6B)	109.5
C(5)-C(6)-H(6C)	109.5
H(6A)-C(6)-H(6C)	109.5
H(6B)-C(6)-H(6C)	109.5
C(5)-C(7)-O(3)	122.26(19)
C(5)-C(7)-C(8)	125.3(2)
O(3)-C(7)-C(8)	112.42(18)
C(7)-C(8)-C(9)	108.67(18)
C(7)-C(8)-C(10)	111.78(18)
C(9)-C(8)-C(10)	112.03(19)

Table 1.3 (continued) Bond lengths [ $\text{\AA}$ ] and angles [ $^\circ$ ] for qedmondson02a\_ucsf.

---

C(7)-C(8)-H(8)	108.1
C(9)-C(8)-H(8)	108.1
C(10)-C(8)-H(8)	108.1
C(8)-C(9)-H(9A)	109.5
C(8)-C(9)-H(9B)	109.5
H(9A)-C(9)-H(9B)	109.5
C(8)-C(9)-H(9C)	109.5
H(9A)-C(9)-H(9C)	109.5
H(9B)-C(9)-H(9C)	109.5
O(4)-C(10)-C(8)	108.54(17)
O(4)-C(10)-C(14)	109.41(17)
C(8)-C(10)-C(14)	112.45(17)
O(4)-C(10)-H(10)	108.8
C(8)-C(10)-H(10)	108.8
C(14)-C(10)-H(10)	108.8
Si(1)-C(11)-H(11A)	109.5
Si(1)-C(11)-H(11B)	109.5
H(11A)-C(11)-H(11B)	109.5
Si(1)-C(11)-H(11C)	109.5
H(11A)-C(11)-H(11C)	109.5
H(11B)-C(11)-H(11C)	109.5
Si(1)-C(12)-H(12A)	109.5
Si(1)-C(12)-H(12B)	109.5
H(12A)-C(12)-H(12B)	109.5
Si(1)-C(12)-H(12C)	109.5
H(12A)-C(12)-H(12C)	109.5
H(12B)-C(12)-H(12C)	109.5
Si(1)-C(13)-H(13A)	109.5
Si(1)-C(13)-H(13B)	109.5
H(13A)-C(13)-H(13B)	109.5
Si(1)-C(13)-H(13C)	109.5
H(13A)-C(13)-H(13C)	109.5
H(13B)-C(13)-H(13C)	109.5
C(15)-C(14)-C(16)	110.43(18)

Table 1.3 (continued) Bond lengths [ $\text{\AA}$ ] and angles [ $^\circ$ ] for qedmondson02a\_ucs.

C(15)-C(14)-C(10)	113.52(19)
C(16)-C(14)-C(10)	109.42(17)
C(15)-C(14)-H(14)	107.8
C(16)-C(14)-H(14)	107.8
C(10)-C(14)-H(14)	107.8
C(14)-C(15)-H(15A)	109.5
C(14)-C(15)-H(15B)	109.5
H(15A)-C(15)-H(15B)	109.5
C(14)-C(15)-H(15C)	109.5
H(15A)-C(15)-H(15C)	109.5
H(15B)-C(15)-H(15C)	109.5
C(17)-C(16)-C(14)	114.83(19)
C(17)-C(16)-H(16A)	108.6
C(14)-C(16)-H(16A)	108.6
C(17)-C(16)-H(16B)	108.6
C(14)-C(16)-H(16B)	108.6
H(16A)-C(16)-H(16B)	107.5
C(18)-C(17)-C(16)	127.3(2)
C(18)-C(17)-Br(1)	117.9(2)
C(16)-C(17)-Br(1)	114.84(17)
C(17)-C(18)-H(18A)	120.0
C(17)-C(18)-H(18B)	120.0
H(18A)-C(18)-H(18B)	120.0

Symmetry transformations used to generate equivalent atoms:

Table 1.4 Anisotropic displacement parameters ( $\text{\AA}^2 \times 10^3$ ) for qedmondson02a\_ucs. The anisotropic displacement factor exponent takes the form:  $-2\pi^2 [ h^2 a^{*2} U^{11} + \dots + 2 h k a^* b^* U^{12} ]$

	$U^{11}$	$U^{22}$	$U^{33}$	$U^{23}$	$U^{13}$	$U^{12}$
Br(1)	29(1)	22(1)	18(1)	0(1)	5(1)	0(1)
Si(1)	16(1)	12(1)	14(1)	0(1)	-1(1)	1(1)
O(1)	18(1)	19(1)	13(1)	-2(1)	4(1)	1(1)

Table 1.4 (continued) Anisotropic displacement parameters ( $\text{\AA}^2 \times 10^3$ ) for qedmondson02a\_ucsf. The anisotropic displacement factor exponent takes the form:  $-2\pi^2 [ h^2 a^{*2} U^{11} + \dots + 2 h k a^* b^* U^{12} ]$

	U <sup>11</sup>	U <sup>22</sup>	U <sup>33</sup>	U <sup>23</sup>	U <sup>13</sup>	U <sup>12</sup>
O(2)	20(1)	24(1)	18(1)	5(1)	5(1)	0(1)
O(3)	21(1)	13(1)	9(1)	-2(1)	2(1)	-1(1)
O(4)	16(1)	14(1)	14(1)	-1(1)	-1(1)	1(1)
C(1)	17(1)	18(1)	9(1)	-2(1)	0(1)	1(1)
C(2)	23(1)	17(1)	16(1)	-6(1)	0(1)	1(1)
C(3)	22(1)	22(1)	19(1)	-1(1)	-5(1)	3(1)
C(4)	16(1)	17(1)	13(1)	2(1)	-1(1)	3(1)
C(5)	19(1)	15(1)	12(1)	0(1)	-2(1)	3(1)
C(6)	24(1)	16(1)	19(1)	1(1)	0(1)	-2(1)
C(7)	17(1)	12(1)	12(1)	-1(1)	-1(1)	2(1)
C(8)	27(1)	12(1)	10(1)	1(1)	2(1)	2(1)
C(9)	37(1)	26(1)	14(1)	4(1)	7(1)	17(1)
C(10)	18(1)	11(1)	11(1)	0(1)	-1(1)	0(1)
C(11)	22(1)	14(1)	21(1)	1(1)	-1(1)	-2(1)
C(12)	29(1)	22(1)	23(1)	1(1)	-6(1)	4(1)
C(13)	18(1)	19(1)	20(1)	-2(1)	1(1)	-1(1)
C(14)	24(1)	13(1)	10(1)	0(1)	0(1)	0(1)
C(15)	41(2)	18(1)	14(1)	-3(1)	-2(1)	-6(1)
C(16)	24(1)	16(1)	12(1)	2(1)	0(1)	-1(1)
C(17)	28(1)	18(1)	16(1)	1(1)	2(1)	-2(1)
C(18)	39(1)	36(1)	14(1)	3(1)	-3(1)	0(1)

Table 1.5 Hydrogen coordinates ( $\times 10^4$ ) and isotropic displacement parameters ( $\text{\AA}^2 \times 10^3$ ) for qedmondson02a\_ucsf.

	x	y	z	U(eq)
H(2A)	2787	6695	7301	28
H(2B)	5280	6615	7273	28
H(2C)	4116	6516	7811	28
H(3A)	5708	4654	7979	31

Table 1.5 (continued) Hydrogen coordinates ( $\times 10^4$ ) and isotropic displacement parameters ( $\text{\AA}^2 \times 10^3$ ) for qedmondson02a\_ucs.f.

	x	y	z	U(eq)
H(3B)	6996	4793	7460	31
H(3C)	5527	3760	7540	31
H(6A)	869	1816	7185	30
H(6B)	2105	1863	6655	30
H(6C)	-246	2298	6689	30
H(8)	2773	3074	6036	19
H(9A)	6907	3766	6305	39
H(9B)	6375	2955	5848	39
H(9C)	5982	2593	6426	39
H(10)	4552	5194	5901	16
H(11A)	3889	6867	6329	29
H(11B)	2391	7878	6225	29
H(11C)	3643	7335	5763	29
H(12A)	-7	6995	5151	37
H(12B)	-1756	7390	5545	37
H(12C)	-1860	6196	5312	37
H(13A)	-2257	5713	6456	29
H(13B)	-1457	6866	6651	29
H(13C)	-249	5791	6818	29
H(14)	5568	4038	5229	19
H(15A)	2992	2722	5222	36
H(15B)	3040	3266	4668	36
H(15C)	1244	3585	5065	36
H(16A)	2457	5529	4875	21
H(16B)	4750	5888	5046	21
H(18A)	2238	5517	3941	36
H(18B)	4297	5146	3608	36

Table 1.6 Torsion angles [°] for qedmondson02a\_ucsf.

---

C(13)-Si(1)-O(4)-C(10)	-118.42(17)
C(11)-Si(1)-O(4)-C(10)	5.24(19)
C(12)-Si(1)-O(4)-C(10)	125.23(17)
C(4)-O(1)-C(1)-O(3)	50.3(2)
C(4)-O(1)-C(1)-C(2)	165.32(18)
C(4)-O(1)-C(1)-C(3)	-71.2(2)
C(7)-O(3)-C(1)-O(1)	-46.7(2)
C(7)-O(3)-C(1)-C(2)	-161.65(19)
C(7)-O(3)-C(1)-C(3)	75.2(2)
C(1)-O(1)-C(4)-O(2)	159.16(19)
C(1)-O(1)-C(4)-C(5)	-25.5(3)
O(2)-C(4)-C(5)-C(7)	170.3(2)
O(1)-C(4)-C(5)-C(7)	-4.6(3)
O(2)-C(4)-C(5)-C(6)	-4.6(3)
O(1)-C(4)-C(5)-C(6)	-179.58(18)
C(4)-C(5)-C(7)-O(3)	7.6(3)
C(6)-C(5)-C(7)-O(3)	-177.87(19)
C(4)-C(5)-C(7)-C(8)	-174.7(2)
C(6)-C(5)-C(7)-C(8)	-0.1(4)
C(1)-O(3)-C(7)-C(5)	19.5(3)
C(1)-O(3)-C(7)-C(8)	-158.55(18)
C(5)-C(7)-C(8)-C(9)	-96.4(3)
O(3)-C(7)-C(8)-C(9)	81.6(2)
C(5)-C(7)-C(8)-C(10)	139.5(2)
O(3)-C(7)-C(8)-C(10)	-42.6(2)
Si(1)-O(4)-C(10)-C(8)	119.66(17)
Si(1)-O(4)-C(10)-C(14)	-117.29(18)
C(7)-C(8)-C(10)-O(4)	-54.4(2)
C(9)-C(8)-C(10)-O(4)	-176.60(18)
C(7)-C(8)-C(10)-C(14)	-175.55(19)
C(9)-C(8)-C(10)-C(14)	62.2(2)
O(4)-C(10)-C(14)-C(15)	-63.4(2)
C(8)-C(10)-C(14)-C(15)	57.3(3)
O(4)-C(10)-C(14)-C(16)	60.5(2)

Table 1.6 (continued). Torsion angles [°] for qedmondson02a\_ucsf.

---

C(8)-C(10)-C(14)-C(16)	-178.85(18)
C(15)-C(14)-C(16)-C(17)	-62.6(3)
C(10)-C(14)-C(16)-C(17)	171.7(2)
C(14)-C(16)-C(17)-C(18)	122.7(3)
C(14)-C(16)-C(17)-Br(1)	-59.1(2)

---

Symmetry transformations used to generate equivalent atoms:

Compound **9c**: CCDC 2402907

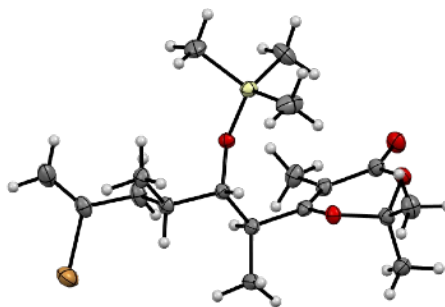
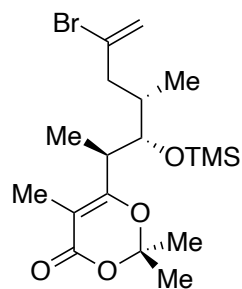


Table 1.7 Crystal data and structure refinement for QEdmondson03\_UCSF.

Identification code	QEdmondson03_UCSF	
Empirical formula	C <sub>18</sub> H <sub>31</sub> Br O <sub>4</sub> Si	
Formula weight	419.43	
Temperature	150(2) K	
Wavelength	1.54184 Å	
Crystal system	Orthorhombic	
Space group	P 21 21 21	
Unit cell dimensions	a = 8.80940(10) Å	α = 90°.
	b = 14.90640(10) Å	β = 90°.
	c = 16.28460(10) Å	γ = 90°.
Volume	2138.44(3) Å <sup>3</sup>	
Z	4	
Density (calculated)	1.303 Mg/m <sup>3</sup>	
Absorption coefficient	3.297 mm <sup>-1</sup>	
F(000)	880	
Crystal size	0.340 x 0.210 x 0.110 mm <sup>3</sup>	
Theta range for data collection	4.020 to 74.466°.	
Index ranges	-10 ≤ h ≤ 11, -18 ≤ k ≤ 18, -20 ≤ l ≤ 18	
Reflections collected	45863	
Independent reflections	4357 [R(int) = 0.0389]	
Completeness to theta = 74.000°	100.0 %	
Absorption correction	Semi-empirical from equivalents	
Max. and min. transmission	1.00000 and 0.76453	
Refinement method	Full-matrix least-squares on F <sup>2</sup>	
Data / restraints / parameters	4357 / 0 / 225	
Goodness-of-fit on F <sup>2</sup>	1.037	



Final R indices [ $I > 2\sigma(I)$ ]	R1 = 0.0289, wR2 = 0.0760
R indices (all data)	R1 = 0.0291, wR2 = 0.0761
Absolute structure parameter	-0.022(5)
Extinction coefficient	n/a
Largest diff. peak and hole	0.528 and -0.508 e.Å <sup>-3</sup>

Table 1.8 Atomic coordinates ( $\times 10^4$ ) and equivalent isotropic displacement parameters ( $\text{Å}^2 \times 10^3$ ) for qedmondson03\_ucsf. U(eq) is defined as one third of the trace of the orthogonalized  $U^{ij}$  tensor.

	x	y	z	U(eq)
Br(1)	-1142(1)	2372(1)	9644(1)	62(1)
Si(1)	3442(1)	1608(1)	6203(1)	36(1)
O(1)	6043(2)	4467(1)	5955(1)	41(1)
O(2)	7947(2)	3899(2)	6661(2)	52(1)
O(3)	3516(2)	4287(1)	6394(1)	37(1)
O(4)	2983(2)	2106(1)	7072(1)	31(1)
C(1)	4572(3)	4879(2)	5998(2)	37(1)
C(2)	4670(4)	5751(2)	6459(2)	47(1)
C(3)	4043(4)	4995(3)	5123(2)	53(1)
C(4)	6598(3)	4055(2)	6641(2)	39(1)
C(5)	5491(3)	3785(2)	7266(2)	37(1)
C(6)	6104(4)	3308(2)	8010(2)	50(1)
C(7)	4006(3)	3888(2)	7105(2)	34(1)
C(8)	2708(3)	3589(2)	7632(2)	36(1)
C(9)	1620(4)	4378(2)	7797(2)	53(1)
C(10)	1880(3)	2788(2)	7240(2)	31(1)
C(11)	2602(5)	465(2)	6190(3)	62(1)
C(12)	2813(6)	2263(3)	5310(2)	70(1)
C(13)	5545(4)	1479(3)	6217(2)	61(1)
C(14)	622(3)	2398(2)	7794(2)	34(1)
C(15)	-371(3)	1746(2)	7326(2)	41(1)
C(16)	1326(3)	1951(3)	8550(2)	47(1)
C(17)	260(3)	1539(2)	9152(2)	44(1)
C(18)	207(4)	701(3)	9378(3)	61(1)

Table 1.9 Bond lengths [Å] and angles [°] for qedmondson03\_ucsf.

---

Br(1)-C(17)	1.926(3)
Si(1)-O(4)	1.6486(19)
Si(1)-C(12)	1.836(4)
Si(1)-C(11)	1.858(4)
Si(1)-C(13)	1.862(4)
O(1)-C(4)	1.366(4)
O(1)-C(1)	1.436(3)
O(2)-C(4)	1.211(4)
O(3)-C(7)	1.372(3)
O(3)-C(1)	1.434(3)
O(4)-C(10)	1.433(3)
C(1)-C(2)	1.504(4)
C(1)-C(3)	1.510(4)
C(2)-H(2A)	0.9800
C(2)-H(2B)	0.9800
C(2)-H(2C)	0.9800
C(3)-H(3A)	0.9800
C(3)-H(3B)	0.9800
C(3)-H(3C)	0.9800
C(4)-C(5)	1.465(4)
C(5)-C(7)	1.344(4)
C(5)-C(6)	1.505(4)
C(6)-H(6A)	0.9800
C(6)-H(6B)	0.9800
C(6)-H(6C)	0.9800
C(7)-C(8)	1.498(4)
C(8)-C(10)	1.538(4)
C(8)-C(9)	1.541(4)
C(8)-H(8)	1.0000
C(9)-H(9A)	0.9800
C(9)-H(9B)	0.9800
C(9)-H(9C)	0.9800
C(10)-C(14)	1.543(3)
C(10)-H(10)	1.0000

Table 1.9 (continued) Bond lengths [ $\text{\AA}$ ] and angles [ $^\circ$ ] for qedmondson03\_ucsf.

---

C(11)-H(11A)	0.9800
C(11)-H(11B)	0.9800
C(11)-H(11C)	0.9800
C(12)-H(12A)	0.9800
C(12)-H(12B)	0.9800
C(12)-H(12C)	0.9800
C(13)-H(13A)	0.9800
C(13)-H(13B)	0.9800
C(13)-H(13C)	0.9800
C(14)-C(15)	1.513(4)
C(14)-C(16)	1.532(4)
C(14)-H(14)	1.0000
C(15)-H(15A)	0.9800
C(15)-H(15B)	0.9800
C(15)-H(15C)	0.9800
C(16)-C(17)	1.489(4)
C(16)-H(16A)	0.9900
C(16)-H(16B)	0.9900
C(17)-C(18)	1.303(5)
C(18)-H(18A)	0.9500
C(18)-H(18B)	0.9500
O(4)-Si(1)-C(12)	111.48(14)
O(4)-Si(1)-C(11)	108.97(15)
C(12)-Si(1)-C(11)	111.0(2)
O(4)-Si(1)-C(13)	106.24(14)
C(12)-Si(1)-C(13)	111.4(2)
C(11)-Si(1)-C(13)	107.6(2)
C(4)-O(1)-C(1)	118.4(2)
C(7)-O(3)-C(1)	116.2(2)
C(10)-O(4)-Si(1)	130.53(16)
O(3)-C(1)-O(1)	110.2(2)
O(3)-C(1)-C(2)	110.2(2)
O(1)-C(1)-C(2)	110.0(2)

Table 1.9 (continued) Bond lengths [ $\text{\AA}$ ] and angles [ $^\circ$ ] for qedmondson03\_ucsf.

---

O(3)-C(1)-C(3)	107.1(2)
O(1)-C(1)-C(3)	106.3(3)
C(2)-C(1)-C(3)	112.9(3)
C(1)-C(2)-H(2A)	109.5
C(1)-C(2)-H(2B)	109.5
H(2A)-C(2)-H(2B)	109.5
C(1)-C(2)-H(2C)	109.5
H(2A)-C(2)-H(2C)	109.5
H(2B)-C(2)-H(2C)	109.5
C(1)-C(3)-H(3A)	109.5
C(1)-C(3)-H(3B)	109.5
H(3A)-C(3)-H(3B)	109.5
C(1)-C(3)-H(3C)	109.5
H(3A)-C(3)-H(3C)	109.5
H(3B)-C(3)-H(3C)	109.5
O(2)-C(4)-O(1)	117.3(3)
O(2)-C(4)-C(5)	125.6(3)
O(1)-C(4)-C(5)	117.0(3)
C(7)-C(5)-C(4)	118.8(3)
C(7)-C(5)-C(6)	124.1(3)
C(4)-C(5)-C(6)	116.7(3)
C(5)-C(6)-H(6A)	109.5
C(5)-C(6)-H(6B)	109.5
H(6A)-C(6)-H(6B)	109.5
C(5)-C(6)-H(6C)	109.5
H(6A)-C(6)-H(6C)	109.5
H(6B)-C(6)-H(6C)	109.5
C(5)-C(7)-O(3)	121.3(3)
C(5)-C(7)-C(8)	126.7(3)
O(3)-C(7)-C(8)	111.9(2)
C(7)-C(8)-C(10)	110.8(2)
C(7)-C(8)-C(9)	110.4(2)
C(10)-C(8)-C(9)	111.8(2)
C(7)-C(8)-H(8)	107.9

Table 1.9 (continued) Bond lengths [ $\text{\AA}$ ] and angles [ $^\circ$ ] for qedmondson03\_ucsf.

---

C(10)-C(8)-H(8)	107.9
C(9)-C(8)-H(8)	107.9
C(8)-C(9)-H(9A)	109.5
C(8)-C(9)-H(9B)	109.5
H(9A)-C(9)-H(9B)	109.5
C(8)-C(9)-H(9C)	109.5
H(9A)-C(9)-H(9C)	109.5
H(9B)-C(9)-H(9C)	109.5
O(4)-C(10)-C(8)	108.0(2)
O(4)-C(10)-C(14)	109.4(2)
C(8)-C(10)-C(14)	113.0(2)
O(4)-C(10)-H(10)	108.8
C(8)-C(10)-H(10)	108.8
C(14)-C(10)-H(10)	108.8
Si(1)-C(11)-H(11A)	109.5
Si(1)-C(11)-H(11B)	109.5
H(11A)-C(11)-H(11B)	109.5
Si(1)-C(11)-H(11C)	109.5
H(11A)-C(11)-H(11C)	109.5
H(11B)-C(11)-H(11C)	109.5
Si(1)-C(12)-H(12A)	109.5
Si(1)-C(12)-H(12B)	109.5
H(12A)-C(12)-H(12B)	109.5
Si(1)-C(12)-H(12C)	109.5
H(12A)-C(12)-H(12C)	109.5
H(12B)-C(12)-H(12C)	109.5
Si(1)-C(13)-H(13A)	109.5
Si(1)-C(13)-H(13B)	109.5
H(13A)-C(13)-H(13B)	109.5
Si(1)-C(13)-H(13C)	109.5
H(13A)-C(13)-H(13C)	109.5
H(13B)-C(13)-H(13C)	109.5
C(15)-C(14)-C(16)	111.0(2)
C(15)-C(14)-C(10)	111.3(2)

Table 1.9 (continued) Bond lengths [ $\text{\AA}$ ] and angles [ $^\circ$ ] for qedmondson03\_ucsf.

C(16)-C(14)-C(10)	110.1(2)
C(15)-C(14)-H(14)	108.1
C(16)-C(14)-H(14)	108.1
C(10)-C(14)-H(14)	108.1
C(14)-C(15)-H(15A)	109.5
C(14)-C(15)-H(15B)	109.5
H(15A)-C(15)-H(15B)	109.5
C(14)-C(15)-H(15C)	109.5
H(15A)-C(15)-H(15C)	109.5
H(15B)-C(15)-H(15C)	109.5
C(17)-C(16)-C(14)	116.9(2)
C(17)-C(16)-H(16A)	108.1
C(14)-C(16)-H(16A)	108.1
C(17)-C(16)-H(16B)	108.1
C(14)-C(16)-H(16B)	108.1
H(16A)-C(16)-H(16B)	107.3
C(18)-C(17)-C(16)	127.1(3)
C(18)-C(17)-Br(1)	118.5(3)
C(16)-C(17)-Br(1)	114.3(3)
C(17)-C(18)-H(18A)	120.0
C(17)-C(18)-H(18B)	120.0
H(18A)-C(18)-H(18B)	120.0

Symmetry transformations used to generate equivalent atoms:

Table 1.10 Anisotropic displacement parameters ( $\text{\AA}^2 \times 10^3$ ) for qedmondson03\_ucsf. The anisotropic displacement factor exponent takes the form:  $-2\pi^2 [ h^2 a^{*2} U^{11} + \dots + 2 h k a^* b^* U^{12} ]$

	$U^{11}$	$U^{22}$	$U^{33}$	$U^{23}$	$U^{13}$	$U^{12}$
Br(1)	69(1)	70(1)	49(1)	-5(1)	17(1)	9(1)
Si(1)	41(1)	33(1)	33(1)	-1(1)	-1(1)	2(1)
O(1)	31(1)	46(1)	45(1)	2(1)	6(1)	2(1)
O(2)	28(1)	58(1)	70(2)	5(1)	1(1)	0(1)

Table 1.10 (continued) Anisotropic displacement parameters ( $\text{\AA}^2 \times 10^3$ ) for qedmondson03\_ucsf. The anisotropic displacement factor exponent takes the form:  $-2\pi^2 [ h^2 a^{*2} U^{11} + \dots + 2 h k a^* b^* U^{12} ]$

	U <sup>11</sup>	U <sup>22</sup>	U <sup>33</sup>	U <sup>23</sup>	U <sup>13</sup>	U <sup>12</sup>
O(3)	27(1)	42(1)	42(1)	2(1)	-1(1)	-5(1)
O(4)	28(1)	32(1)	33(1)	0(1)	-1(1)	2(1)
C(1)	27(1)	41(1)	44(2)	3(1)	4(1)	-2(1)
C(2)	43(2)	37(2)	61(2)	1(1)	6(1)	-1(1)
C(3)	45(2)	68(2)	47(2)	9(2)	-3(1)	-3(2)
C(4)	30(1)	36(1)	52(2)	0(1)	-1(1)	-2(1)
C(5)	33(1)	35(1)	43(2)	-1(1)	-2(1)	-6(1)
C(6)	44(2)	49(2)	56(2)	11(1)	-10(2)	-8(2)
C(7)	34(1)	30(1)	38(1)	-5(1)	0(1)	-5(1)
C(8)	33(1)	35(1)	40(1)	-5(1)	4(1)	-5(1)
C(9)	49(2)	38(2)	73(2)	-13(2)	22(2)	-4(1)
C(10)	25(1)	31(1)	37(1)	0(1)	-1(1)	0(1)
C(11)	77(3)	44(2)	66(2)	-17(2)	11(2)	-8(2)
C(12)	116(4)	56(2)	39(2)	-4(2)	-12(2)	19(2)
C(13)	47(2)	84(3)	53(2)	-8(2)	14(2)	7(2)
C(14)	24(1)	38(1)	41(1)	2(1)	-1(1)	-1(1)
C(15)	30(1)	45(2)	49(2)	1(1)	-2(1)	-8(1)
C(16)	28(1)	71(2)	43(2)	13(1)	-2(1)	-5(1)
C(17)	31(1)	60(2)	40(2)	7(1)	1(1)	-1(1)
C(18)	46(2)	72(2)	64(2)	24(2)	14(2)	10(2)

Table 1.11 Hydrogen coordinates ( $\times 10^4$ ) and isotropic displacement parameters ( $\text{\AA}^2 \times 10^3$ ) for qedmondson03\_ucsf.

	x	y	z	U(eq)
H(2A)	3656	6016	6505	70
H(2B)	5341	6164	6164	70
H(2C)	5079	5641	7010	70
H(3A)	3979	4407	4856	80
H(3B)	4767	5374	4825	80
H(3C)	3041	5280	5119	80

Table 1.11 (continued) Hydrogen coordinates ( $\times 10^4$ ) and isotropic displacement parameters ( $\text{\AA}^2 \times 10^3$ ) for qedmondson03\_ucsf.

	x	y	z	U(eq)
H(6A)	5616	3547	8505	75
H(6B)	7203	3403	8045	75
H(6C)	5892	2665	7964	75
H(8)	3131	3388	8171	43
H(9A)	1016	4498	7304	80
H(9B)	2210	4914	7939	80
H(9C)	944	4226	8254	80
H(10)	1416	2986	6710	37
H(11A)	2789	170	6718	94
H(11B)	3068	112	5748	94
H(11C)	1506	509	6095	94
H(12A)	1706	2327	5325	106
H(12B)	3112	1953	4805	106
H(12C)	3286	2858	5325	106
H(13A)	6022	2073	6201	92
H(13B)	5868	1131	5737	92
H(13C)	5851	1167	6720	92
H(14)	-31	2905	7986	41
H(15A)	-770	2039	6833	62
H(15B)	-1217	1555	7676	62
H(15C)	231	1221	7167	62
H(16A)	2031	1478	8358	57
H(16B)	1940	2406	8843	57
H(18A)	901	280	9152	73
H(18B)	-525	511	9770	73

Table 1.12 Torsion angles [ $^\circ$ ] for qedmondson03\_ucsf.

C(12)-Si(1)-O(4)-C(10)	19.0(3)
C(11)-Si(1)-O(4)-C(10)	-103.8(3)
C(13)-Si(1)-O(4)-C(10)	140.6(2)



Table 1.12 (continued). Torsion angles [°] for qedmondson03\_ucs.f.

---

C(7)-O(3)-C(1)-O(1)	46.5(3)
C(7)-O(3)-C(1)-C(2)	-75.1(3)
C(7)-O(3)-C(1)-C(3)	161.7(3)
C(4)-O(1)-C(1)-O(3)	-45.8(3)
C(4)-O(1)-C(1)-C(2)	75.8(3)
C(4)-O(1)-C(1)-C(3)	-161.6(3)
C(1)-O(1)-C(4)-O(2)	-163.1(3)
C(1)-O(1)-C(4)-C(5)	20.9(4)
O(2)-C(4)-C(5)-C(7)	-170.3(3)
O(1)-C(4)-C(5)-C(7)	5.4(4)
O(2)-C(4)-C(5)-C(6)	2.6(5)
O(1)-C(4)-C(5)-C(6)	178.3(3)
C(4)-C(5)-C(7)-O(3)	-4.1(4)
C(6)-C(5)-C(7)-O(3)	-176.5(3)
C(4)-C(5)-C(7)-C(8)	174.9(3)
C(6)-C(5)-C(7)-C(8)	2.5(5)
C(1)-O(3)-C(7)-C(5)	-23.1(4)
C(1)-O(3)-C(7)-C(8)	157.7(2)
C(5)-C(7)-C(8)-C(10)	-108.9(3)
O(3)-C(7)-C(8)-C(10)	70.2(3)
C(5)-C(7)-C(8)-C(9)	126.8(3)
O(3)-C(7)-C(8)-C(9)	-54.1(3)
Si(1)-O(4)-C(10)-C(8)	-122.5(2)
Si(1)-O(4)-C(10)-C(14)	114.1(2)
C(7)-C(8)-C(10)-O(4)	53.7(3)
C(9)-C(8)-C(10)-O(4)	177.2(2)
C(7)-C(8)-C(10)-C(14)	174.8(2)
C(9)-C(8)-C(10)-C(14)	-61.6(3)
O(4)-C(10)-C(14)-C(15)	-71.4(3)
C(8)-C(10)-C(14)-C(15)	168.3(2)
O(4)-C(10)-C(14)-C(16)	52.1(3)
C(8)-C(10)-C(14)-C(16)	-68.2(3)
C(15)-C(14)-C(16)-C(17)	-56.4(4)
C(10)-C(14)-C(16)-C(17)	179.9(3)

Table 1.12 (continued). Torsion angles [°] for qedmondson03\_ucs.

---

C(14)-C(16)-C(17)-C(18)	120.1(4)
C(14)-C(16)-C(17)-Br(1)	-61.1(4)

---

Symmetry transformations used to generate equivalent atoms:

## 1.5 References

1. Dinos, G. P. The macrolide antibiotic renaissance. *Br. J. Pharmacol.* **174**, 2967–2983 (2017).
2. Kannan, K. *et al.* The general mode of translation inhibition by macrolide antibiotics. *Proc. Natl. Acad. Sci.* **111**, 15958–15963 (2014).
3. Katz, L. & Ashley, G. W. Translation and Protein Synthesis: Macrolides. *Chem. Rev.* **105**, 499–528 (2005).
4. Wilson, D. N. Ribosome-targeting antibiotics and mechanisms of bacterial resistance. *Nat. Rev. Microbiol.* **12**, 35–48 (2014).
5. Corbaz, R. *et al.* Stoffwechselprodukte von Actinomyceten. 1. Mitteilung. Narbomycin. *Helv. Chim. Acta* **38**, 935–942 (1955).
6. Brockmann, H. & Henkel, W. Pikromycin, ein neues Antibiotikum aus Actinomyceten. *Naturwissenschaften* **37**, 138–139 (1950).
7. Putnam, S. D., Castanheira, M., Moet, G. J., Farrell, D. J. & Jones, R. N. CEM-101, a novel fluoroketolide: antimicrobial activity against a diverse collection of Gram-positive and Gram-negative bacteria. *Diagn. Microbiol. Infect. Dis.* **66**, 393–401 (2010).
8. Almutairi, M. M. *et al.* Co-produced natural ketolides methymycin and pikromycin inhibit bacterial growth by preventing synthesis of a limited number of proteins. *Nucleic Acids Res.* **45**, 9573–9582 (2017).
9. Vázquez-Laslop, N. *et al.* Role of antibiotic ligand in nascent peptide-dependent ribosome stalling. *Proc. Natl. Acad. Sci.* **108**, 10496–10501 (2011).
10. Oh, H.-S. & Kang, H.-Y. Total Synthesis of Pikromycin. *J. Org. Chem.* **77**, 1125–1130 (2012).
11. Seiple, I. B. *et al.* A platform for the discovery of new macrolide antibiotics. *Nature* **533**, 338–345 (2016).

12. Boeckman, R. K. Jr. & Pruitt, J. R. A new, highly efficient, selective methodology for formation of medium-ring and macrocyclic lactones via intramolecular ketene trapping: an application to a convergent synthesis of (-)-kromycin. *J. Am. Chem. Soc.* **111**, 8286–8288 (1989).
13. Boeckman, R. K. Jr. & Perni, R. B. Studies directed toward the synthesis of naturally occurring acyltetramic acids. 2. Preparation of the macrocyclic subunit of ikarugamycin. *J. Org. Chem.* **51**, 5486–5489 (1986).
14. Zhang, Z., Kitamura, Y. & Myers, A. G. An Efficient Directed Claisen Reaction Allows for Rapid Construction of 5,6-Disubstituted 1,3-Dioxin-4-ones. *Synthesis* **47**, 2709–2712 (2015).
15. Simsek, S. & Kalesse, M. Enantioselective synthesis of polyketide segments through vinylogous Mukaiyama aldol reactions. *Tetrahedron Lett.* **50**, 3485–3488 (2009).
16. Boeckman, Robert K., Pero, J. E. & Boehmler, D. J. Toward the Development of a General Chiral Auxiliary. Enantioselective Alkylation and a New Catalytic Asymmetric Addition of Silyloxyfurans: Application to a Total Synthesis of (-)-Rasfonin. *J. Am. Chem. Soc.* **128**, 11032–11033 (2006).
17. Chérest, M., Felkin, H. & Prudent, N. Torsional strain involving partial bonds. The stereochemistry of the lithium aluminium hydride reduction of some simple open-chain ketones. *Tetrahedron Lett.* **9**, 2199–2204 (1968).
18. Nguyen Trong Anh, ., Eisenstein, O., Lefour, J. M. & Tran Huu Dau, M. E. Orbital factors and asymmetric induction. *J. Am. Chem. Soc.* **95**, 6146–6147 (1973).
19. Kalesse, M., Cordes, M., Symkenberg, G. & Lu, H.-H. The vinylogous Mukaiyama aldol reaction (VMAR) in natural product synthesis. *Nat. Prod. Rep.* **31**, 563–594 (2014).

20. Curti, C., Battistini, L., Sartori, A. & Zanardi, F. New Developments of the Principle of Vinylogy as Applied to  $\pi$ -Extended Enolate-Type Donor Systems. *Chem. Rev.* **120**, 2448–2612 (2020).
21. Shirokawa, S. *et al.* Remote Asymmetric Induction with Vinylketene Silyl N,O-Acetal. *J. Am. Chem. Soc.* **126**, 13604–13605 (2004).
22. May, A. E. & Hoye, T. R. Room Temperature Acylketene Formation? 1,3-Dioxin-4-ones via Silver(I) Activation of Phenylthioacetate in the Presence of Ketones. *J. Org. Chem.* **75**, 6054–6056 (2010).

## **Chapter 2. Total synthesis of narbomycin using an unprecedented macrocyclization**

## 2.1 Revised synthetic route to narbomycin: the right and left halves

From the outset, we envisioned narbomycin and other minimal macrolide analogues that could be assembled from commercially available or easily synthesized building blocks. These building blocks could then be stitched together in a modular and convergent manner. Any intended synthetic derivitizations of narbomycin could be incorporated in the respective building block and the chemistry used to assemble the macrolide analogue could remain relatively unchanged. Our efforts began with the synthesis of the right half of the molecule, that is, C1 to C8 (Figure 2.1).

Now that the synthetic strategy to employ a vinylogous dioxinone Mukaiyama aldol to set the

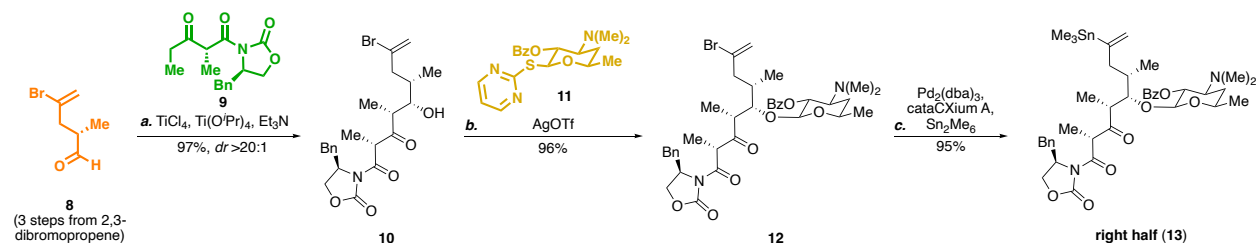


**Figure 2.1.** Synthesis of the right half. Reagents and conditions: (a) **9**,  $\text{TiCl}_4$ ,  $\text{Ti}(\text{O}^i\text{Pr})_4$ ,  $\text{CH}_2\text{Cl}_2$ ,  $-78^\circ\text{C}$ , 4 h, 97 %; (b) **11**,  $\text{AgOTf}$ ,  $\text{CH}_2\text{Cl}_2/\text{PhMe}$  (2:1),  $0^\circ\text{C}$ , 2 h, 96%; (c)  $\text{Pd}_2(\text{dba})_3$  (5 mol %), *cataCXium A* (30 mol %),  $\text{Sn}_2\text{Me}_6$ ,  $\text{PhMe}$ ,  $50^\circ\text{C}$ , 16 h, 95%.

C4/C5 stereocenters, and thus the acyl ketene method of cyclization, seemed to be out of reach, we reevaluated our initial approach. Evans' work in the total synthesis of C6-deoxy macrolide aglycons, like oleandolide, demonstrated that the C4/C5 configuration could be set through a  $\beta$ -keto-imide aldol.<sup>1,2</sup> Following a similar strategy, our synthesis of the right half of narbomycin commenced with an aldol to join building blocks **8**<sup>3</sup> and **9**. Aldehyde **8** was synthesized from commercially available 2,3-dibromopropene in three steps (68% yield), establishing the C6 stereocenter. **10** could then be synthesized by joining the freshly made aldehyde **8** and  $\beta$ -keto-imide **9** in 97% yield and high diastereoselectivity. The aldol product **10** was then glycosidated using the desosamine glycosyl donor **11**<sup>4,5</sup>, using an excess of silver triflate to yield the  $\beta$ -glycoside

**12** in 96% yield. **12** could then be converted to the vinyl stannane **13** in a palladium-catalyzed manner. It is important to note that the bulky di(adamantly)-alkyl phosphine ligand (cataCXium A) was crucial to the success of this reaction. We rationalize the necessity of the bulky ligand to occlude the multiple coordinating functionalities on **12** (i.e., the tertiary amine and the three carbonyls) from the palladium center. With the fully furnished right half **13** in hand, we next focused our attention on the left half of narbomycin (C9 to C13).

As seen in Figure 2.2, the synthesis of the left half of the molecule commenced with an

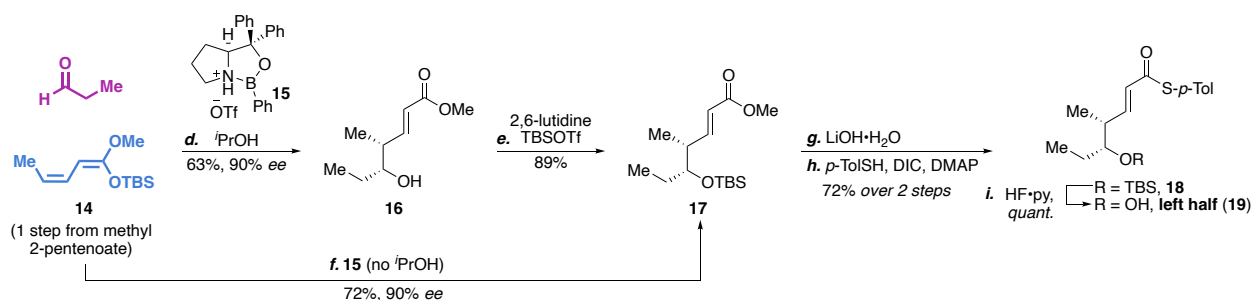


**Figure 2.2.** Synthesis of the left half. Reagents and conditions: (d) **15** (50 mol %), *i*PrOH, CH<sub>2</sub>Cl<sub>2</sub>, -78 °C, 2 h, 63%; (e) 2,6-lutidine, TBSOTf, CH<sub>2</sub>Cl<sub>2</sub>, 0 °C, 90 min, 89%; (f) **15** (50 mol %), CH<sub>2</sub>Cl<sub>2</sub>, -78 °C, 18 h, 72%; (g) LiOH·H<sub>2</sub>O, THF/MeOH/H<sub>2</sub>O (1:1:1), 0 °C to 20 °C, 18 h, *quantitative*; (h) *p*-TolSH, DIC, DMAP, 0 °C, 2 h, 72%; (i) HF·py, THF, 0 °C, 4 h, *quantitative*.

enantioselective vinylogous Mukaiyama aldol between the silyl ketene acetal **14** and propionaldehyde using the prolyl-type oxazaborolidine catalyst with a Brønsted acid co-catalyst<sup>6</sup> to yield aldol product **16** in good yield and high enantiomeric excess. The secondary alcohol was then TBS-protected to form the silyl ether **17**. It was observed that a small amount of silyl-transfer side product (i.e., **17**) was formed in the aldol reaction. This is usually circumvented by inclusion of a sacrificial alcohol, like *i*PrOH, but since we desired the protected alcohol, omitting *i*PrOH from the otherwise identical aldol conditions yielded **17** directly, bypassing the separate protection step, in 72% yield without any decline in enantioselectivity. The thioester **18** was synthesized by saponification and thioesterification in 72% yield over two steps. Careful control of the



temperature of the thioester formation reaction was critical to the outcome of the reaction: Even with substoichiometric amounts of thiol, at temperature above 0 °C, conjugate addition into newly formed thioester were observed as a side product. The final left half **19** was produced upon the removal of the TBS group with HF•pyridine in quantitative yield.

## 2.2 Coupling the halves and macrocyclization

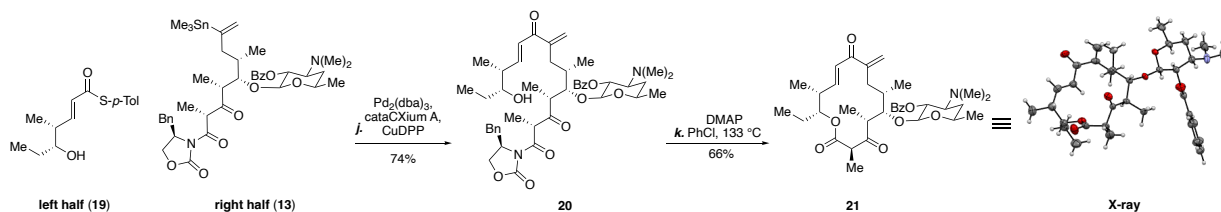


**Figure 2.3**, Coupling of the halves and macrocyclization. Reagents and conditions: (j)  $\text{Pd}_2(\text{dba})_3$  (5 mol %), *cataCXium A* (30 mol %),  $\text{CuDPP}$  (1.30 equiv), **19** (1.50 equiv), THF (degassed), 20 °C, 4 h, 74%; (k) DMAP (0.10 equiv),  $\text{PhCl}$  (~1 mM), 133 °C, 15 h, 66%.

The left and right halves were successfully coupled with an acylative palladium/copper-catalyzed cross coupling reaction, sometimes known as a Liebeskind-Srogl coupling,<sup>7</sup> to yield the linear macrocyclization precursor **20** in 74% yield (Figure 2.3). While screening conditions, there were a few observations that proved vital to the success of the cross coupling. First, the copper(I) source had to be the diphenylphosphinate salt, which is common when using stannane nucleophiles for this reaction, as opposed to the traditionally used thiophene carbonylate salt. Second, as with the stannylation, while some bulky phosphine ligands could be used to generate **20** successfully, *cataCXium A* proved to produce the highest yield. Third, the loading of  $\text{CuDPP}$  and thioester **19** relative to the vinyl stannane **13** were important in avoiding proto-destannylation side product, a common pitfall of this reaction thought to be caused by a transmetallation side reaction between the copper and the tin.<sup>8,9</sup> This coupling was also successful between **13** and TBS-protected thioester **18**, yielding the TBS-protected linear molecule in 92% yield. The silyl group could then be removed with HF•pyridine in 85% yield, which generates **20** in approximately the same yield

(over 2 steps) as the aforementioned coupling (1 step). It is also worth noting that the catalyst and ligand combination used in this transformation is the same as it was in the stannylation reaction and telescoping the two reactions (i.e., **12** and **19** to **20**) gave product, albeit in much lower yield (ca. 13%). Additionally whether **20** was synthesized directly from the cross coupling or in the two-step coupling/protecting group removal fashion, the linear macrocyclization precursor was seen by  $^1\text{H}$  NMR as a 5:1 mixture of diastereomers. Although the  $\alpha$ -proton of  $\beta$ -keto-imides is thought to be not very acidic<sup>10</sup> ( $\text{pK}_a \sim 18^{11}$ ), we hypothesized that the other product was a C2 epimer of **20**. We were not concerned with the scrambling of this stereocenter, because we anticipated that upon cyclization the C2 methyl group would equilibrate to its natural configuration, avoiding *syn*-pentane interactions, as documented for other macrolides.<sup>12,13</sup>

With the linear molecule in hand, we turned our attention to macrocyclization strategies. Unlike dioxinones, which are known to thermolyze at 90-130 °C to generate acylketenes which can be captured by nucleophiles, of Evans-style imides and  $\beta$ -ketoimides have only been shown to thermalize forcing thermal conditions (>133 °C) or with assistance from Lewis acids<sup>14</sup>, and are always captured with an excess of nucleophile (usually as solvent). Direct intramolecular displacement of the auxiliary has not been documented to our knowledge. Despite this lack of precedent, we decided to subject the substrate to attempt macrocyclization using the same thermal conditions used in the dioxinone acyl ketene cyclization. If successful, this strategy would avoid risky, multistep options that would likely proceed through highly unstable  $\beta$ -ketoacids. To our delight, after 16 h in refluxing PhCl we were able to isolate the macrocycle **21** in 33% yield as a single diastereomer, recovering 66% of remaining starting material. Unfortunately, the yield could not be improved by increasing the temperature, increasing the length of the reaction time, addition of Lewis acid, nor through microwave irradiation. However, upon addition of a catalytic amount of

DMAP, the reaction yield could be brought to 66% in a single pass. The macrocycle **21** was crystallized and its structure was determined by X-ray crystallography (Figure 2.3), which confirmed the correct stereochemical configuration of all stereocenters in the molecule thus far.

### 2.3 Optimization of the C8 reduction and the total synthesis of narbomycin

The final steps in this synthesis of narbomycin were 1) chemo-, regio-, and stereoselective reduction of the C8 methylene, and 2) removal of the benzoyl group on the desosamine C2'-OH.

The first transformation was notably difficult to achieve in any capacity due to the nature of intermediate **21**. The macrocycle has two  $\alpha$ ,  $\beta$ -unsaturated systems that share a common carbonyl, both of which adopt an *s-cis* conformation in the crystal structure, although this may not accurately reflect the configuration in solution (Figure 2.3). Because of the stereoelectronic similarity between the two electrophilic  $\beta$  positions, we anticipated four possible products (Figure 2.4).

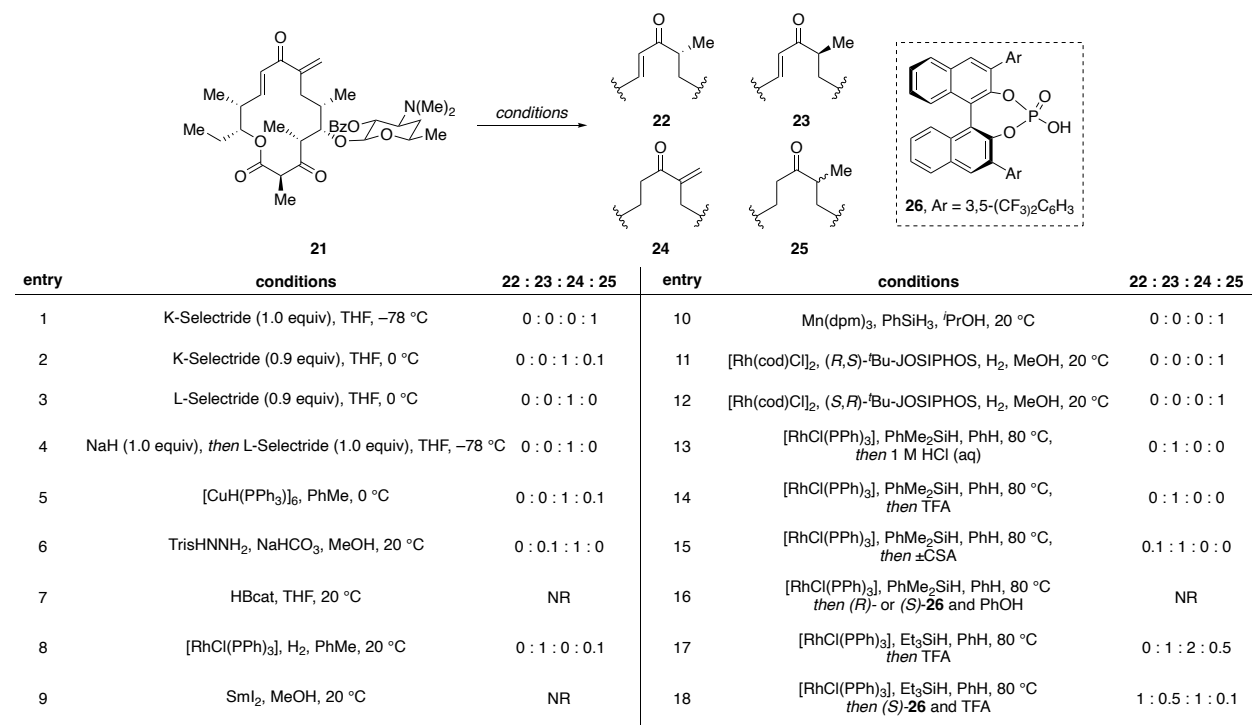


**Figure 2.4**, Representative list of attempted conditions for the selective reduction of C8 olefin. Note: this is not an exhaustive list of attempted conditions.

The desired product, **22**, would require selective conjugate reduction of the C8 olefin such that the resultant enolate, if the reaction proceeded through such an intermediate, would then collapse and be protonated stereoselectively from the beta face. Product **23** would arise from protonation from the undesired alpha face. Conjugate addition occurring with undesired regiochemistry (i.e., C10/C11 reduction) would yield **24**. Lastly, if the conjugate reduction were to proceed twice, then the over-reduced product **25** would arise. Though the product is not depicted in Figure 2.4, 1,2-reduction to deliver a doubly allylic alcohol is also a possible undesired product under certain conditions.

Our initial attempts at this transformation were using bulky hydrides, including several Selectrides and Stryker's reagent (entries 1–5), anticipating that a bulky hydride source would be selective for the 1,1-substituted alkene over the 1,2-substituted alkene. This approach resulted in predominantly over-reduced product **25**, despite variations in temperature and loading of the reducing agent. We had several hypotheses as to why this might happen, one of which was that the enolate intermediate was being quenched intermolecularly by the C2 proton on another molecule of **21**, priming the singly reduced product for another reduction. To test this, we first introduced a single equivalent of NaH to deprotonate C2, thus 'protecting' this proton as a sodium enolate. However, incorrect regiochemical reduction product **24** predominated, as well as some 1,2-reduction (not pictured). Similar results were observed with aluminum and copper hydride reducing agents (not shown).

We next turned our attention to alternative methods like diimide reductions (entry 6), conjugate hydroborations (entry 7), and radical MHAT reductions (entries 9 and 10). Unfortunately, these failed to yield any of the desired product. More conventional hydrogenation conditions using Pd/C and Pt/C led to overreduction, but hydrogenation with Wilkinson's catalyst (entry 8) was selective for reduction product **23** with minimal over-reduction. Performing a rhodium catalyzed

hydrogenation with chiral phosphine ligands resulted in over-reduction. Inspired by Danishefsky's synthesis of guanacastepene A<sup>15</sup>, we tried a rhodium-catalyzed conjugate hydrosilylation approach<sup>16–18</sup> using Wilkinson's catalyst and the tertiary silane PhMe<sub>2</sub>SiH. To our surprise, this produced a highly regioselective hydrosilylation to provide stable silyl enol ether. Numerous attempts to collapse this intermediate with a variety of acids, both achiral and chiral, and fluoride

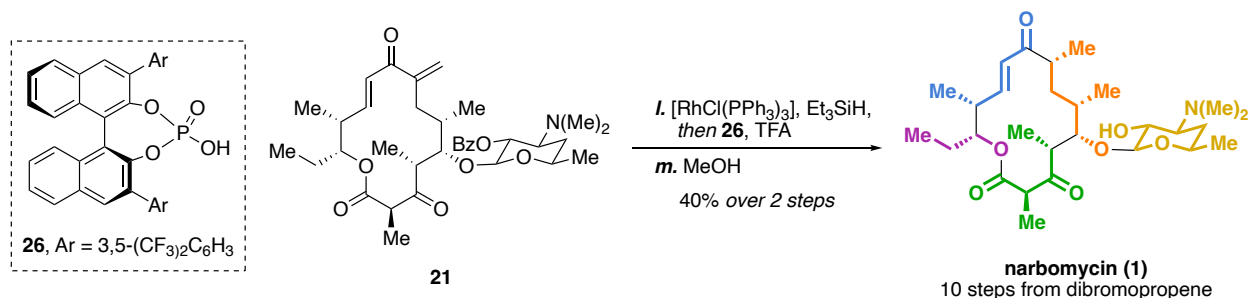


**Figure 2.5**, Completion of the total synthesis of narbomycin. Reagents and conditions: (l) [RhCl(PPh<sub>3</sub>)<sub>3</sub>] (10 mol %), Et<sub>3</sub>SiH (1.50 equiv), PhH, 80 °C, 20 min, then **26** (10 mol %), TFA (20 equiv), PhH, 0 °C, 30 min; (m) MeOH, 40 °C, 16 h, 40% over two steps.

sources failed to produce any appreciable amount of **22**. Instead, protonation from the undesired face of the silyl enol ether predominated, yielding **23** almost exclusively (entries 13-16). When swapping the silane used for the transformation with the less bulky Et<sub>3</sub>SiH, the required reaction time was longer and the regioselectivity of the reduction was considerably lower; however, when the corresponding silyl enol ether was slowly quenched with a mixture of the chiral Brønsted acid **26** and TFA in benzene (entry 18), a mixture of products, including a significant amount of the desired product **22** was observed. The products were difficult to separate chromatographically, so the crude of this reaction was taken forward to the final benzoyl deprotection step in warm MeOH and narbomycin (**1**) was isolated in 40% yield over two steps (Figure 2.5). The <sup>1</sup>H and <sup>13</sup>C NMR of synthetic **1** matched reported literature spectra as well as that of an authentic sample of narbomycin from fermentative isolation.

## 2.4 Conclusion and outlook

This synthetic route provides access to narbomycin in 10 steps (longest linear sequence) in a modular, convergent manner. Though the final steps would benefit from further optimization, this

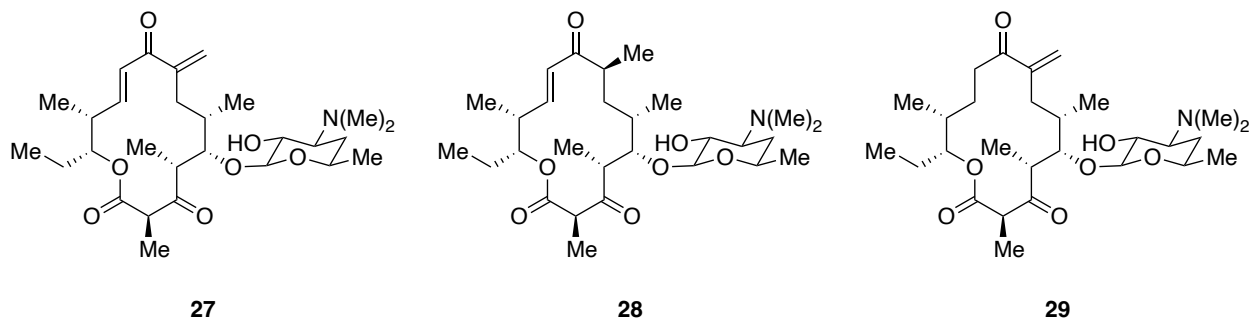


Figure 2.6, First series of analogues.

is a promising first step towards generating a library of minimal macrolides that are designed to overcome known resistance mechanisms or optimize interactions with other antibiotics that can simultaneously bind a neighboring site in the bacterial ribosome, the peptidyl transferase center.<sup>19</sup>

The next steps in this story are further confirm the identity of our synthetic narbomycin through antimicrobial tests (e.g., minimal inhibitory concentration assays), and to test the activity of our first ‘analogues’, which are essentially any products generated after the cyclization that have the C2-OBz group removed (Figure 2.6). Of particular interest are compounds that bear the exocyclic C8 olefin enone system (**27** and **29**), since this may act as an electrophile for any proximity-induced covalent interactions with rRNA residues in the NPET.<sup>20</sup>

## 2.5 General Experimental Procedures

All reactions were performed in flame- or oven-dried glassware fitted with rubber septa under a positive pressure of nitrogen or argon, unless otherwise noted. All reaction mixtures were stirred throughout the course of each procedure using Teflon-coated magnetic stir bars. Air- and moisture-sensitive liquids were transferred via syringe or stainless-steel cannula. Solutions were concentrated by rotary evaporation below 35 °C. Analytical thin-layer chromatography (TLC) was performed using glass plates pre-coated with silica gel (0.25-mm, 60-Å pore size, 230–400 mesh, SILICYCLE INC) impregnated with a fluorescent indicator (254 nm). TLC plates were visualized by exposure to ultraviolet light (UV), and then were stained by submersion in a basic aqueous solution of potassium permanganate or with an acidic ethanolic solution of anisaldehyde, followed by brief heating.

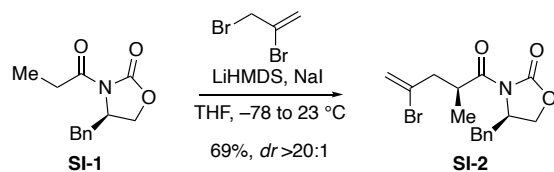
**Materials:** CH<sub>2</sub>Cl<sub>2</sub>, THF, ethyl ether, and acetonitrile to be used in anhydrous reaction mixtures were dried by passage through activated alumina columns immediately prior to use. Hexanes used were ≥85% n-hexane. Other commercial solvents and reagents were used as received, unless otherwise noted.

**Instrumentation:** Unless otherwise noted, proton nuclear magnetic resonance (<sup>1</sup>H NMR) spectra and carbon nuclear magnetic resonance (<sup>13</sup>C NMR) spectra were recorded on a 400 MHz Bruker Avance III HD 2-channel NMR spectrometer at 23 °C or a 500 MHz Bruker DRX 4-channel NMR spectrometer at 23 °C. Proton chemical shifts are expressed in parts per million (ppm, δ scale) and are referenced to residual protium in the NMR solvent (CHCl<sub>3</sub>: δ 7.26). Carbon chemical shifts are expressed in parts per million (ppm, δ scale) and are referenced to the carbon resonance of the NMR solvent (CDCl<sub>3</sub>: δ 77.0). Data are represented as follows: chemical shift, multiplicity (s = singlet, d = doublet, t = triplet, q = quartet, dd = doublet of doublets, dt = doublet of triplets, sxt =

sextet, m = multiplet, br = broad, app = apparent), integration, and coupling constant (J) in hertz (Hz). High-resolution mass spectra were obtained at the QB3/Chemistry Mass Spectrometry Facility at University of California, Berkeley using a Thermo LTQ-FT mass spectrometer.



## Vinyl bromide imide **SI-2**



*n*-Butyllithium (2.0-M in hexanes, 22.5 mL, 45.0 mmol, 1.05 equiv) was added dropwise to a 0 °C solution of bis-trimethylsilylamide (9.4 mL, 45.01 mmol, 1.05 equiv) in 50 mL THF in a 50-mL round bottom flask. The resulting mixture was stirred at 0 °C for 30 min, and was then cooled to -78 °C. A solution of **SI-1**<sup>21</sup> (10.00 g, 42.87 mmol, 1equiv) in 30 mL THF was added dropwise and the resulting light yellow solution was stirred at -78 °C for 1 h. In a separate flame-dried flask, NaI (16.06 g, 107.2 mmol, 2.50 equiv) was suspended in 20 mL THF and 2,3-dibromopropene (10.5 mL, 107.2 mmol, 2.50 equiv) was added. The flask was covered with aluminum foil to shield from incident light and the suspension was stirred vigorously. After 1 h, the iodide solution was filtered through a medium-porosity fritted funnel and the filtrate was added dropwise to the enolate mixture and the reaction was stirred at -78 °C for 30 min. The reaction was allowed to slowly come to ambient temperature (approximately 20 °C) over the course of 1 h. After 16 h, the reaction was cooled to 0 °C and 100 mL saturated aqueous NH<sub>4</sub>Cl solution was added. The phases were separated, and the aqueous phase was extracted with CH<sub>2</sub>Cl<sub>2</sub> (2 x 100 mL). The combined organic layers were washed with brine (150 mL), dried over sodium sulfate, filtered, and the filtrate was concentrated. The crude mixture was purified by flash chromatography (silica gel, eluent: 10-40% EtOAc/hexanes) to provide **SI-2** (10.35 g, 69 %) as a dark yellow oil.

**TLC** (30% EtOAc/hexanes):  $R_f = 0.53$  (UV, *p*-anisaldehyde).

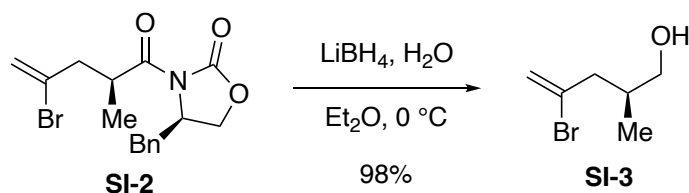
**<sup>1</sup>H NMR** (400 MHz, CDCl<sub>3</sub>)  $\delta$  7.37 – 7.17 (m, 5H), 5.68 (d,  $J = 1.3$  Hz, 1H), 5.49 (d,  $J = 1.6$  Hz, 1H), 4.68 (ddt,  $J = 9.5, 7.6, 3.3$  Hz, 1H), 4.25 – 4.12 (m, 3H), 3.27 (dd,  $J = 13.4, 3.4$  Hz, 1H), 3.00

(ddd,  $J = 14.5, 7.6, 1.1$  Hz, 1H), 2.74 (dd,  $J = 13.4, 9.5$  Hz, 1H), 2.52 (ddd,  $J = 14.5, 6.7, 1.0$  Hz, 1H), 1.21 (d,  $J = 6.9$  Hz, 3H).

$^{13}\text{C}$  NMR (100 MHz,  $\text{CDCl}_3$ )  $\delta$  175.9, 153.1, 135.3, 131.2, 129.6, 129.1, 127.5, 119.2, 66.2, 55.5, 44.7, 38.0, 36.7, 17.1.

**HRMS (ESI-TOF)**  $m/z$  calcd for  $\text{C}_{16}\text{H}_{19}\text{BrNO}_3$   $[\text{M} + \text{H}]^+$  352.0548, found 352.0542

### Alcohol **SI-3**<sup>22</sup>



$\text{LiBH}_4$  (4.0 M in THF, 6.08 mL, 24.3 mmol, 1.70 equiv) was added dropwise to a solution of **SI-2** (5.04 g, 14.4 mmol, 1.00 equiv) in 200 mL ethyl ether at 0 °C. Deionized water (0.36 mL, 20.0 mmol, 1.40 equiv) was added and the mixture was stirred at 0 °C. After 30 min, 200 mL phosphate buffer solution (pH 7) was added. The layers were separated and the aqueous layer was extracted with  $\text{CH}_2\text{Cl}_2$  (3 x 200 mL). The combined organic layers were washed with brine (200 mL), dried over sodium sulfate, filtered, and the filtrate was concentrated. The crude yellow oil was purified by flash chromatography (silica gel, eluent: 15-100% EtOAc/hexanes) to provide **SI-3** (2.50 g, 98 %) as a pale, yellow liquid.

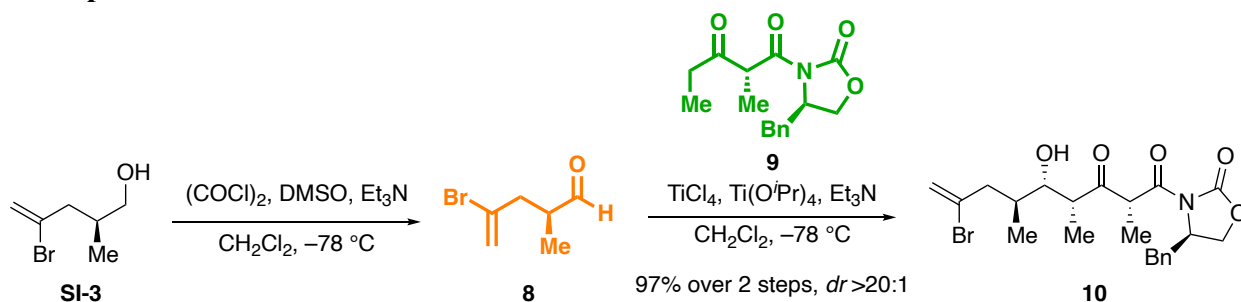
**TLC** (30% EtOAc/hexanes):  $R_f = 0.42$  (*p*-anisaldehyde).

$^1\text{H}$  NMR (400 MHz,  $\text{CDCl}_3$ )  $\delta$  5.62 (q,  $J = 1.2$  Hz, 1H), 5.48 (d,  $J = 1.5$  Hz, 1H), 3.56 (d,  $J = 5.7$  Hz, 2H), 2.61 (ddd,  $J = 14.2, 6.0, 1.2$  Hz, 1H), 2.26 (ddd,  $J = 14.2, 8.1, 0.9$  Hz, 1H), 2.15 – 2.02 (m, 1H), 0.98 (d,  $J = 6.7$  Hz, 3H).

$^{13}\text{C}$  NMR (100 MHz,  $\text{CDCl}_3$ )  $\delta$  133.1, 118.1, 67.0, 45.1, 34.1, 15.8.

**HRMS (ESI-TOF)** The compound failed to ionize under electrospray in both positive and negative modes.

### Aldol product **10**<sup>2</sup>



A solution of DMSO (2.38 mL, 33.5 mmol, 4.00 equiv) in 10 mL  $\text{CH}_2\text{Cl}_2$  was added dropwise to a solution of oxalyl dichloride (1.44 mL, 16.8 mmol, 2.00 equiv) in 20 mL  $\text{CH}_2\text{Cl}_2$  at  $-78\text{ }^\circ\text{C}$ . After 15 min, a solution of **SI-3** (1.50 g, 8.38 mmol, 1.00 equiv) in 10 mL  $\text{CH}_2\text{Cl}_2$  was added dropwise. The mixture was stirred at  $-65\text{ }^\circ\text{C}$  for 1 h before cooling back down to  $-78\text{ }^\circ\text{C}$  (warming to  $-65\text{ }^\circ\text{C}$  was found to be critical for conversion).  $\text{Et}_3\text{N}$  (6.31 mL, 45.2 mmol, 5.40 equiv) was added dropwise and the resulting pale yellow solution was stirred at  $-70\text{ }^\circ\text{C}$ , coming to  $-10\text{ }^\circ\text{C}$  over 5 h. After 5 h, the reaction mixture was partitioned between pentane (80 mL) and water (100 mL). The aqueous layer was extracted with pentanes (80 mL). The combined organic layers were washed with 1 M  $\text{NaHSO}_4$  (50 mL) and brine (50 mL), dried over sodium sulfate, filtered, and the filtrate was concentrated. The crude gold oil was used immediately in the next step without further purification.

In a flame-dried flask, 42 mL of  $\text{CH}_2\text{Cl}_2$  was cooled to  $0\text{ }^\circ\text{C}$  and a 1.0 M solution of  $\text{TiCl}_4$  (9.70 mL, 9.70 mmol, 1.16 equiv) in  $\text{CH}_2\text{Cl}_2$  was added, followed by dropwise addition of  $\text{Ti}(\text{O}i\text{Pr})_4$  (0.99 mL, 3.26 mmol, 0.39 equiv). The pale yellow mixture was stirred at  $0\text{ }^\circ\text{C}$  for 15 min, then a solution of  $\beta$ -keto-imide **9**<sup>1</sup> (3.60 g, 12.5 mmol, 1.49 equiv) in 24 mL  $\text{CH}_2\text{Cl}_2$  was added dropwise

This mixture was cooled to  $-20\text{ }^{\circ}\text{C}$ , and  $\text{Et}_3\text{N}$  (1.86 mL, 13.4 mmol, 1.60 equiv) was added dropwise. The dark red mixture was stirred at  $-20\text{ }^{\circ}\text{C}$  for 1 h before being cooled to  $-78\text{ }^{\circ}\text{C}$  and a solution of the crude aldehyde **8** (1.48 g, 8.36 mmol, 1.00 equiv) in 24 mL  $\text{CH}_2\text{Cl}_2$  was added dropwise and allowed to react at this temperature. After 12 h, 120 mL saturated aqueous  $\text{NH}_4\text{Cl}$  was added, the reaction was removed from the cold bath, and warmed to ambient temperature with stirring. The mixture was diluted with 60 mL deionized water and 120 mL  $\text{Et}_2\text{O}$ . The layers were separated, and the aqueous layer was extracted with  $\text{Et}_2\text{O}$  (2 x 60 mL). The combined organic layers were washed with saturated aqueous  $\text{NaHCO}_3$  (60 mL), brine (60 mL), dried over sodium sulfate, filtered, and the filtrate was concentrated. The crude mixture was purified by flash chromatography (silica gel, eluent: 0-25%  $\text{EtOAc}$ /hexanes) to provide the aldol product **10** (3.90 g, 97% over 2 steps) as a colorless oil.

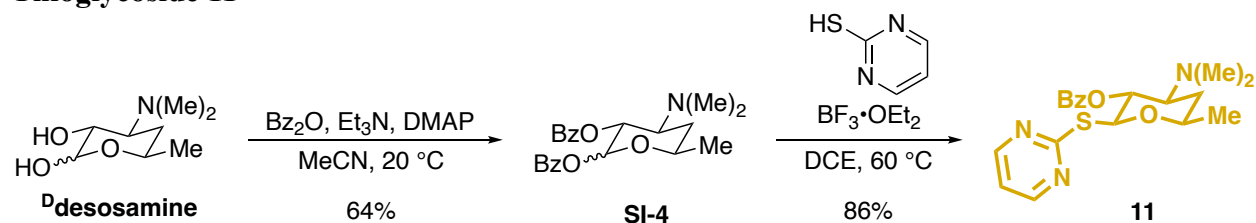
**TLC** (30%  $\text{EtOAc}$ /hexanes):  $R_f = 0.34$  (UV, *p*-anisaldehyde).

**$^1\text{H}$  NMR** (400 MHz,  $\text{CDCl}_3$ )  $\delta$  7.38 – 7.27 (m, 3H), 7.23 – 7.15 (m, 2H), 5.59 (s, 1H), 5.46 (s, 1H), 4.84 (q,  $J = 7.3$  Hz, 1H), 4.77 (ddt,  $J = 9.5, 8.0, 3.2$  Hz, 1H), 4.29 (t,  $J = 8.6$  Hz, 1H), 4.20 (dd,  $J = 9.2, 3.0$  Hz, 1H), 3.88 – 3.80 (m, 1H), 3.29 (dd,  $J = 13.3, 3.4$  Hz, 1H), 3.12 – 2.97 (m, 2H), 2.89 (d,  $J = 3.3$  Hz, 1H), 2.79 (dd,  $J = 13.4, 9.5$  Hz, 1H), 2.13 (dd,  $J = 14.3, 10.3$  Hz, 1H), 2.04 – 1.89 (m, 1H), 1.49 (d,  $J = 7.3$  Hz, 3H), 1.15 (d,  $J = 7.0$  Hz, 3H), 0.88 (d,  $J = 6.7$  Hz, 3H).

**$^{13}\text{C}$  NMR** (100 MHz,  $\text{CDCl}_3$ )  $\delta$  211.8, 170.1, 154.1, 134.9, 133.8, 129.4, 129.0, 127.5, 118.2, 74.0, 66.7, 55.3, 51.8, 46.3, 45.2, 38.0, 34.3, 14.7, 13.2, 8.4.

**HRMS (ESI-TOF)**  $m/z$  calcd for  $\text{C}_{22}\text{H}_{29}\text{BrNO}_5$   $[\text{M} + \text{H}]^+$  466.1229, found 466.1221

## Thioglycoside 11<sup>5</sup>



A round-bottom flask containing the crude desosamine•HCl (22.2 g, 105 mmol, 1.00 equiv.) cleaved from erythromycin<sup>23</sup> was charged with a stir bar, flushed with nitrogen, and suspended in 750 mL MeCN and placed in a cool water bath. Et<sub>3</sub>N (46 mL, 1.05 mol, 10 equiv) was added slowly, followed sequentially by DMAP (3.84 g, 31.5 mmol, 0.30 equiv) and benzoic anhydride (71.2 g, 315 mmol, 3.00 equiv). The reaction was allowed to stir at ambient temperature for 18 h, after which the mixture was concentrated to an orange oil with a white precipitate. This residue was suspended in ethyl acetate (300 mL) and saturated aqueous NaHCO<sub>3</sub> (500 mL) was added. The mixture was stirred vigorously for 30 minutes, until gas evolution stopped, and was then transferred to a separatory funnel. The layers were separated, and the aqueous layer was extracted with ethyl acetate (2 x 300 mL). The combined organic layers were dried over sodium sulfate, filtered, and the filtrate was concentrated. The crude mixture was purified by flash chromatography (silica gel, eluent: 0-100% EtOAc/hexanes + 0.1% Et<sub>3</sub>N) to provide a 1:2 mixture of α:β anomers of the benzoylated desosamine **SI-4** (25.7 g, 64% over 2 steps) as a yellow foam.

**TLC** (60% EtOAc/hexanes + 0.1% Et<sub>3</sub>N): R<sub>f</sub> = 0.4 (UV, *p*-anisaldehyde).

**<sup>1</sup>H NMR** (1:2 α:β anomeric mixture, minor peaks reported separately from major peaks when possible, overlapping major and minor chemical shifts are reported as seen, 400 MHz, CDCl<sub>3</sub>) δ 8.10 – 8.06 (m, minor 1H), 8.02 – 7.95 (m, 4H), 7.95 – 7.90 (m, minor 1H), 7.64 – 7.58 (m, minor 1H), 7.52 – 7.45 (m, app 3H), 7.39 – 7.32 (m, app 6H), 6.59 (d, J = 3.6 Hz, minor 1H), 5.96 (d, J = 7.9 Hz, 1H), 5.48 – 5.39 (m, app 1.5H), 4.29 – 4.17 (m, minor 1H), 3.95 – 3.83 (m, 1H), 3.44

(ddd,  $J = 12.3, 10.9, 4.1$  Hz, minor 1H), 3.08 (ddd,  $J = 12.3, 10.5, 4.3$  Hz, 1H), 2.37 (s, minor 6H), 2.35 (s, 6H), 2.02 – 1.94 (m, minor 1H), 1.90 (ddd,  $J = 13.3, 4.4, 2.0$  Hz, 1H), 1.67 – 1.50 (m, app 1.5H), 1.34 (d,  $J = 6.1$  Hz, 3H), 1.27 (d,  $J = 6.2$  Hz, minor 3H).

$^{13}\text{C}$  NMR (1:2  $\alpha$ : $\beta$  anomeric mixture, peaks are reported collectively, 100 MHz,  $\text{CDCl}_3$ )  $\delta$  165.7, 165.6, 165.2, 164.9, 133.4, 133.3, 133.0, 132.9, 130.1, 130.0, 129.8, 129.7, 129.1, 128.6, 128.4, 128.3, 94.4, 91.6, 70.7, 70.3, 69.6, 67.6, 63.3, 58.6, 40.9, 40.8, 32.9, 31.7, 21.2, 21.1.

**HRMS (ESI-TOF)**  $m/z$  calcd for  $\text{C}_{22}\text{H}_{26}\text{NO}_5$   $[\text{M} + \text{H}]^+$  384.1810, found 384.1807

A round-bottom flask with a stir bar and Celite (13 g) were carefully flame-dried under vacuum. After cooling to room temperature, the flask was placed under an argon atmosphere and a solution of **SI-4** (13.2 g, 34.4 mmol, 1.00 equiv) in 150 mL 1,2-dichloroethane was transferred to the flask. Pyrimidine-2-thiol (5.79 g, 51.6 mmol, 1.10 equiv) was then added as a solid in a single portion.  $\text{BF}_3 \cdot \text{OEt}_2$  (12.7 mL, 103 mmol, 3.00 equiv) was then added dropwise to the yellow suspension and the reaction mixture was then heated to 60 °C for 17 h. The reaction was cooled to ambient temperature and saturated aqueous  $\text{NaHCO}_3$  (150 mL) was added to the mixture and stirred for 30 min. The mixture was then filtered through a pad of Celite, and the pad was rinsed with  $\text{CH}_2\text{Cl}_2$  (150 mL). The filtrate was then extracted with  $\text{CH}_2\text{Cl}_2$  (3 x 200 mL), and the combined organic layers were dried over sodium sulfate, filtered, and the filtrate was concentrated to a dark yellow oil. The crude mixture was purified by flash chromatography (silica gel, eluent: 0-100% EtOAc/hexanes + 0.1%  $\text{Et}_3\text{N}$ ) to provide the thioglycoside **11** (1.09 g, 86%) as a dark yellow foam.

**TLC** (100% EtOAc + 0.1%  $\text{Et}_3\text{N}$ ):  $R_f = 0.31$  (UV, *p*-anisaldehyde).

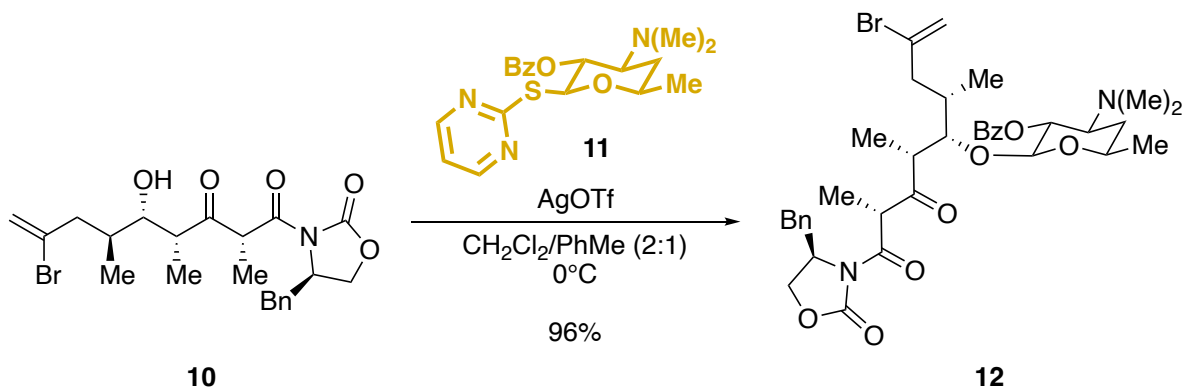
$^1\text{H}$  NMR (400 MHz,  $\text{CDCl}_3$ )  $\delta$  8.44 (d,  $J = 4.8$  Hz, 2H), 7.99 – 7.92 (m, 2H), 7.50 – 7.42 (m, 1H), 7.37 – 7.29 (m, 2H), 6.91 (t,  $J = 4.8$  Hz, 1H), 5.82 (d,  $J = 10.1$  Hz, 1H), 5.32 (t,  $J = 10.0$  Hz, 1H),

3.89 – 3.76 (m, 1H), 3.07 (ddd,  $J = 12.3, 9.9, 4.3$  Hz, 1H), 2.31 (s, 6H), 1.90 (ddd,  $J = 13.2, 4.4, 2.0$  Hz, 1H), 1.63 – 1.49 (m, 1H), 1.29 (d,  $J = 6.1$  Hz, 3H).

$^{13}\text{C}$  NMR (100 MHz,  $\text{CDCl}_3$ )  $\delta$  170.5, 165.6, 157.3, 132.9, 130.3, 129.9, 128.2, 117.2, 83.5, 74.0, 69.2, 65.1, 40.9, 32.3, 21.5.

HRMS (ESI-TOF)  $m/z$  calcd for  $\text{C}_{19}\text{H}_{24}\text{N}_3\text{O}_3\text{S}$   $[\text{M} + \text{H}]^+$  374.1538, found 374.1534

### Glycoside 12



A flame-dried round-bottom flask charged with a stir bar, 2 g activated  $4\text{\AA}$  molecular sieves were added and were suspended in 15 mL PhMe and 10 mL  $\text{CH}_2\text{Cl}_2$ . This mixture was then cooled to  $0^\circ\text{C}$  and covered with aluminum foil to shield from incident light before  $\text{AgOTf}$  (17.8 g, 69.5 mmol, 20.00 equiv) was added as a solid in a single and stirred vigorously. A solution of alcohol **10** (1.62 g, 3.47 mmol, 1.00 equiv; dried via azeotropic distillation from PhMe thrice before use) in 15 mL  $\text{CH}_2\text{Cl}_2$  was added, followed by a solution of thioglycoside donor **11** (3.89 g, 10.4 mmol, 3.00 equiv; dried via azeotropic distillation from PhMe thrice before use) in 20 mL  $\text{CH}_2\text{Cl}_2$  was added dropwise at  $0^\circ\text{C}$  and stirred vigorously (Note: the reaction is a heterogenous suspension that must be stirred well to avoid silver salt and crushed molecular sieve aggregates from forming. Additionally, retro-aldol side products are produced at temperatures above  $0^\circ\text{C}$ .) After 2 h, 15 mL  $\text{CH}_2\text{Cl}_2$  and 15 mL saturated aqueous  $\text{NH}_4\text{Cl}$  were added and stirred for 5 min before 50 mL saturated aqueous  $\text{NaHCO}_3$  was added and this biphasic mixture is stirred vigorously, coming to

room temperature until the evolution of gas stopped. The mixture was filtered through a pad of Celite, and the filter cake was rinsed with CH<sub>2</sub>Cl<sub>2</sub> (50 mL). The layers were separated, and the aqueous layer was extracted with CH<sub>2</sub>Cl<sub>2</sub> (50 mL). The combined organic layers were dried over sodium sulfate, filtered, and the filtrate was concentrated to a pink oil. The crude mixture was purified by flash chromatography (silica gel, eluent: 0-20% acetone/hexanes + 0.1% Et<sub>3</sub>N) to provide glycoside **12** (2.42 g, 96%) as a yellow foam.

**TLC** (35% acetone/hexanes + 0.1% Et<sub>3</sub>N): R<sub>f</sub> = 0.47 (UV, *p*-anisaldehyde).

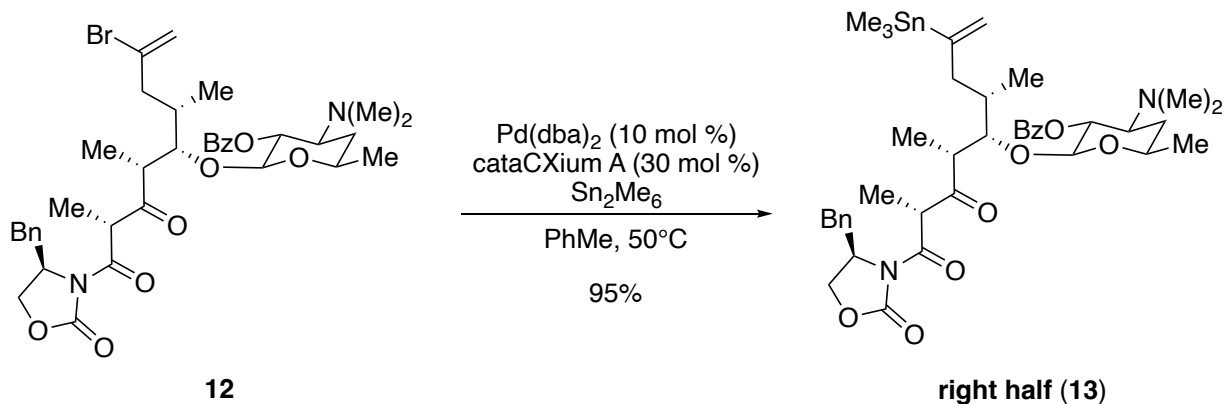
**<sup>1</sup>H NMR** (400 MHz, CDCl<sub>3</sub>) δ 8.07 – 8.03 (m, 2H), 7.60 – 7.51 (m, 1H), 7.48 – 7.39 (m, 2H), 7.39 – 7.29 (m, 3H), 7.23 – 7.16 (m, 2H), 5.62 (s, 1H), 5.42 (d, J = 1.4 Hz, 1H), 5.08 (dd, J = 10.5, 7.6 Hz, 1H), 4.80 – 4.67 (m, 2H), 4.61 (d, J = 7.6 Hz, 1H), 4.30 – 4.15 (m, 2H), 4.02 (t, J = 4.6 Hz, 1H), 3.66 – 3.56 (m, 1H), 3.28 (dd, J = 13.4, 3.3 Hz, 1H), 2.97 – 2.86 (m, 2H), 2.77 (dd, J = 13.4, 9.5 Hz, 1H), 2.69 (dd, J = 14.4, 4.2 Hz, 1H), 2.30 (s, 6H), 2.29 – 2.15 (m, 1H), 2.11 – 1.98 (m, 1H), 1.85 – 1.77 (m, 1H), 1.53 – 1.39 (m, 1H), 1.35 – 1.26 (m, 6H), 1.01 – 0.86 (m, 6H).

**<sup>13</sup>C NMR** (100 MHz, CDCl<sub>3</sub>) δ 209.4, 170.6, 165.6, 153.4, 135.1, 134.6, 133.0, 130.6, 129.9, 129.5, 129.2, 128.4, 127.6, 118.1, 101.9, 79.7, 72.0, 69.2, 66.5, 63.6, 55.5, 51.0, 48.5, 44.3, 41.0, 37.9, 35.8, 31.9, 21.2, 16.3, 13.4, 12.5.

**HRMS (ESI-TOF)** m/z calcd for C<sub>37</sub>H<sub>48</sub>BrN<sub>2</sub>O<sub>8</sub> [M + H]<sup>+</sup> 727.2594, found 727.2586



### Vinyl stannane **13** (right half)



A flame-dried round-bottom flask charged with a stir bar was placed under an atmosphere of argon gas. A solution of **12** (1.10 g, 1.51 mmol, 1.00 equiv; dried via azeotropic distillation from PhMe thrice before use) in 40 mL PhMe was added to the flask followed by sequential addition of  $\text{Sn}_2\text{Me}_6$  (0.63 mL, 3.0 mmol, 2.00 equiv),  $\text{Pd}_2\text{dba}_3$  (69 mg, 0.76 mmol, 0.05 equiv), and cataCXium A (di(1-adamantanyl)-*n*-butylphosphine) (163 mg, 0.45 mmol, 0.30 equiv). The maroon solution was heated to 50 °C. After 16 h, the reaction was cooled to ambient temperature and 25 mL saturated aqueous  $\text{CuSO}_4$  was added. The reaction mixture was extracted with  $\text{Et}_2\text{O}$  (2 x 40 mL), and the combined organic layers were washed with brine (50 mL), dried over sodium sulfate, filtered, and the filtrate was concentrated to a brown oil. The crude mixture was purified by flash chromatography (silica gel, eluent: 16-26% acetone/hexanes + 0.1%  $\text{Et}_3\text{N}$ ) to provide the vinyl stannane right half **13** (1.16 g, 95 %) as an olive-green foam.

**TLC** (35% acetone/hexanes + 0.1%  $\text{Et}_3\text{N}$ ):  $R_f = 0.5$  (UV, *p*-anisaldehyde).

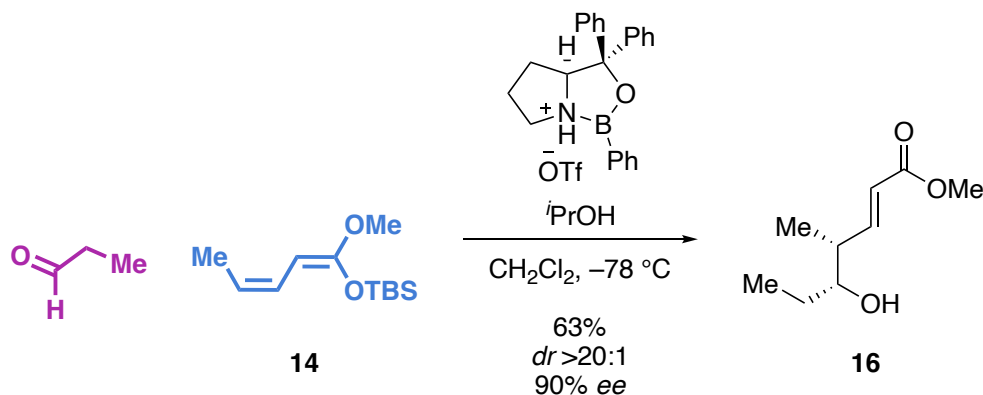
**$^1\text{H NMR}$**  (400 MHz,  $\text{CDCl}_3$ )  $\delta$  8.07 – 8.02 (m, 2H), 7.57 – 7.46 (m, 1H), 7.42 (dd,  $J = 8.3, 7.0$  Hz, 2H), 7.36 – 7.26 (m, 3H), 7.20 – 7.15 (m, 2H), 5.61 (t,  $J = 2.2$  Hz, 1H), 5.16 (d,  $J = 2.1$  Hz, 1H), 5.05 (dd,  $J = 10.6, 7.5$  Hz, 1H), 4.75 – 4.65 (m, 2H), 4.61 (d,  $J = 7.6$  Hz, 1H), 4.27 – 4.12 (m, 2H), 4.07 (dd,  $J = 6.2, 2.3$  Hz, 1H), 3.65 – 3.53 (m, 1H), 3.26 (dd,  $J = 13.4, 3.3$  Hz, 1H), 2.94 – 2.82 (m,

2H), 2.81 – 2.66 (m, 2H), 2.27 (s, 6H), 1.91 – 1.77 (m, 1H), 1.79 – 1.68 (m, 2H), 1.49 – 1.36 (m, 1H), 1.29 – 1.23 (m, 6H), 0.92 (d,  $J = 7.3$  Hz, 3H), 0.78 (d,  $J = 6.6$  Hz, 3H), 0.23 – 0.02 (m, 9H).

$^{13}\text{C}$  NMR (100 MHz,  $\text{CDCl}_3$ )  $\delta$  209.5, 170.7, 165.5, 155.4, 153.3, 135.0, 132.6, 130.8, 129.8, 129.4, 129.0, 128.2, 127.5, 125.5, 101.3, 78.6, 72.0, 68.9, 66.3, 63.4, 55.3, 50.6, 47.0, 44.4, 40.8, 37.8, 37.1, 31.9, 21.2, 15.3, 13.3, 11.3, -9.4.

HRMS (ESI-TOF)  $m/z$  calcd for  $\text{C}_{40}\text{H}_{57}\text{N}_2\text{O}_8\text{Sn}$   $[\text{M} + \text{H}]^+$  813.3136, found 813.3123

### Vinylogous Mukaiyama aldol product 16



A flame-dried round-bottom flask was charged with phenylboronic acid (4.860 g, 39.86 mmol, 0.50 equiv) and (*S*)-diphenyl(pyrrolidin-2-yl)methanol (10.10 g, 39.86 mmol, 0.50 equiv). The vessel was equipped with a Dean-Stark apparatus with reflux condenser and the system was evacuated and flushed with nitrogen (3 times). PhMe (150 mL) was added, and the resulting clear solution was brought to reflux. After 17 h, the mixture was allowed to cool to ambient temperature and was concentrated. The resulting white solid was dried at  $\leq 1$  Torr for 1 h. The vessel was flushed with nitrogen, and  $\text{CH}_2\text{Cl}_2$  (400 mL) was added. The resulting colorless solution was cooled to  $-78$  °C, and TfOH (3.19 mL, 35.88 mmol, 0.45 equiv) in 10 mL  $\text{CH}_2\text{Cl}_2$  was added dropwise over 5 min by means of cannula (CAUTION: TfOH rapidly corrodes most plastic syringes!). Some of the TfOH froze upon contact with the solution. After 15 min, the solids had dissolved, and a mixture of **14**<sup>6</sup> (18.21 g, 79.73 mmol, 1.00 equiv), propionaldehyde (5.8 mL, 80.52 mmol, 1.01

equiv), and isopropanol (6.7 mL, 87.70 mmol, 1.10 equiv) in CH<sub>2</sub>Cl<sub>2</sub> (40 mL) was added dropwise by cannula over 30 min. The mixture was stirred at -78 °C for another 2 h, and saturated aqueous NaHCO<sub>3</sub> (350 mL) was added in one portion. The vessel was removed from the cooling bath and was allowed to warm to ambient temperature while it was rapidly stirred. The biphasic mixture was transferred to a separatory funnel, and the layers were separated. The aqueous layer was extracted with CH<sub>2</sub>Cl<sub>2</sub> (2 x 350 mL). The combined organic layers were washed with water (350 mL) and brine (350 mL), and the washed solution was dried over sodium sulfate, filtered, and the filtrate was concentrated to a viscous clear oil. The crude mixture was purified by flash chromatography (silica gel, eluent: 0-30% EtOAc/hexanes) to provide aldol product **16** (8.65 g, 63%) as a colorless oil.

**TLC** (25% EtOAc/hexanes): R<sub>f</sub> = 0.24 (UV, *p*-anisaldehyde).

**<sup>1</sup>H NMR** (400 MHz, CDCl<sub>3</sub>) δ 6.94 (dd, J = 15.7, 7.9 Hz, 1H), 5.84 (dd, J = 15.7, 1.3 Hz, 1H), 3.71 (s, 3H), 3.46 (ddd, J = 8.9, 5.4, 3.8 Hz, 1H), 2.41 (dddd, J = 8.0, 6.7, 5.4, 1.3 Hz, 1H), 1.60 – 1.45 (m, 1H), 1.45 – 1.29 (m, 1H), 1.07 (d, J = 6.8 Hz, 3H), 0.94 (t, J = 7.4 Hz, 3H).

**<sup>13</sup>C NMR** (100 MHz, CDCl<sub>3</sub>) δ 167.1, 151.6, 121.0, 75.8, 51.5, 42.2, 27.3, 14.0, 10.2.

**HRMS (ESI-TOF)** m/z calcd for C<sub>9</sub>H<sub>17</sub>O<sub>3</sub> [M + H]<sup>+</sup> 173.1177, found 173.1172

Determination of enantiomeric excess:

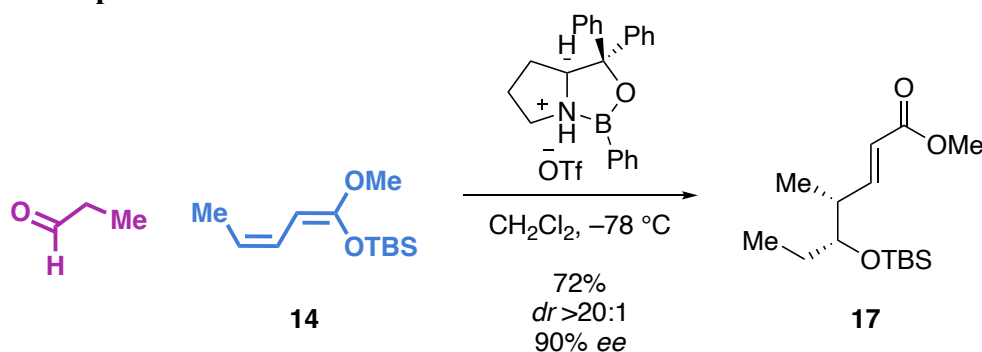
To a solution of **16** (20 mg, 0.11 mmol, 1.00 equiv) in CH<sub>2</sub>Cl<sub>2</sub> (2 mL), at 19 °C was added successively Et<sub>3</sub>N (0.12 mL, 0.86 mmol, 8 equiv), DMAP (18 mg, 0.15 mmol, 1.4 equiv) and either (*S*)- or (*R*)-Mosher acid chloride (0.08 mL, 0.43 mmol, 4 equiv). After 2 h, the mixture was diluted with EtOAc (15 mL). The mixture was transferred to a separatory funnel and washed successively with 1 M aqueous NaHSO<sub>4</sub> solution (3 x 5 mL), 1 M aqueous NaOH solution (5 mL), and saturated

aqueous NaHCO<sub>3</sub> solution (3 x 5 mL). The organic phase was dried over sodium sulfate, filtered, and concentrated. The crude residue was analyzed by <sup>1</sup>H-NMR.

For (S)-3,3,3-trifluoro-2-methoxy-2-phenylpropanoyl chloride: The enantiomeric excess was calculated from integration of the doublet of doublets at 6.94 ppm (major), 6.84 ppm (minor). The ee was 90%.

For (R)-3,3,3-trifluoro-2-methoxy-2-phenylpropanoyl chloride: The enantiomeric excess was calculated from integration of the doublet of doublets at 6.84 ppm (major), 6.94 ppm (minor). The ee was 90%.

### Silyl ether aldol product 17



A flame-dried round-bottom flask was charged with phenylboronic acid (248 mg, 2.03 mmol, 0.50 equiv) and (*S*)-diphenyl(pyrrolidin-2-yl)methanol (515 mg, 2.03 mmol, 0.50 equiv). The vessel was equipped with a Dean-Stark apparatus with reflux condenser and the system was evacuated and flushed with nitrogen (3 times). PhMe (15 mL) was added, and the resulting clear solution was brought to reflux. After 17 h, the mixture was allowed to cool to ambient temperature and was concentrated. The resulting white solid was dried at ≤1 Torr for 1 h. The vessel was flushed with

nitrogen, and CH<sub>2</sub>Cl<sub>2</sub> (20 mL) was added. The resulting colorless solution was cooled to -78 °C, and TfOH (0.16 mL, 0.45 Eq, 35.88 mmol) was added dropwise over 5 min by means of glass syringe (CAUTION: TfOH rapidly corrodes most plastic syringes!). Some of the TfOH froze upon contact with the solution. After 1 h, the solids had dissolved, and a mixture of **14** (929 mg, 4.07 mmol, 1.00 equiv) and propionaldehyde (0.3 mL, 80.52 mmol, 1.01 equiv) in CH<sub>2</sub>Cl<sub>2</sub> (5 mL) was added dropwise by means of syringe pump over 30 min. The mixture was stirred at -78 °C for another 18 h, and saturated aqueous NaHCO<sub>3</sub> (15 mL) was added in one portion. The vessel was removed from the cooling bath and was allowed to warm to ambient temperature while it was rapidly stirred. The biphasic mixture was transferred to a separatory funnel, and the layers were separated. The aqueous layer was extracted with CH<sub>2</sub>Cl<sub>2</sub> (2 x 14 mL). The combined organic layers were washed with water (30 mL) and brine (30 mL), and the washed solution was dried over sodium sulfate, filtered, and the filtrate was concentrated to a pale-yellow oil. The crude mixture was purified by flash chromatography (silica gel, eluent: 0-10% EtOAc/hexanes) to provide the silyl ether aldol product **17** (830 mg, 72%) as a pale-yellow oil. The enantiomeric excess was determined after removing the TBS group with HF•pyr (*vide infra*) and using the above-mentioned protocol, finding that the ee was 90%.

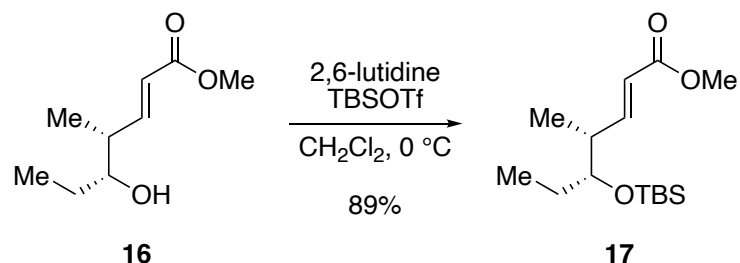
**TLC** (5% EtOAc/hexanes): R<sub>f</sub> = 0.41 (UV, *p*-anisaldehyde).

**<sup>1</sup>H NMR** (400 MHz, CDCl<sub>3</sub>) δ 6.97 (dd, *J* = 15.8, 7.5 Hz, 1H), 5.77 (dd, *J* = 15.8, 1.4 Hz, 1H), 3.68 (s, 3H), 3.55 – 3.47 (m, 1H), 2.50 – 2.37 (m, 1H), 1.52 – 1.28 (m, 2H), 0.99 (d, *J* = 6.9 Hz, 3H), 0.86 (s, 9H), 0.83 (t, *J* = 7.4 Hz, 3H), 0.01 (s, 3H), 0.00 (s, 3H).

**<sup>13</sup>C NMR** (100 MHz, CDCl<sub>3</sub>) δ 167.2, 152.4, 120.4, 76.4, 51.4, 41.4, 26.9, 25.9, 18.2, 14.2, 9.6, -4.3, -4.5.

**HRMS (ESI-TOF)** *m/z* calcd for C<sub>15</sub>H<sub>31</sub>O<sub>3</sub>Si [M + H]<sup>+</sup> 287.2042, found 287.2036

### Silyl ether **17** via TBS protection



In a flame-dried round-bottom flask charged with a stir bar and under argon gas, **16** (6.58 g, 38.2 mmol, 1.00 equiv) was solubilized in CH<sub>2</sub>Cl<sub>2</sub> (220 mL) and cooled to 0 °C. 2,6-lutidine (5.5 mL, 47.8 mmol, 1.25 equiv) and TBSOTf (9.66 mL, 42.0 mmol, 1.10 equiv) were added sequentially and allowed to react at 0 °C. After 1.5 h, the reaction was slowly quenched with 14 mL MeOH and stirred for 5 min. The mixture was diluted into 300 mL EtOAc and washed with 1M NaHSO<sub>4</sub> (100 mL), saturated aqueous NaHCO<sub>3</sub> (100 mL), and brine (200 mL), dried over sodium sulfate, filtered, and the filtrate concentrated to a white oil. The crude mixture was purified by flash chromatography (silica gel, eluent: 0-10% EtOAc/hexanes) to provide silyl ether **17** (9.72 g, 89 %) as a yellow oil.

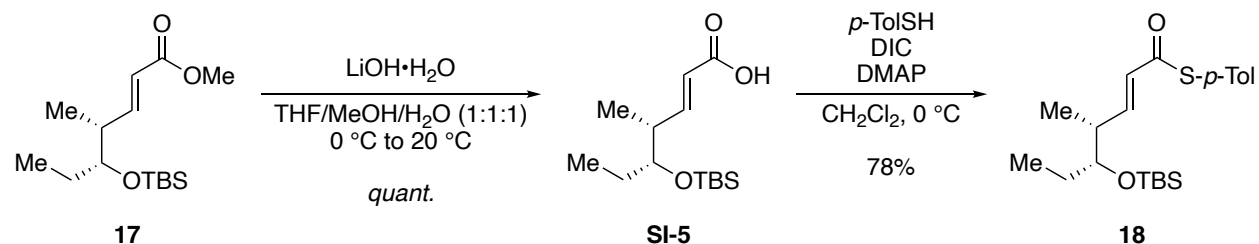
**TLC** (5% EtOAc/hexanes): R<sub>f</sub> = 0.41 (UV, *p*-anisaldehyde).

**<sup>1</sup>H NMR** (400 MHz, CDCl<sub>3</sub>) δ 6.97 (dd, *J* = 15.8, 7.5 Hz, 1H), 5.77 (dd, *J* = 15.8, 1.4 Hz, 1H), 3.68 (s, 3H), 3.55 – 3.47 (m, 1H), 2.50 – 2.37 (m, 1H), 1.52 – 1.28 (m, 2H), 0.99 (d, *J* = 6.9 Hz, 3H), 0.86 (s, 9H), 0.83 (t, *J* = 7.4 Hz, 3H), 0.01 (s, 3H), 0.00 (s, 3H).

**<sup>13</sup>C NMR** (100 MHz, CDCl<sub>3</sub>) δ 167.2, 152.4, 120.4, 76.4, 51.4, 41.4, 26.9, 25.9, 18.2, 14.2, 9.6, -4.3, -4.5.

**HRMS (ESI-TOF)** *m/z* calcd for C<sub>15</sub>H<sub>31</sub>O<sub>3</sub>Si [M + H]<sup>+</sup> 287.2042, found 287.2036

### Thioester 18



**17** (4.36 g, 15.2 mmol, 1.00 equiv) was solubilized in a 1:1:1 solution of water (50 mL), MeOH (50 mL), and THF (50 mL), and cooled to 0 °C. LiOH·H<sub>2</sub>O (12.8 g, 304 mmol, 20.00 equiv) was added in portions to the reaction. This cloudy white suspension was removed from the cooling bath and allowed to stir to ambient temperature. After 18 h, the reaction was cooled to 0 °C and carefully acidified with cold aqueous 1M HCl. The white precipitate acid was then extracted with Et<sub>2</sub>O (3 x 100 mL). The combined organic layers were washed with water (2 x 100 mL), brine (100 mL), dried over sodium sulfate, filtered, and the filtrate was concentrated to provide carboxylic acid **SI-5** (4.15 g, *quantitative*) as a clear oil, which was pure by both TLC and <sup>1</sup>H NMR and thus not subject to purification. Reactions that required purification could be done by flash chromatography (silica gel, eluent: 0-10% EtOAc/hexanes + 0.1% AcOH).

**TLC** (30% EtOAc/hexanes + 0.1% AcOH): R<sub>f</sub> = 0.59 (UV, *p*-anisaldehyde).

**<sup>1</sup>H NMR** (400 MHz, CDCl<sub>3</sub>) δ 11.92 (s, 1H), 7.13 (dd, *J* = 15.8, 7.4 Hz, 1H), 5.81 (dd, *J* = 15.7, 1.4 Hz, 1H), 3.56 (dt, *J* = 6.6, 5.1 Hz, 1H), 2.57 – 2.44 (m, 1H), 1.57 – 1.31 (m, 2H), 1.04 (d, *J* = 6.8 Hz, 3H), 0.89 (s, 9H), 0.86 (d, *J* = 7.4 Hz, 3H), 0.04 (s, 3H), 0.04 (s, 3H).

**<sup>13</sup>C NMR** (100 MHz, CDCl<sub>3</sub>) δ 172.5, 155.3, 120.3, 76.4, 41.6, 27.0, 26.0, 18.3, 14.0, 9.8, -4.2, -4.4.

**HRMS (ESI-TOF)** *m/z* calcd for C<sub>14</sub>H<sub>27</sub>O<sub>3</sub>Si [M – H]<sup>–</sup> 271.1729, found 271.1737

**SI-5** (4.49 g, 16.5 mmol, 1.00 equiv) and DMAP (604 mg, 4.94 mmol, 0.30 equiv) were solubilized in 100 mL CH<sub>2</sub>Cl<sub>2</sub> and cooled to 0 °C. DIC (2.8 mL, 19.8 mmol, 1.20 equiv) was added dropwise and allowed to stir for 5 min. 4-methylbenzenethiol (1.94 g, 15.7 mmol, 0.95 equiv) in 50 mL CH<sub>2</sub>Cl<sub>2</sub> was slowly added dropwise and the mixture was stirred at 0 °C (Note: the temperature of the mixture must be kept cool and a slight sub-stoichiometric amount of thiol is necessary to avoid conjugate addition side-reaction). After 2 h, the reaction was filtered through a pad of Celite to remove precipitates that formed during the reaction and the Celite pad was rinsed with 50 mL CH<sub>2</sub>Cl<sub>2</sub>. The filtrate was washed with saturated aqueous NaHCO<sub>3</sub> (150 mL), water (150 mL), brine (150 mL), dried over sodium sulfate, filtered, and the filtrate was concentrated. The crude was purified by flash chromatography (silica gel, eluent: 0-5% EtOAc/hexanes) to provide the thioester **18** (4.89 g, 78%) as a clear colorless oil.

**TLC** (10% EtOAc/hexanes):  $R_f = 0.69$  (UV, *p*-anisaldehyde).

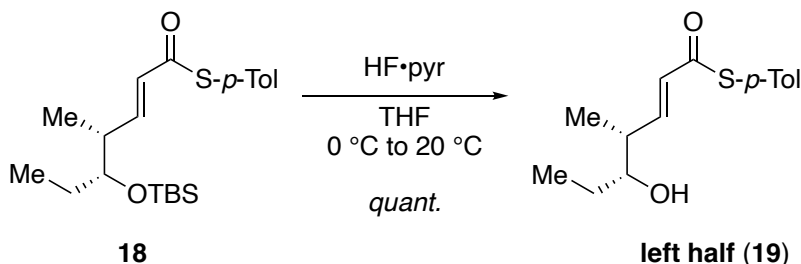
**<sup>1</sup>H NMR** (400 MHz, CDCl<sub>3</sub>)  $\delta$  7.35 – 7.30 (m, 2H), 7.24 – 7.18 (m, 2H), 7.04 (dd,  $J = 15.7, 7.2$  Hz, 1H), 6.16 (dd,  $J = 15.7, 1.3$  Hz, 1H), 3.62 – 3.56 (m, 1H), 2.54 – 2.45 (m, 1H), 2.37 (s, 3H), 1.56 – 1.35 (m, 2H), 1.05 (d,  $J = 6.8$  Hz, 3H), 0.91 (s, 9H), 0.88 (t,  $J = 7.4$  Hz, 3H), 0.06 (s, 6H).

**<sup>13</sup>C NMR** (100 MHz, CDCl<sub>3</sub>)  $\delta$  188.7, 149.7, 139.7, 134.8, 130.1, 127.4, 124.3, 76.4, 41.5, 27.0, 26.0, 21.5, 18.3, 14.0, 9.9, -4.2, -4.4.

**HRMS (ESI-TOF)**  $m/z$  calcd for C<sub>21</sub>H<sub>35</sub>O<sub>2</sub>SSi [M + H]<sup>+</sup> 379.2127, found 379.2119



### Thioester **19** (left half)



**18** (160 mg, 423  $\mu\text{mol}$ , 1.00 equiv) was solubilized in THF (1 mL) in a polypropylene reaction vessel and cooled to 0 °C. HF·pyr (0.38 mL, 4.23 mmol, 10 equiv) was added dropwise and the reaction was allowed to stir to ambient temperature. After 4 h, the reaction was cooled to 0°C and quenched slowly with saturated aqueous NaHCO<sub>3</sub> until the gas evolution stopped. The suspension was extracted with Et<sub>2</sub>O (3 x 10 mL), and the combined organic layers were washed with brine (10 mL), dried over sodium sulfate, filtered, and the filtrate was concentrated to a pale yellow oil. The crude was purified by flash chromatography (silica gel, eluent: 0-25% EtOAc/hexanes) to provide the  $\delta$ -hydroxy thioester **19** (111 mg, *quantitative*) as a clear colorless oil.

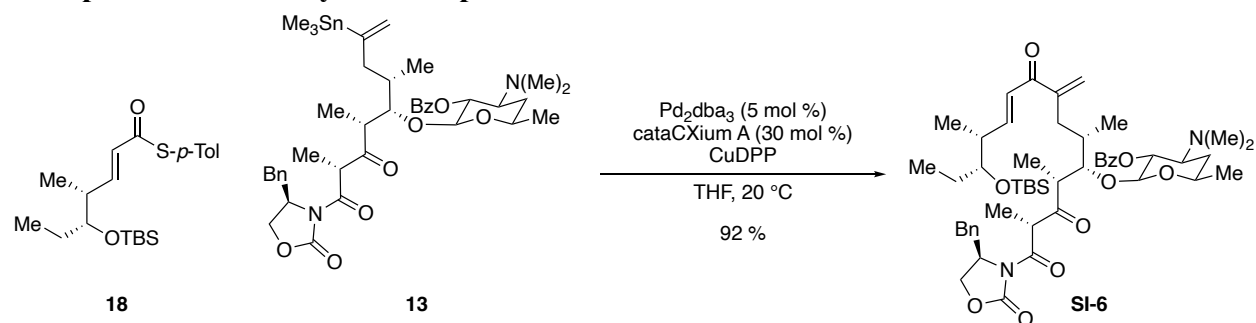
**TLC** (30% EtOAc/hexanes):  $R_f = 0.47$  (UV, *p*-anisaldehyde).

**<sup>1</sup>H NMR** (400 MHz, CDCl<sub>3</sub>)  $\delta$  7.36 – 7.28 (m, 2H), 7.23 (d,  $J = 7.9$  Hz, 2H), 6.95 (dd,  $J = 15.6$ , 7.8 Hz, 1H), 6.21 (dd,  $J = 15.6$ , 1.2 Hz, 1H), 3.51 (ddd,  $J = 9.0$ , 5.3, 3.8 Hz, 1H), 2.51 – 2.40 (m, 1H), 2.38 (s, 3H), 1.63 – 1.48 (m, 1H), 1.48 – 1.33 (m, 1H), 1.11 (d,  $J = 6.8$  Hz, 3H), 0.97 (t,  $J = 7.4$  Hz, 3H).

**<sup>13</sup>C NMR** (100 MHz, CDCl<sub>3</sub>)  $\delta$  188.7, 148.4, 139.8, 134.7, 130.1, 127.9, 124.1, 76.0, 42.5, 27.6, 21.5, 14.0, 10.4.

**HRMS (ESI-TOF)**  $m/z$  calcd for C<sub>15</sub>H<sub>21</sub>O<sub>2</sub>S [M + H]<sup>+</sup> 265.1262, found 265.1256

## TBS-protected macrocyclization precursor SI-6



A flame-dried flask with stir bar under an argon atmosphere was charged with  $\text{Pd}_2\text{dba}_3$  (56 mg, 0.61 mmol, 0.05 equiv), *cata*CXium A (131 mg, 0.34 mmol, 0.30 equiv) and CuDPP (448 mg, 1.59 mmol, 1.30 equiv). A solution of **18** (693 mg, 1.83 mmol, 1.50 equiv; dried via azeotropic distillation from PhMe thrice before use) in 15 mL THF (sparged with argon gas for 20 minutes prior) was added to the flask and stirred for a minute at ambient temperature, followed by dropwise addition of a solution of **13** (989 mg, 1.22 mmol, 1.00 equiv; dried via azeotropic distillation from PhMe thrice before use) in 10 mL THF (sparged with argon gas for 20 minutes prior) was added dropwise and stirred at ambient temperature. After 4 h, the reaction was diluted with 40 mL  $\text{Et}_2\text{O}$  and filtered through a pad of Celite. The pad was rinsed with 40 mL  $\text{Et}_2\text{O}$ , and the combined filtrate was concentrated to a black oil. The crude mixture was purified by flash chromatography (silica gel, eluent: 16-26% acetone/hexanes + 0.1%  $\text{Et}_3\text{N}$ ) to provide the linear, TBS-protected macrocycle precursor **SI-6** (1.01 g, 92%) as a gold foam.

**TLC** (35% acetone/hexanes + 0.1%  $\text{Et}_3\text{N}$ ):  $R_f = 0.49$  (UV, *p*-anisaldehyde).

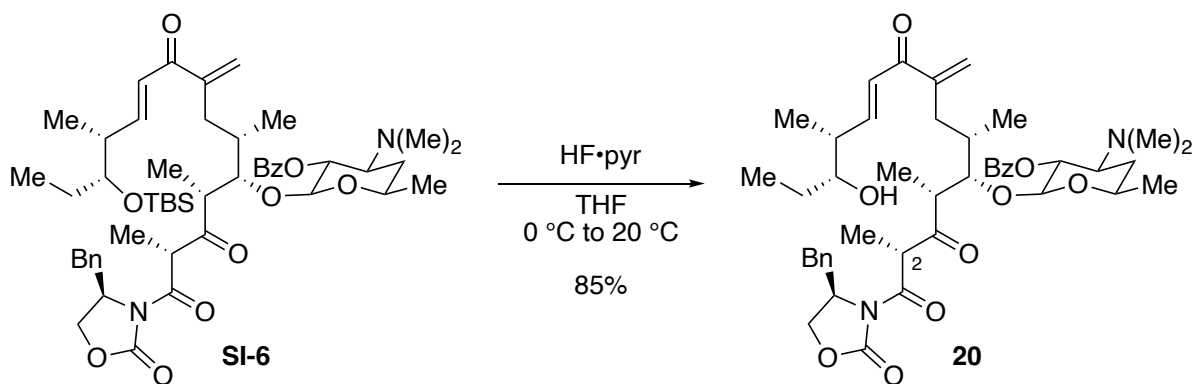
**$^1\text{H NMR}$**  (400 MHz,  $\text{CDCl}_3$ )  $\delta$  8.06 – 8.00 (m, 2H), 7.53 (t,  $J = 7.3$  Hz, 1H), 7.41 (t,  $J = 7.7$  Hz, 2H), 7.36 – 7.27 (m, 3H), 7.20 – 7.15 (m, 2H), 6.79 (dd,  $J = 15.6, 7.4$  Hz, 1H), 6.52 (dd,  $J = 15.6, 1.2$  Hz, 1H), 5.90 (s, 1H), 5.75 (s, 1H), 5.11 – 5.05 (m, 1H), 4.83 (q,  $J = 7.0$  Hz, 1H), 4.76 (td,  $J = 7.5, 6.5, 3.2$  Hz, 1H), 4.61 (d,  $J = 7.6$  Hz, 1H), 4.29 (t,  $J = 8.4$  Hz, 1H), 4.20 – 4.10 (m, 1H), 3.99 (t,  $J = 4.1$  Hz, 1H), 3.62 – 3.56 (m, 1H), 3.52 (q,  $J = 5.4$  Hz, 1H), 3.24 (dd,  $J = 13.3, 3.5$  Hz, 1H),

3.06 – 2.95 (m, 1H), 2.91 – 2.87 (m, 2H), 2.73 (dd,  $J = 13.7, 9.2$  Hz, 1H), 2.57 (dd,  $J = 14.2, 4.1$  Hz, 1H), 2.51 – 2.41 (m, 1H), 2.28 (s, 6H), 1.98 (dd,  $J = 14.1, 10.1$  Hz, 1H), 1.76 (s, 1H), 1.64 (s, 1H), 1.51 – 1.35 (m, 2H), 1.32 (d,  $J = 7.0$  Hz, 3H), 1.27 (d,  $J = 6.2$  Hz, 6H), 1.02 (d,  $J = 6.8$  Hz, 3H), 0.92 (d,  $J = 7.2$  Hz, 3H), 0.89 – 0.83 (m, 12H), 0.03 (d,  $J = 1.8$  Hz, 3H), 0.00 (s, 3H).

$^{13}\text{C}$  NMR (126 MHz,  $\text{CDCl}_3$ )  $\delta$  209.8, 192.7, 170.7, 165.6, 153.5, 150.7, 148.4, 135.3, 132.8, 129.9, 129.5, 129.1, 128.4, 127.5, 125.7, 125.1, 101.9, 79.9, 76.5, 72.0, 69.1, 66.45, 63.6, 55.5, 50.9, 48.2, 41.8, 41.0, 37.9, 37.0, 33.9, 29.9, 27.0, 26.0, 21.2, 18.3, 16.5, 14.6, 13.5, 13.0, 9.7, -4.2, -4.3.

HRMS (ESI-TOF)  $m/z$  calcd for  $\text{C}_{51}\text{H}_{75}\text{N}_2\text{O}_{10}\text{Si}$   $[\text{M} + \text{H}]^+$  903.5191, found 903.5185

### Macrocyclization precursor 20



SI-6 (1.74 g, 1.93 mmol, 1.00 equiv) was solubilized in THF (30 mL) in a polypropylene reaction vessel and cooled to 0 °C. HF·pyr (3.47 mL, 38.5 mmol, 20 equiv) was added dropwise and the reaction was allowed to stir to ambient temperature. After 16 h, the reaction was cooled to 0 °C and quenched slowly with saturated aqueous  $\text{NaHCO}_3$  until the gas evolution stopped. The suspension was extracted with  $\text{Et}_2\text{O}$  (3 x 50 mL), and the combined organic layers were washed with brine (50 mL), dried over sodium sulfate, filtered, and the filtrate was concentrated to a gold

oil. The crude was purified by flash chromatography (silica gel, eluent: 0-40% acetone/hexanes + 0.1% Et<sub>3</sub>N) to provide the macrocyclization precursor **20** (1.29 g, 85%) as a gold foam.

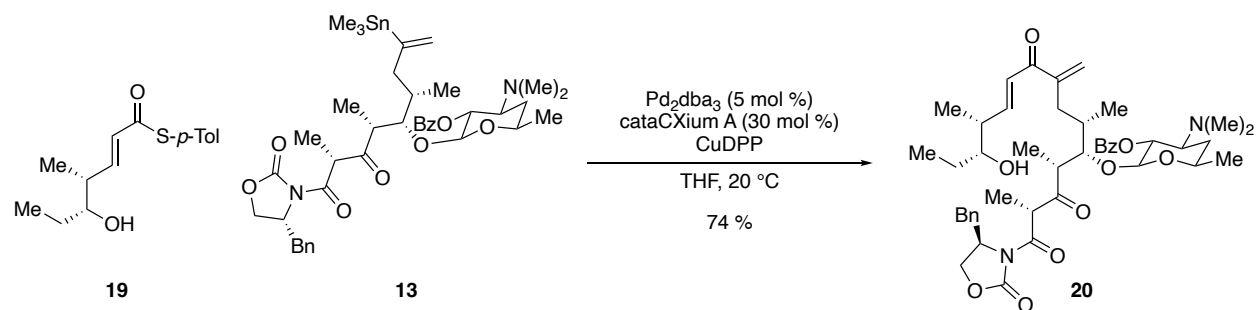
**TLC** (35% acetone/hexanes + 0.1% Et<sub>3</sub>N): R<sub>f</sub> = 0.30 (UV, *p*-anisaldehyde).

**<sup>1</sup>H NMR** (5:1 mixture of C-2 epimers, minor peaks reported separately from major peaks when possible, overlapping major and minor chemical shifts are reported as seen, 400 MHz, CDCl<sub>3</sub>) δ 8.10 – 8.06 (m, minor 1H), 8.06 – 8.02 (m, 2H), 7.59 – 7.47 (m, 1.2H), 7.47 – 7.37 (m, 2H), 7.36 – 7.17 (m, 5H), 6.84 (dd, *J* = 15.7, 8.4 Hz, minor 1H), 6.77 (dd, *J* = 15.6, 7.8 Hz, 1H), 6.67 – 6.55 (m, 1.2H), 5.99 – 5.91 (m, 1.2H), 5.75 (s, 1.2H), 5.14 – 5.06 (m, 1.2H), 4.87 (q, *J* = 7.1 Hz, 1H), 4.83 – 4.72 (m, 1H), 4.69 – 4.64 (m, minor 1H), 4.62 (d, *J* = 7.7 Hz, 1H), 4.55 (d, *J* = 7.6 Hz, minor 1H), 4.30 (t, *J* = 8.5 Hz, 1H), 4.21 – 4.12 (m, 1.2H), 4.03 – 3.91 (m, 1.2H), 3.67 – 3.54 (m, 1H), 3.53 – 3.46 (m, 1H), 3.42 (dd, *J* = 13.5, 3.4 Hz, minor 1H), 3.26 (dd, *J* = 13.4, 4.0 Hz, 1H), 3.12 – 2.97 (m, 1H), 2.90 (ddd, *J* = 12.3, 10.3, 4.4 Hz, 1H), 2.81 – 2.70 (m, 1.2H), 2.64 (dd, *J* = 14.0, 4.8 Hz, 1H), 2.53 – 2.39 (m, 1.2H), 2.29 (s, 7H), 2.03 – 1.94 (m, 1.2 H), 1.92 – 1.84 (m, minor 1H), 1.82 – 1.71 (m, 2H), 1.65 – 1.58 (m, 1H), 1.56 – 1.50 (m, 1H), 1.49 – 1.40 (m, 1H), 1.33 (d, *J* = 7.1 Hz, 3H), 1.31 – 1.27 (m, 3H), 1.11 – 1.07 (m, 4H), 1.00 – 0.96 (m, 4H), 0.93 (d, *J* = 7.3 Hz, 3H), 0.91 – 0.86 (m, 9H).

**<sup>13</sup>C NMR** (5:1 mixture of C-2 epimers, peaks are reported collectively, 100 MHz, CDCl<sub>3</sub>) δ 209.7, 209.5, 192.8, 192.3, 170.5, 165.5, 153.5, 150.2, 148.3, 148.2, 135.5, 135.2, 132.7, 130.6, 129.9, 129.8, 129.4, 129.4, 128.9, 128.3, 127.4, 127.3, 126.1, 125.8, 125.1, 101.8, 101.3, 80.1, 79.6, 76.0, 76.0, 71.9, 69.1, 69.0, 66.4, 63.5, 55.5, 51.3, 50.6, 48.1, 47.8, 42.6, 42.4, 40.8, 37.8, 37.6, 36.9, 36.6, 34.7, 34.5, 34.1, 31.8, 31.6, 30.9, 29.1, 27.4, 27.3, 25.3, 22.7, 21.1, 20.7, 17.0, 16.6, 14.1, 13.8, 13.5, 13.2, 12.7, 11.4, 10.4, 10.4.

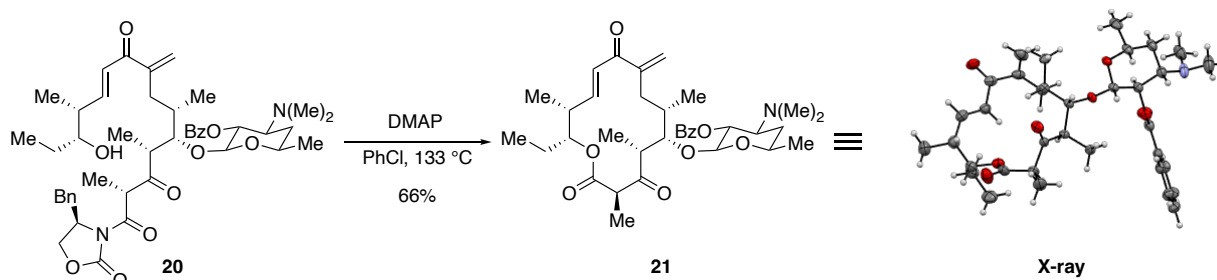
**HRMS (ESI-TOF)** *m/z* calcd for C<sub>45</sub>H<sub>61</sub>N<sub>2</sub>O<sub>10</sub> [M + H]<sup>+</sup> 789.4326, found 789.4318

## Macrocyclization precursor **20** via Liebeskind-Srogl coupling



A flame-dried flask with stir bar under an argon atmosphere was charged with Pd<sub>2</sub>dba<sub>3</sub> (5 mg, 5.5 μmol, 0.05 equiv), cataCXium A (12 mg, 33 μmol, 0.30 equiv) and CuDPP (40 mg, 0.14 mmol, 1.30 equiv). A solution of **19** (43 mg, 0.16 mmol, 1.50 equiv; dried via azeotropic distillation from PhMe thrice before use) in 2 mL THF (sparged with argon gas for 20 minutes prior) was added to the flask and stirred for a minute at ambient temperature, followed by dropwise addition of a solution of **13** (89 mg, 0.11 mmol, 1.00 equiv; dried via azeotropic distillation from PhMe thrice before use) in 2 mL THF (sparged with argon gas for 20 minutes prior) was added dropwise and stirred at ambient temperature. After 4 h, the reaction was diluted with 10 mL Et<sub>2</sub>O and filtered through a pad of Celite. The pad was rinsed with 4 mL Et<sub>2</sub>O, and the combined filtrate was concentrated to a black oil. The crude mixture was purified by flash chromatography (silica gel, eluent: 16-26% acetone/hexanes + 0.1% Et<sub>3</sub>N) to provide the linear macrocycle precursor **20** (64 mg, 74%) as a gold foam. Characterization data for this product is identical to that obtained from the TBS removal step.

## Macrocycle 21



In a flame-dried flask with stir bar, **20** (269 mg, 1.00 Eq, 341  $\mu\text{mol}$ ) and DMAP (4.2 mg, 34  $\mu\text{mol}$ , 0.10 equiv) (both combined and dried via azeotropic distillation from PhMe thrice before use) were solubilized in PhCl (340 mL, 1mM) and sparged with argon gas for 20 minutes. The vessel was equipped with a reflux condenser, evacuated and backfilled with nitrogen three times, then placed under argon and heated to reflux. After 15 h, the reaction was cooled to ambient temperature and concentrated (50 °C water bath) to a brown oil. The crude mixture was purified by flash chromatography (silica gel, eluent: 0-20% acetone/hexanes + 0.1% Et<sub>3</sub>N) to provide macrocycle **21** (138 mg, 66 %) as a pale-yellow oil. Product could be crystallized from an acetone/hexanes mixture.

**TLC** (35% acetone/hexanes + 0.1% Et<sub>3</sub>N):  $R_f = 0.46$  (UV, *p*-anisaldehyde).

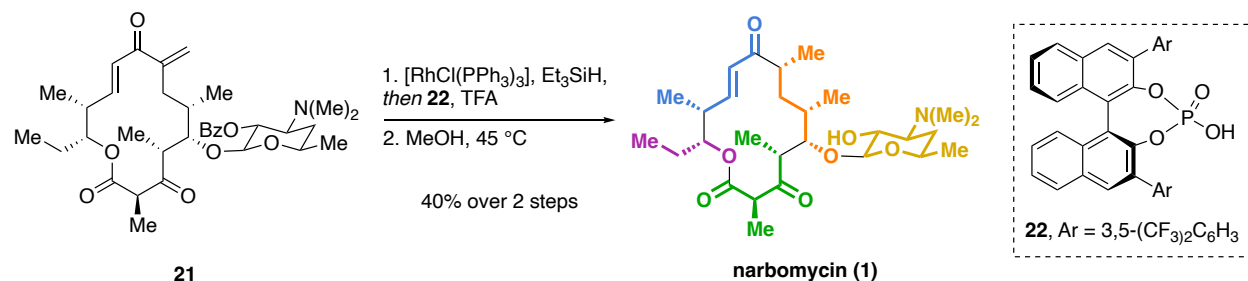
**<sup>1</sup>H NMR** (some satellite peaks, unreported, are observed due to small presence of C-3 keto-enol tautomer 400 MHz, CDCl<sub>3</sub>)  $\delta$  8.04 (d,  $J = 7.2$  Hz, 2H), 7.56 (t,  $J = 7.4$  Hz, 1H), 7.43 (t,  $J = 7.6$  Hz, 3H), 6.73 (dd,  $J = 15.8, 5.7$  Hz, 1H), 6.26 (dd,  $J = 15.8, 1.7$  Hz, 1H), 5.60 (d,  $J = 1.7$  Hz, 1H), 5.36 (s, 1H), 5.14 (dd,  $J = 10.6, 7.7$  Hz, 1H), 4.92 (ddd,  $J = 8.5, 5.1, 2.6$  Hz, 1H), 4.52 (d,  $J = 7.6$  Hz, 1H), 3.92 (dt,  $J = 7.0, 3.5$  Hz, 1H), 3.65 – 3.56 (m, 2H), 2.96 (s, 1H), 2.74 (p,  $J = 7.4$  Hz, 1H), 2.66 (td,  $J = 7.9, 7.3, 3.6$  Hz, 1H), 2.47 (dd,  $J = 14.6, 6.1$  Hz, 1H), 2.33 (s, 6H), 2.26 (dd,  $J = 14.6, 8.2$  Hz, 1H), 1.88 – 1.80 (m, 2H), 1.67 – 1.46 (m, 2H), 1.30 (d,  $J = 6.1$  Hz, 3H), 1.08 (d,  $J = 2.6$  Hz,

3H), 1.06 (d,  $J = 2.6$  Hz, 3H), 0.96 (d,  $J = 3.7$  Hz, 3H), 0.95 (d,  $J = 3.3$  Hz, 3H), 0.87 (t,  $J = 7.4$  Hz, 3H).

$^{13}\text{C}$  NMR (100 MHz,  $\text{CDCl}_3$ )  $\delta$  207.2, 195.4, 169.5, 165.5, 149.8, 148.9, 133.0, 130.6, 129.9, 128.5, 127.4, 122.0, 102.7, 81.2, 77.8, 72.0, 69.3, 63.8, 53.6, 50.9, 50.2, 40.9, 38.4, 36.3, 35.3, 31.5, 24.1, 21.1, 18.0, 14.3, 13.8, 11.5, 10.5.

HRMS (ESI-TOF)  $m/z$  calcd for  $\text{C}_{35}\text{H}_{50}\text{NO}_8$   $[\text{M} + \text{H}]^+$  612.3536, found 612.3529

### Narbomycin (1)



A flame-dried flask with stir bar under an argon atmosphere was charged with  $[\text{RhCl}(\text{PPh}_3)_3]$  (0.4 mg, 0.4  $\mu\text{mol}$ , 0.10 equiv), then a solution of **21** (2.5 mg, 4.1  $\mu\text{mol}$ , 1.00 equiv) in PhH (2.0 mL) and  $\text{Et}_3\text{SiH}$  (1  $\mu\text{L}$ , 6  $\mu\text{mol}$ , 1.50 equiv) were added sequentially, and the mixture was heated to 80 °C. After 20 h, the reaction was cooled to 0 °C and a solution of TFA (6  $\mu\text{L}$ , 82  $\mu\text{mol}$ , 20.00 equiv) and **26** (0.4 mg, 0.4  $\mu\text{mol}$ , 0.10 equiv) in PhH (1 mL) was slowly added dropwise. After 30 min, the reaction was quenched with saturated aqueous  $\text{NaHCO}_3$  until the evolution of gas stopped. The aqueous layer was extracted with  $\text{Et}_2\text{O}$  (3 x 1 mL), and the combined organic layers were dried over sodium sulfate, filtered, and the filtrate was concentrated to a brown film. The crude reaction was solubilized in MeOH (2 mL), and heated to 40 °C. After 16 h, the reaction was concentrated and purified by preparative TLC (silica gel, 3% MeOH/DCM +  $\text{NH}_4\text{OH}$ ) to provide narbomycin **1** (1.5 mg, 40 % over two steps) as a clear film.

TLC (35% acetone/hexanes + 0.1%  $\text{Et}_3\text{N}$ ):  $R_f = 0.39$  (UV, *p*-anisaldehyde).

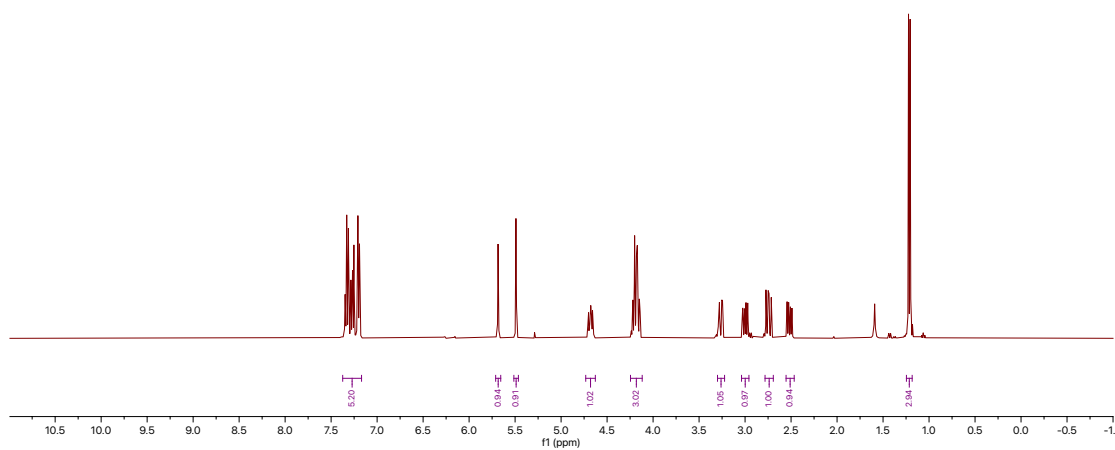
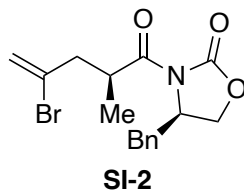
**<sup>1</sup>H NMR** (400 MHz, CDCl<sub>3</sub>) δ 6.70 (dd, *J* = 16.6, 6.4 Hz, 1H), 6.16 (d, *J* = 16.0 Hz, 1H), 4.98 – 4.91 (m, 1H), 4.33 (d, *J* = 7.4 Hz, 1H), 4.19 (s, 1H), 3.88 (q, *J* = 6.9 Hz, 1H), 3.62 – 3.52 (m, 1H), 3.31 – 3.23 (m, 1H), 3.00 – 2.93 (m, 1H), 2.82 – 2.71 (m, 2H), 2.57 – 2.45 (m, 1H), 2.30 (s, 6H), 1.76 – 1.65 (m, 3H), 1.61 – 1.57 (m, 1H), 1.56 – 1.49 (m, 1H), 1.39 (d, *J* = 6.9 Hz, 6H), 1.27 (d, *J* = 6.4 Hz, 6H), 1.14 (d, *J* = 6.5 Hz, 3H), 1.12 (d, *J* = 7.0 Hz, 3H), 1.05 (d, *J* = 7.1 Hz, 3H), 0.92 (t, *J* = 7.4 Hz, 4H).

**HRMS (ESI-TOF)** *m/z* calcd for C<sub>28</sub>H<sub>48</sub>NO<sub>7</sub> [M + H]<sup>+</sup> 510.3430, found 510.3421

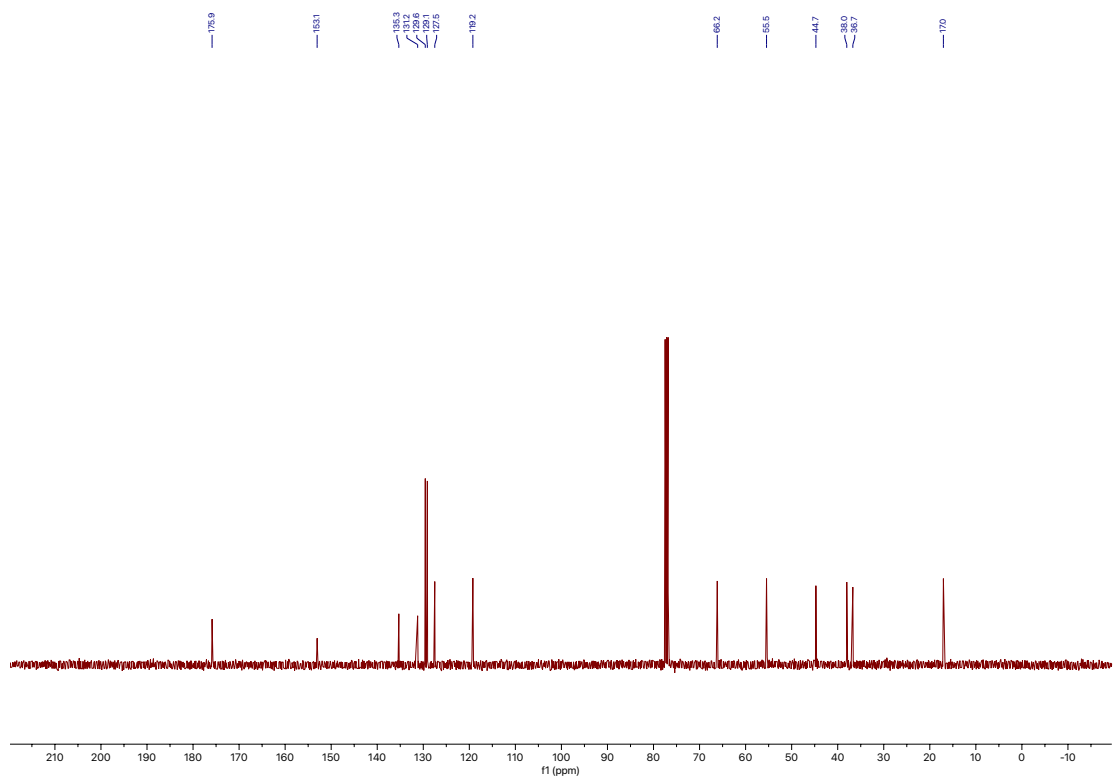


# $^1\text{H}$ NMR and $^{13}\text{C}$ NMR Spectra for Compounds

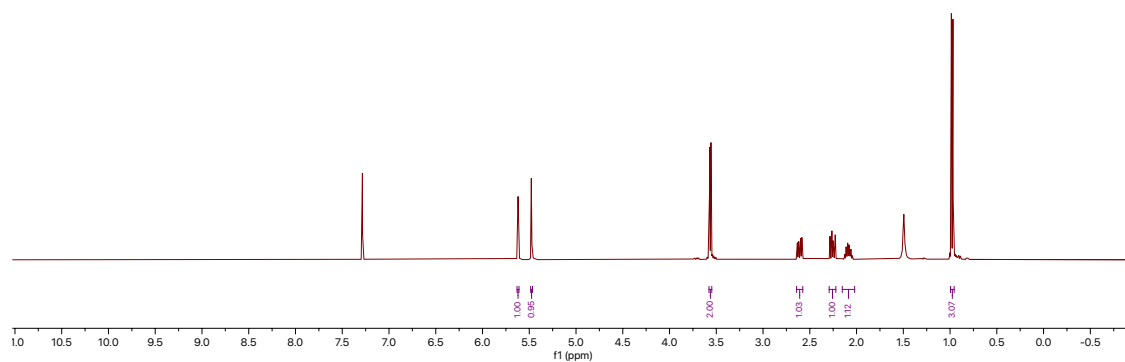
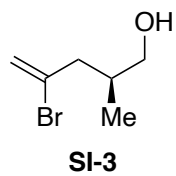
( $^1\text{H}$  NMR,  $\text{CDCl}_3$ , 400 MHz)



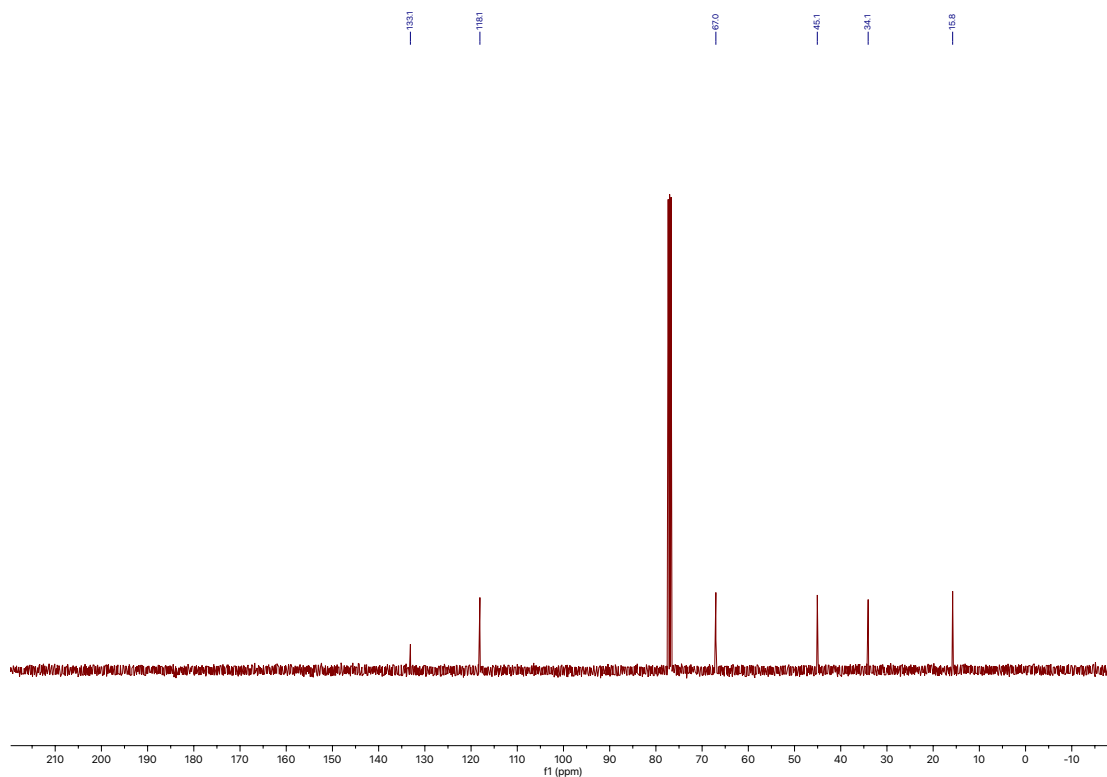
( $^{13}\text{C}$  NMR,  $\text{CDCl}_3$ , 100 MHz)



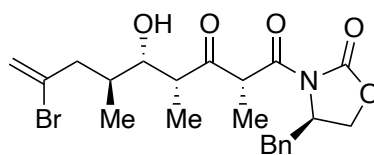
(<sup>1</sup>H NMR, CDCl<sub>3</sub>, 400 MHz)



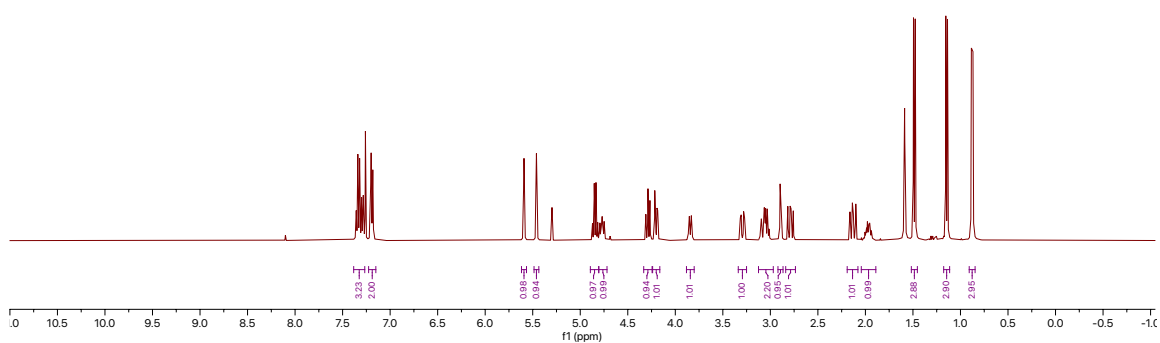
(<sup>13</sup>C NMR, CDCl<sub>3</sub>, 100 MHz)



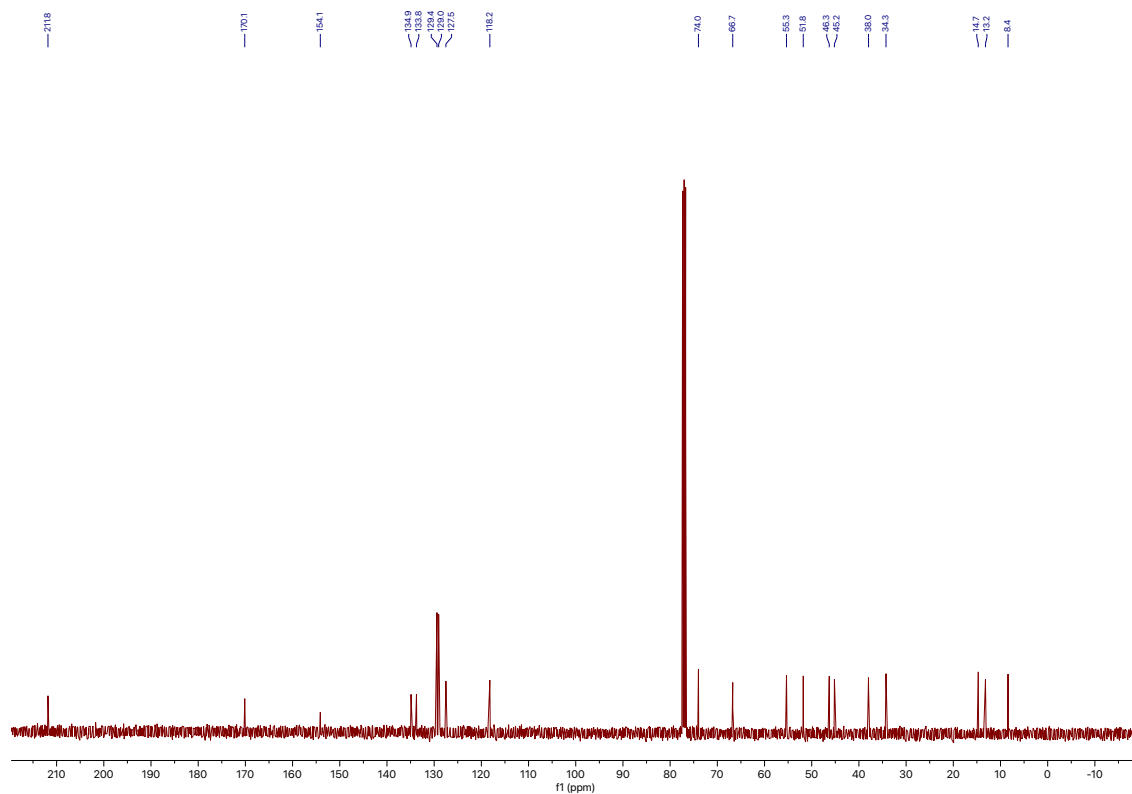
(<sup>1</sup>H NMR, CDCl<sub>3</sub>, 400 MHz)



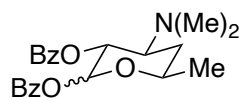
**10**



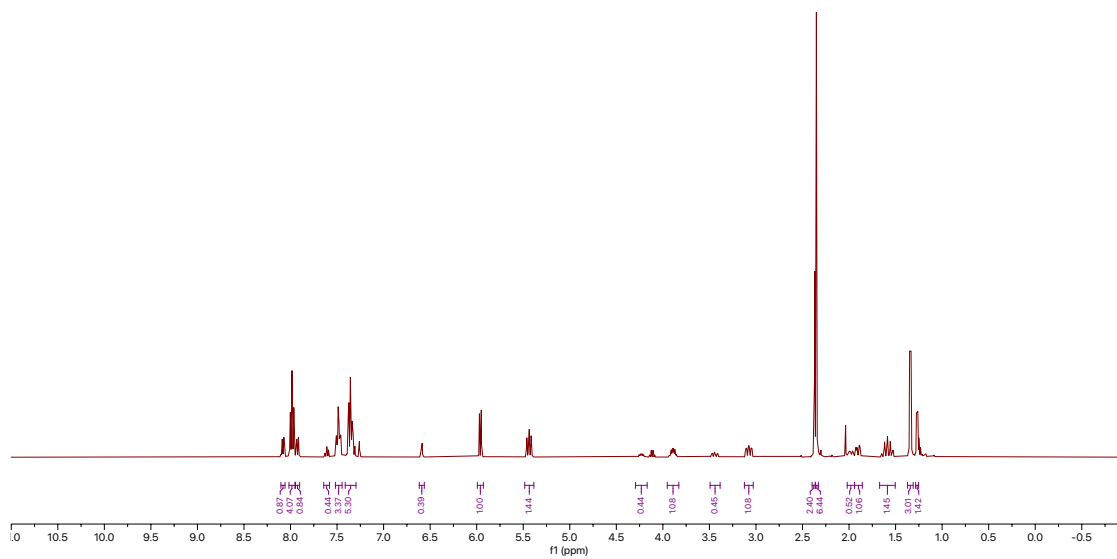
(<sup>13</sup>C NMR, CDCl<sub>3</sub>, 100 MHz)



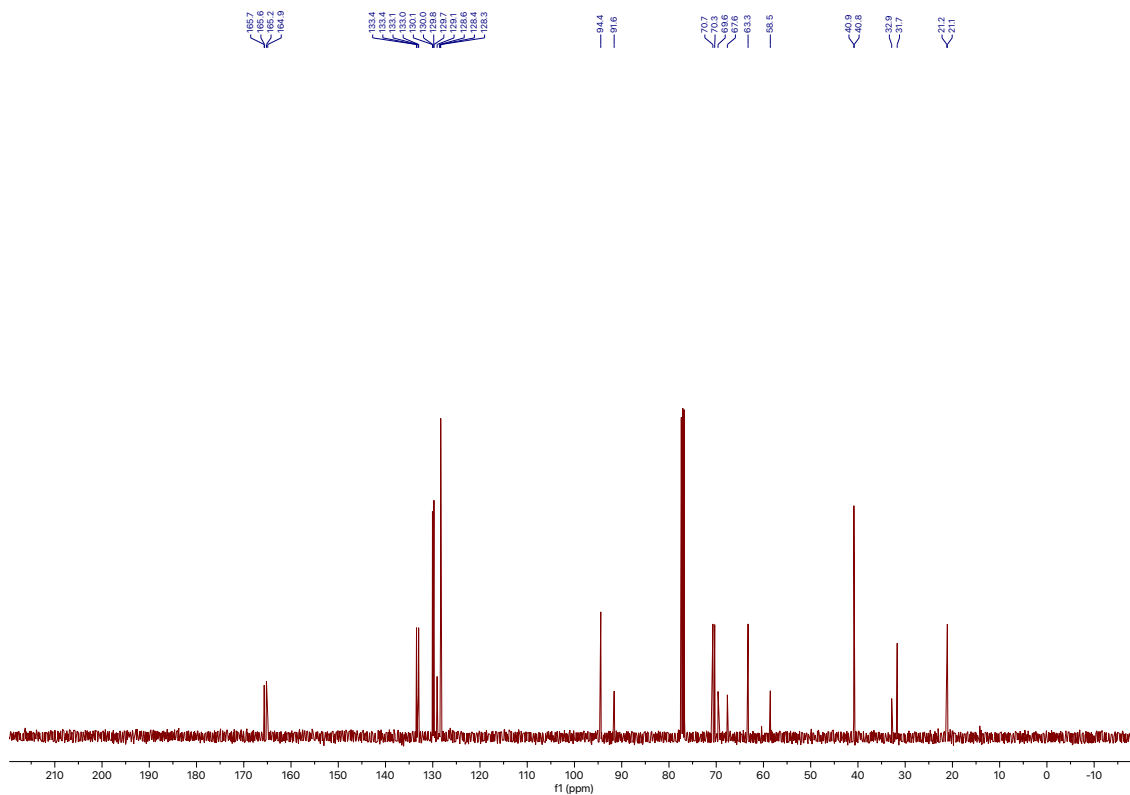
(<sup>1</sup>H NMR, CDCl<sub>3</sub>, 400 MHz)



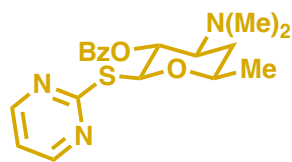
SI-4



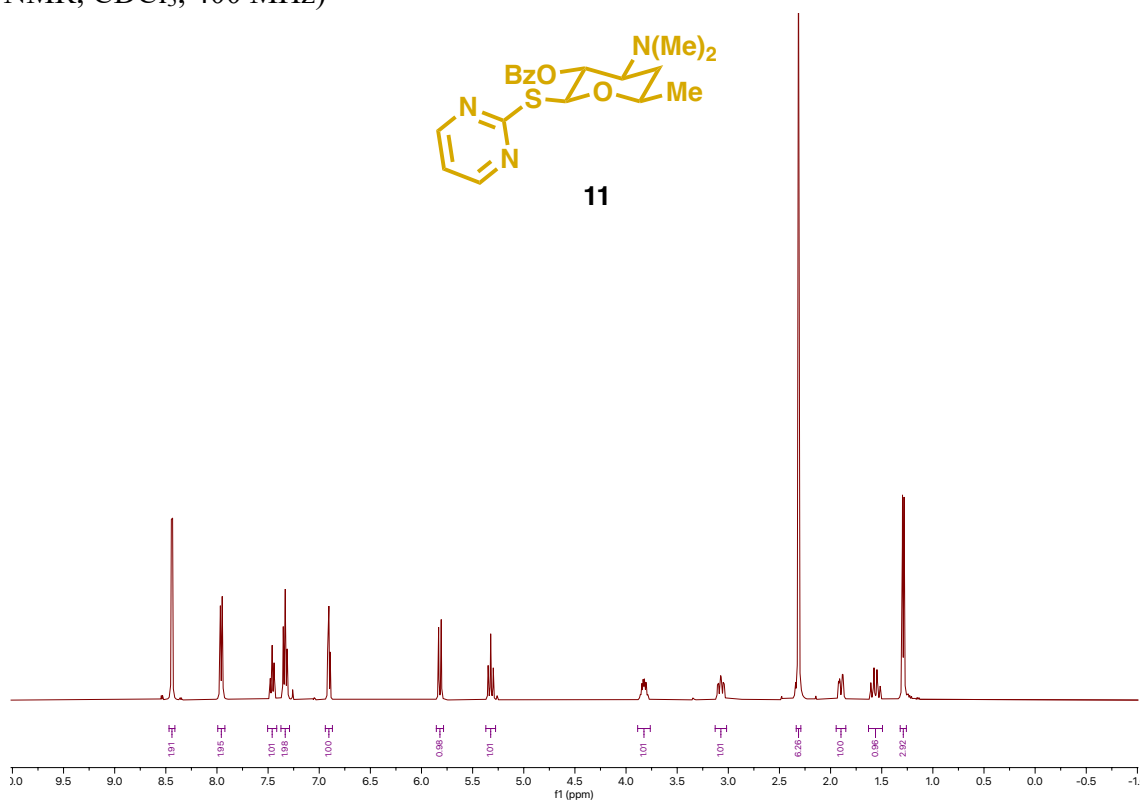
(<sup>13</sup>C NMR, CDCl<sub>3</sub>, 100 MHz)



(<sup>1</sup>H NMR, CDCl<sub>3</sub>, 400 MHz)

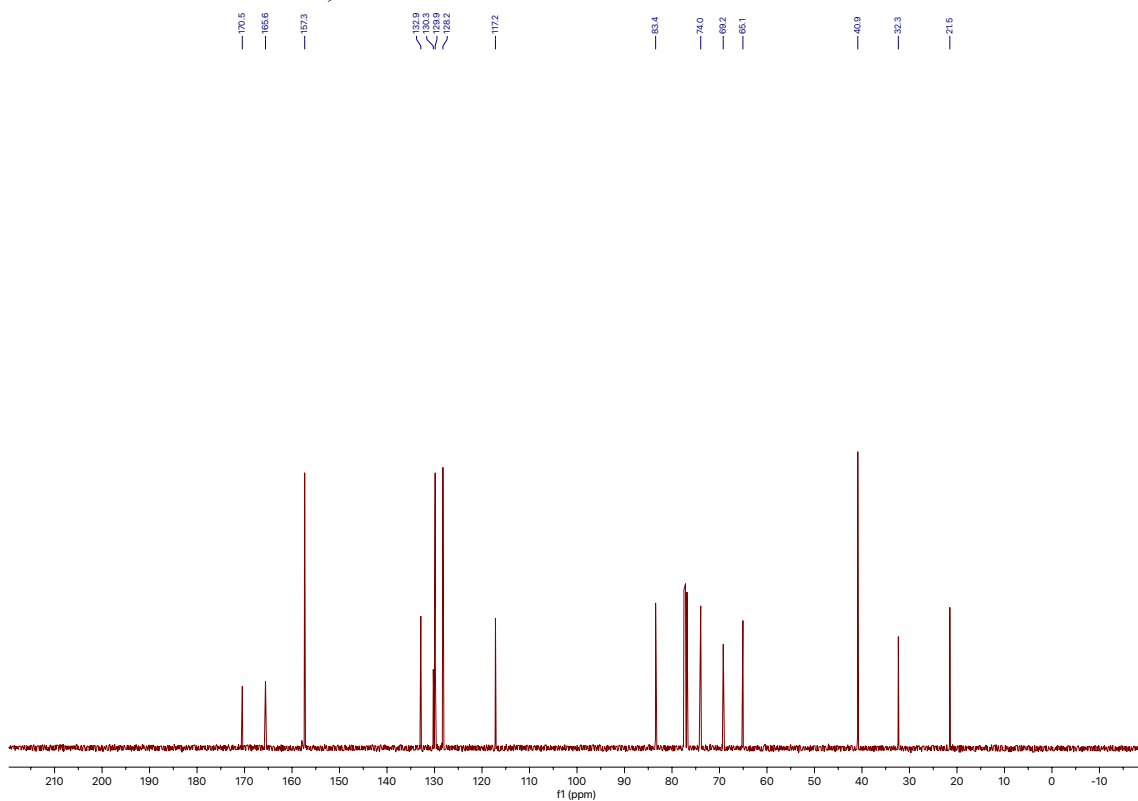


11

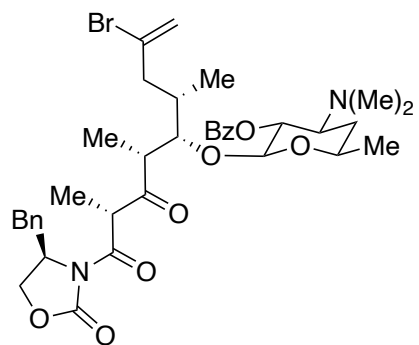


(<sup>13</sup>C NMR, CDCl<sub>3</sub>, 100 MHz)

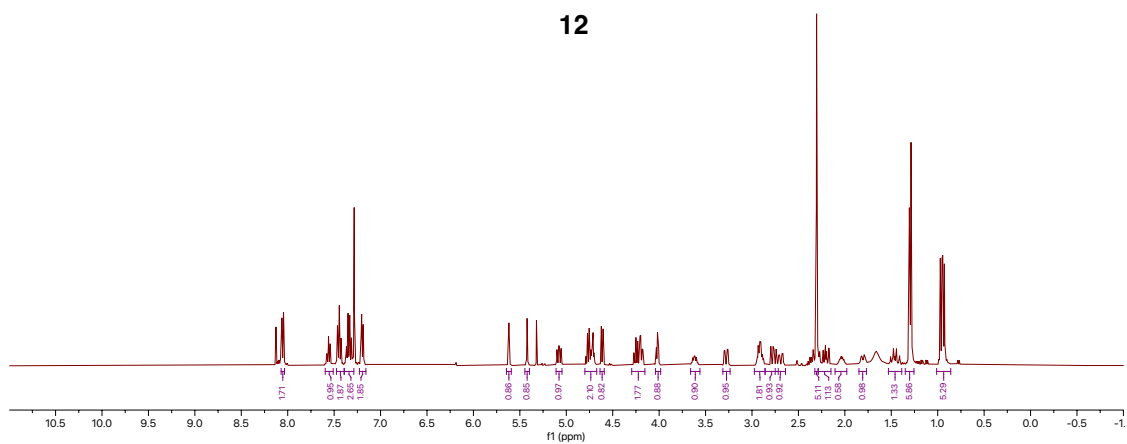
170.5  
165.6  
157.3  
132.9  
130.3  
128.2  
117.2  
83.4  
74.0  
69.2  
68.1  
40.9  
32.3  
21.5



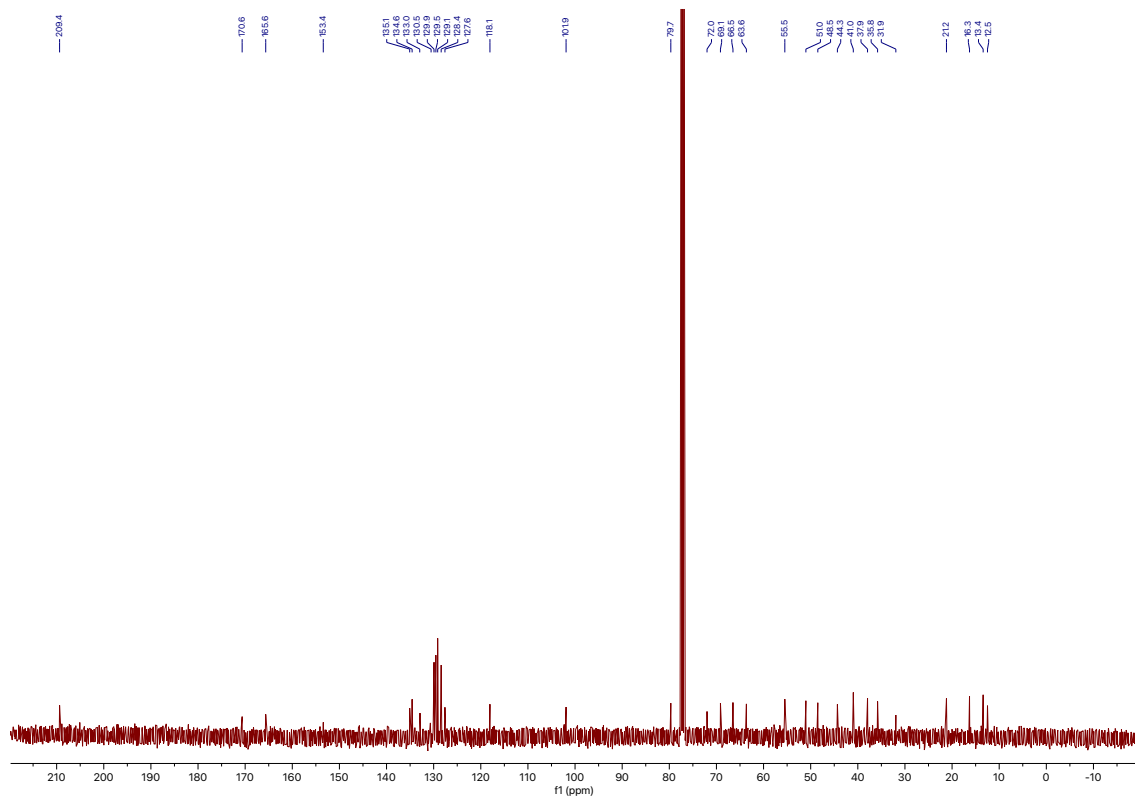
(<sup>1</sup>H NMR, CDCl<sub>3</sub>, 400 MHz)



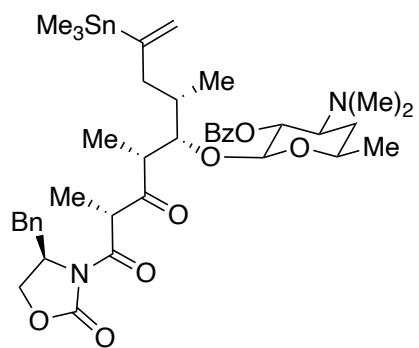
12



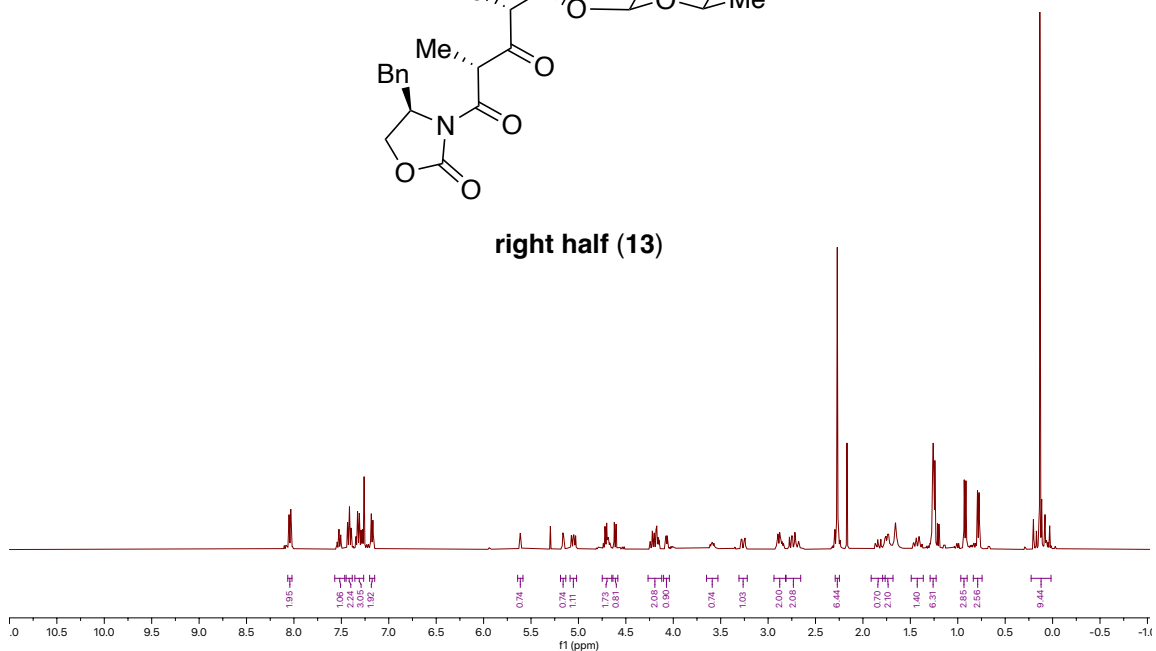
(<sup>13</sup>C NMR, CDCl<sub>3</sub>, 100 MHz)



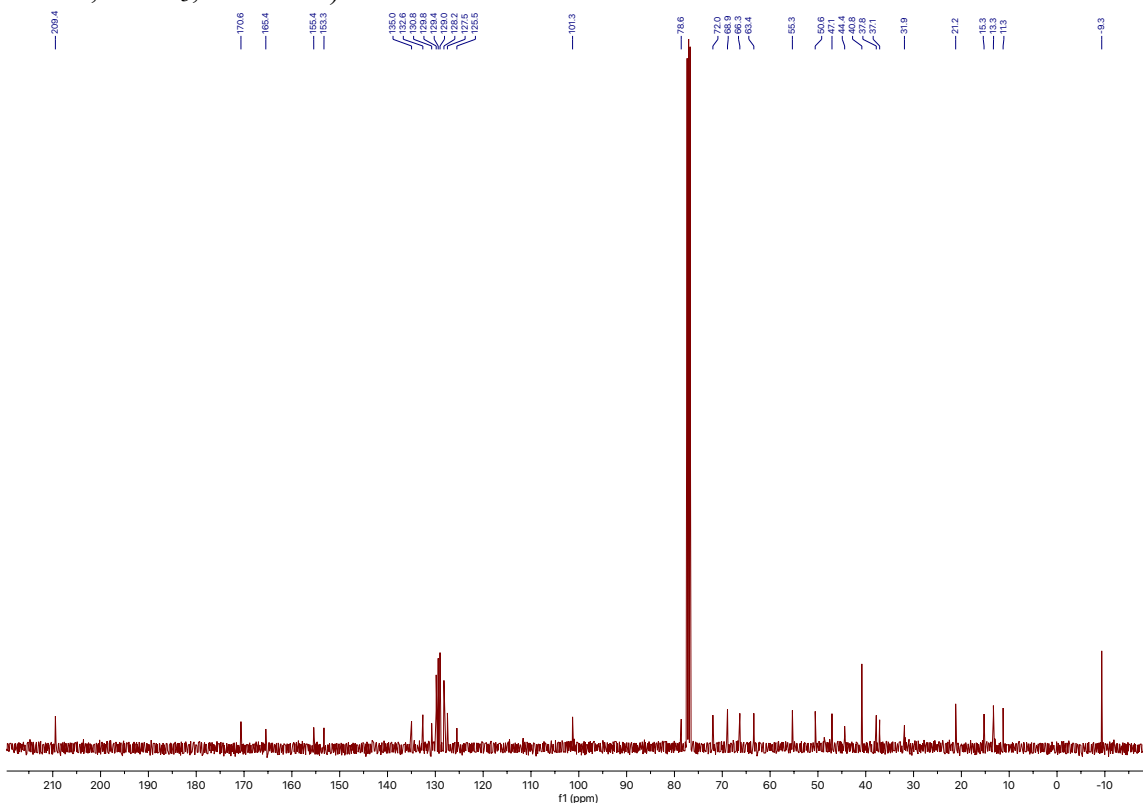
(<sup>1</sup>H NMR, CDCl<sub>3</sub>, 400 MHz)



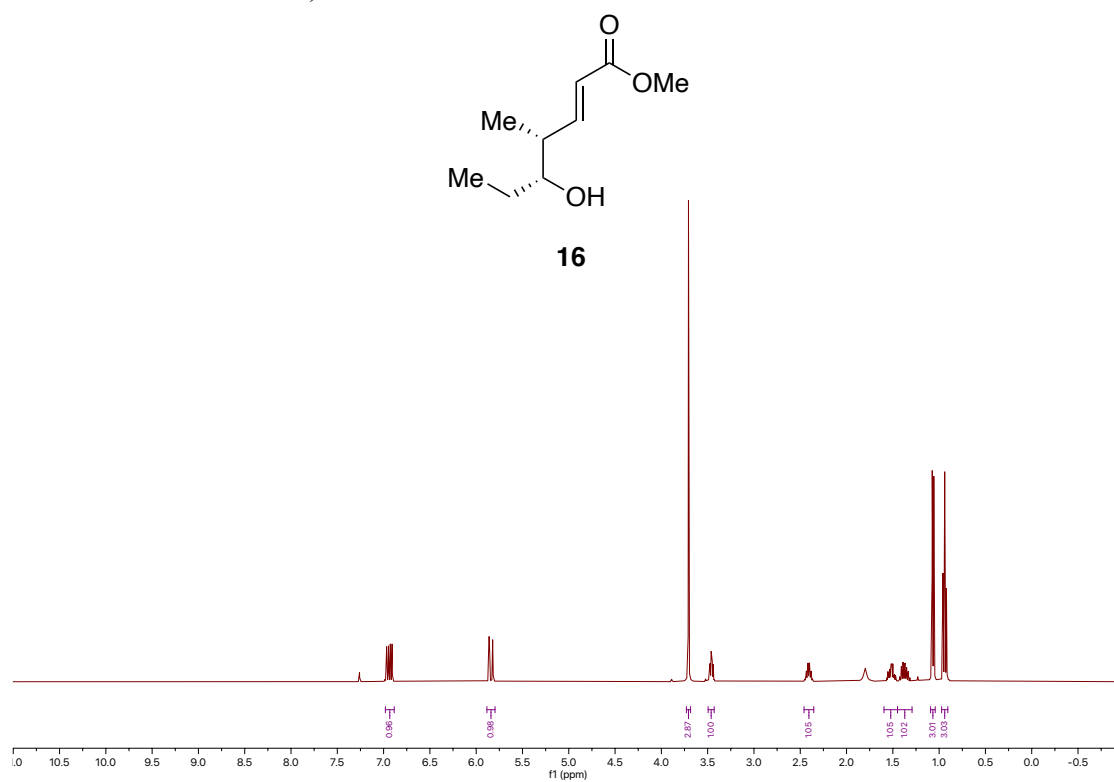
right half (13)



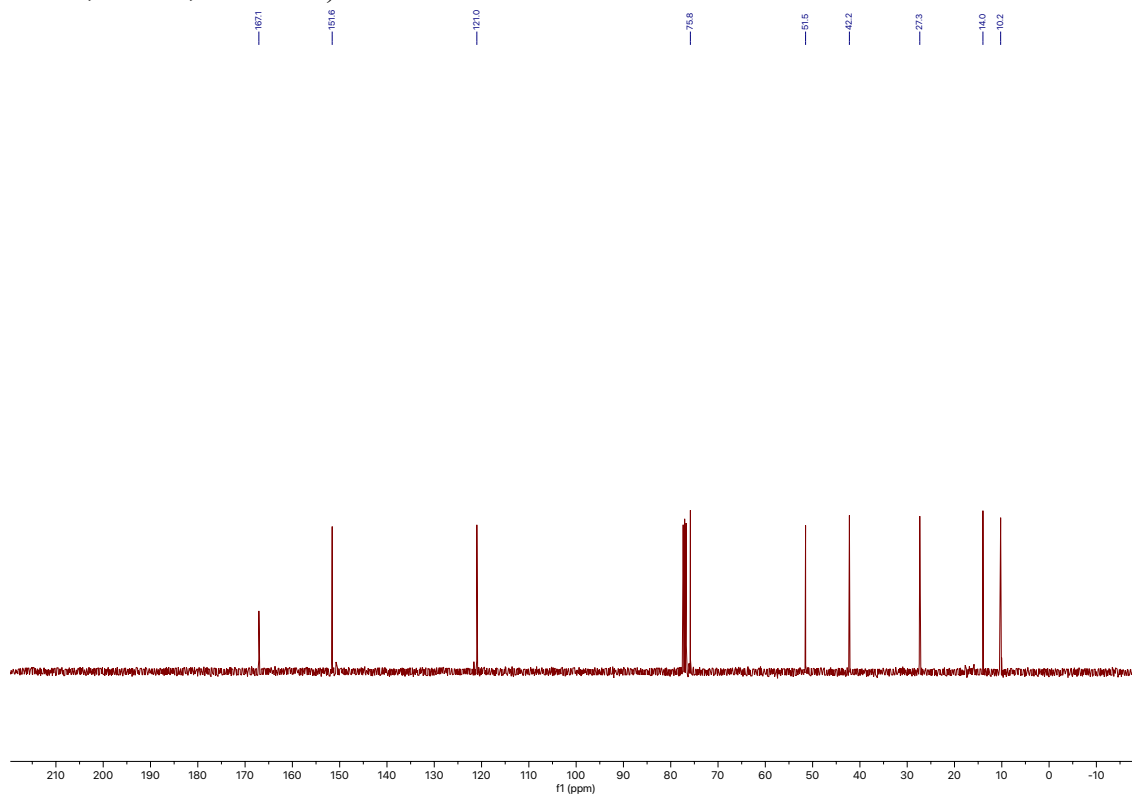
(<sup>13</sup>C NMR, CDCl<sub>3</sub>, 100 MHz)



(<sup>1</sup>H NMR, CDCl<sub>3</sub>, 400 MHz)

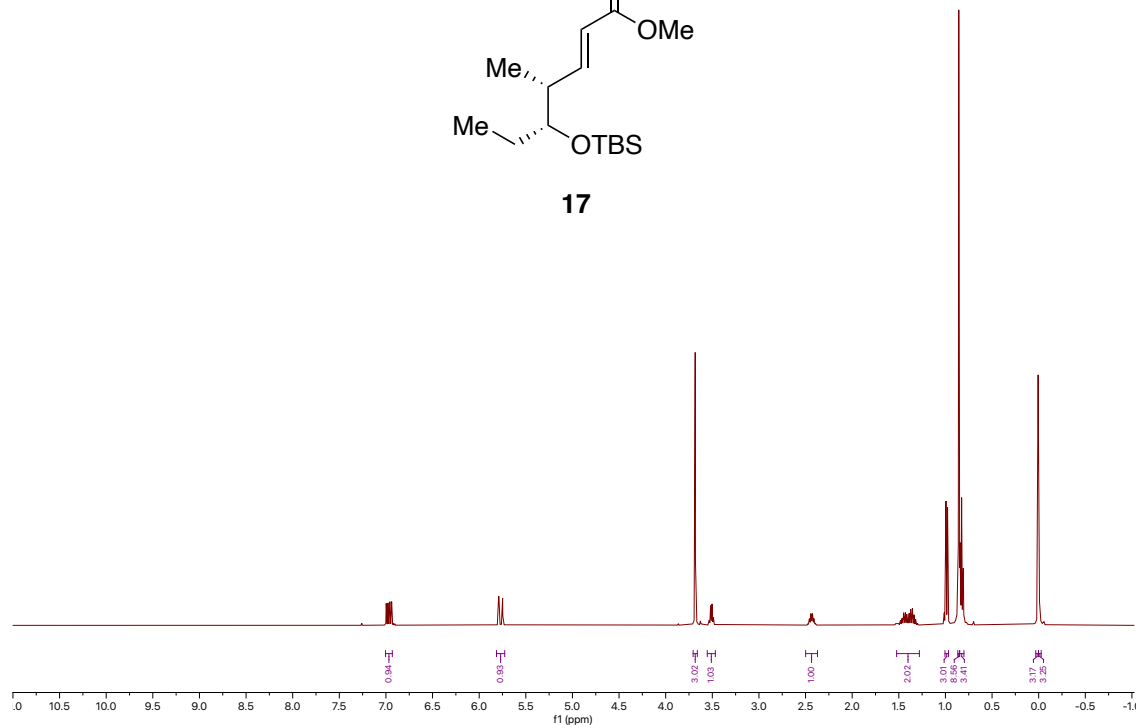
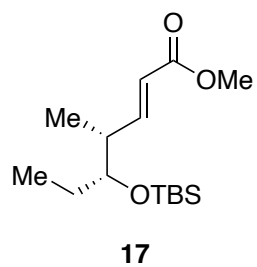


(<sup>13</sup>C NMR, CDCl<sub>3</sub>, 100 MHz)

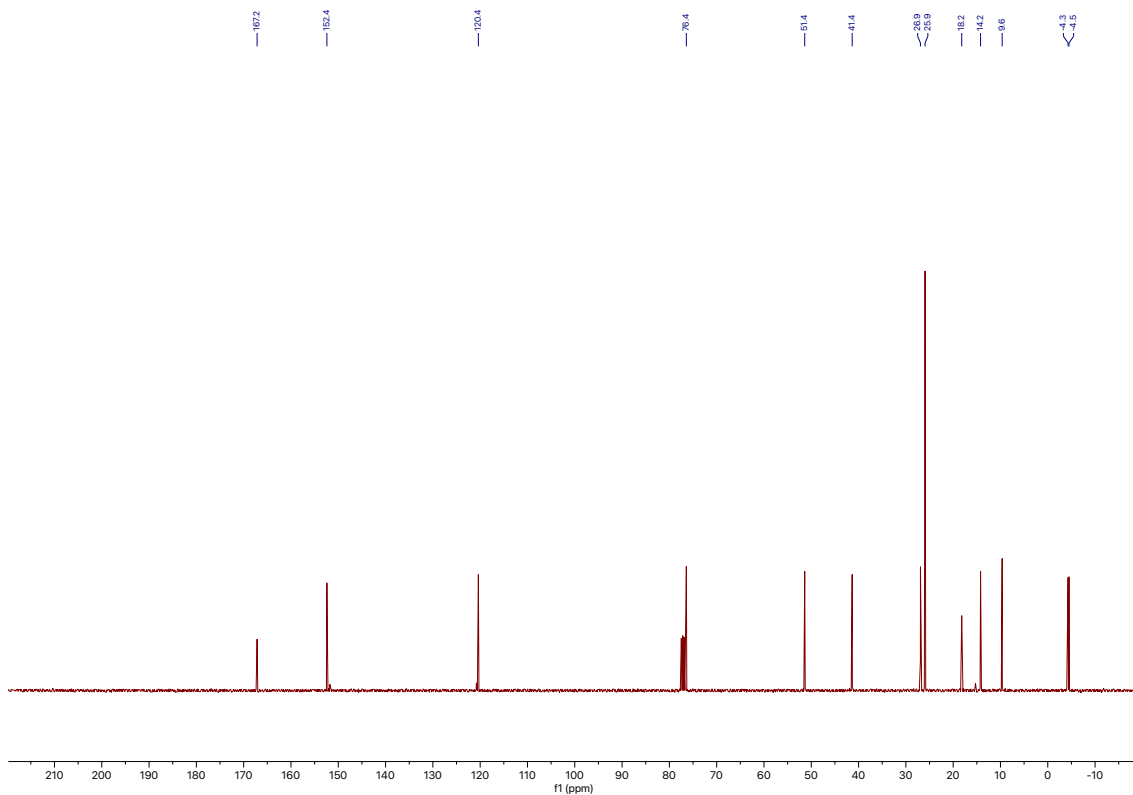




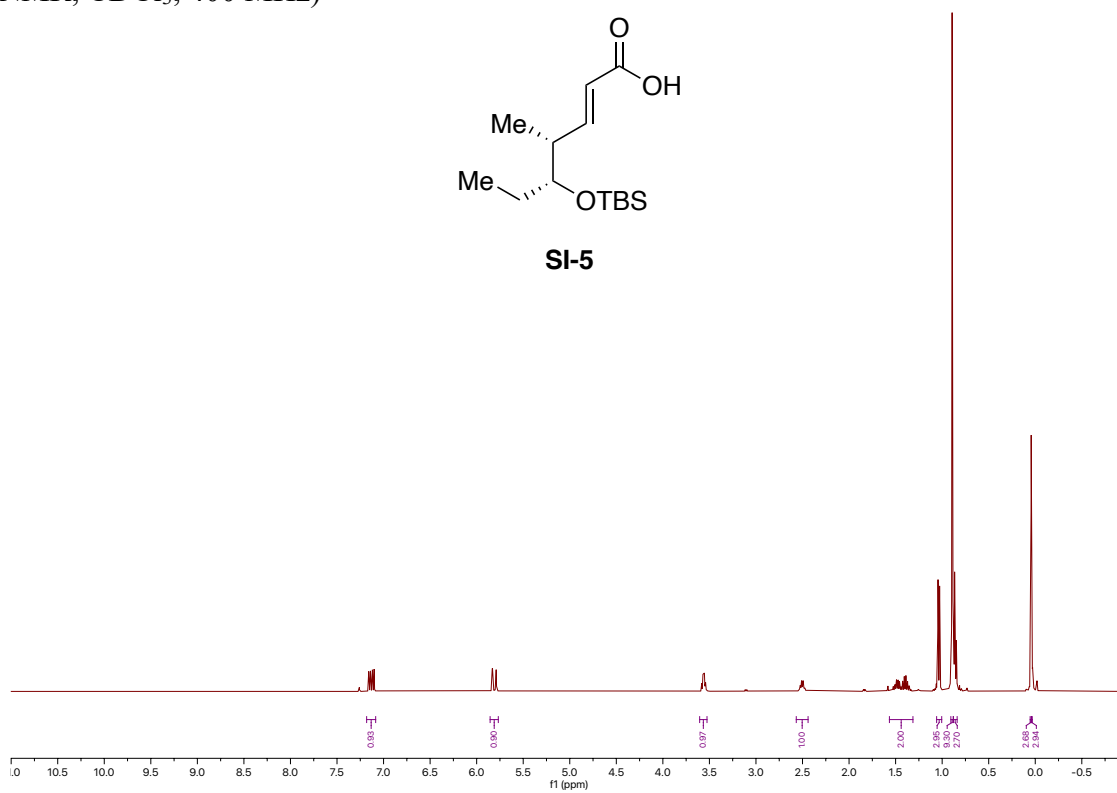
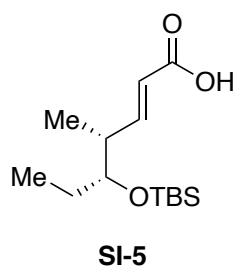
(<sup>1</sup>H NMR, CDCl<sub>3</sub>, 400 MHz)



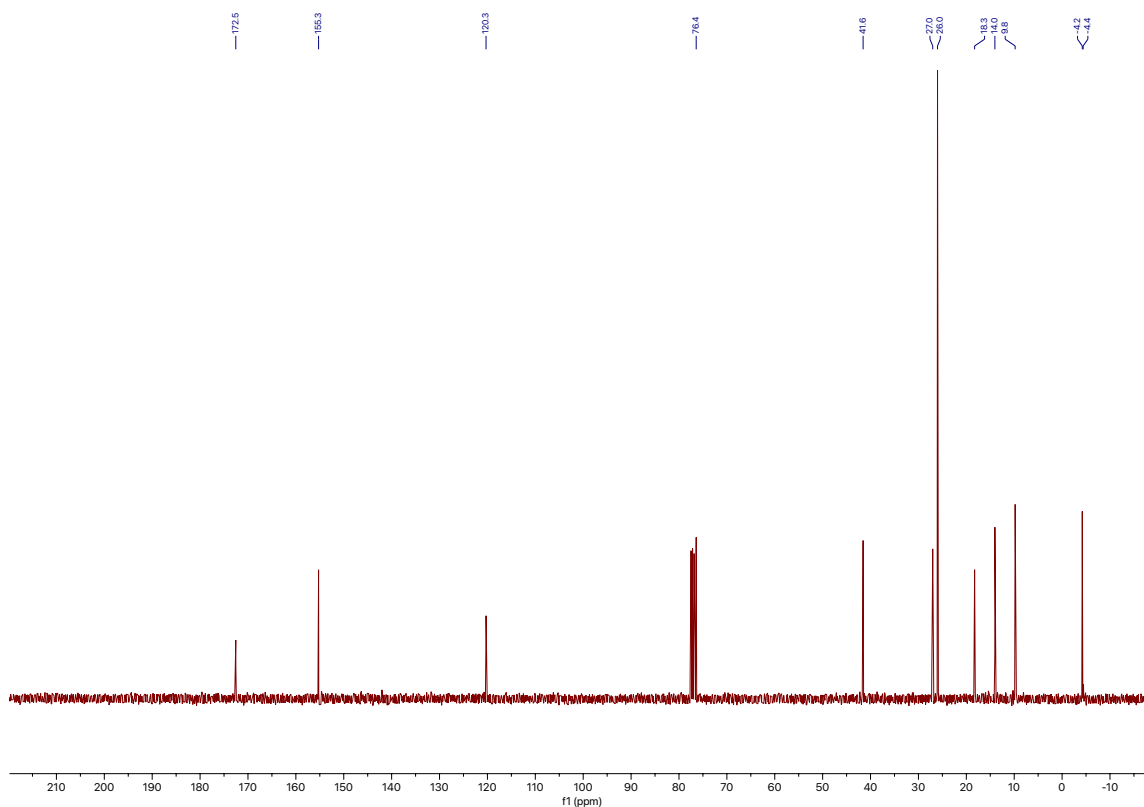
(<sup>13</sup>C NMR, CDCl<sub>3</sub>, 100 MHz)



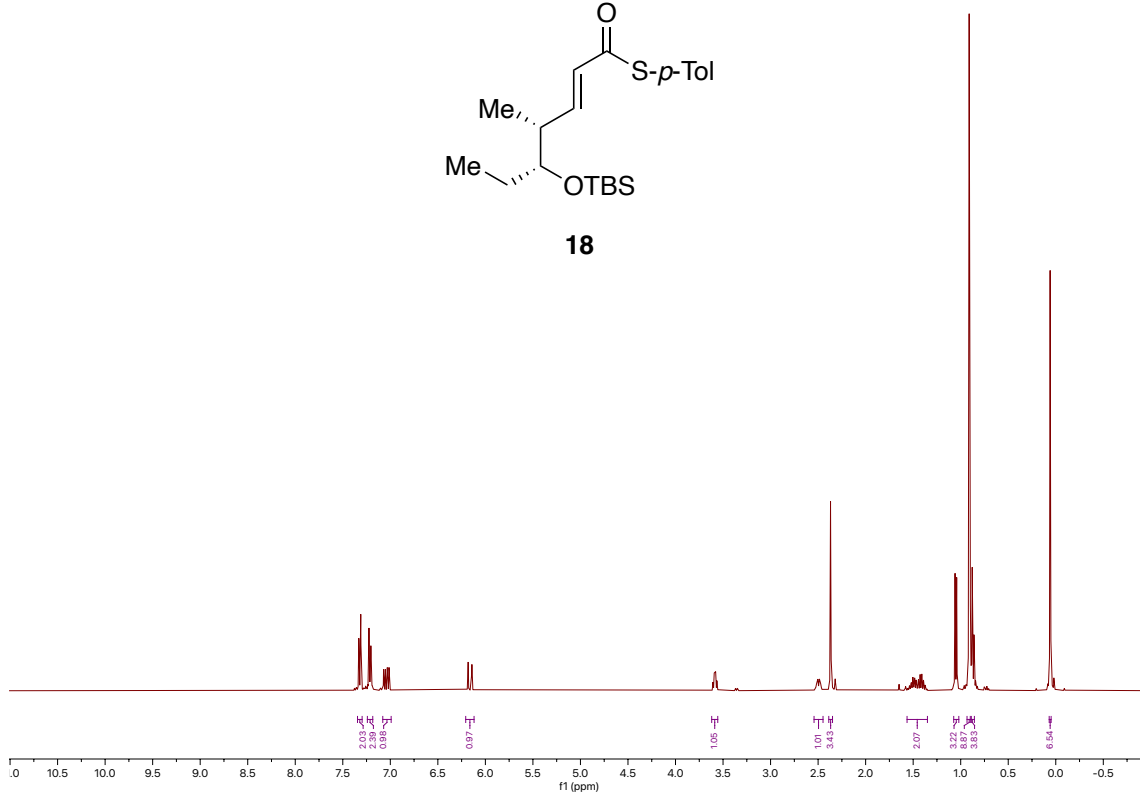
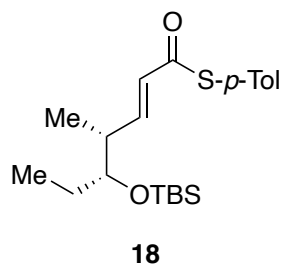
(<sup>1</sup>H NMR, CDCl<sub>3</sub>, 400 MHz)



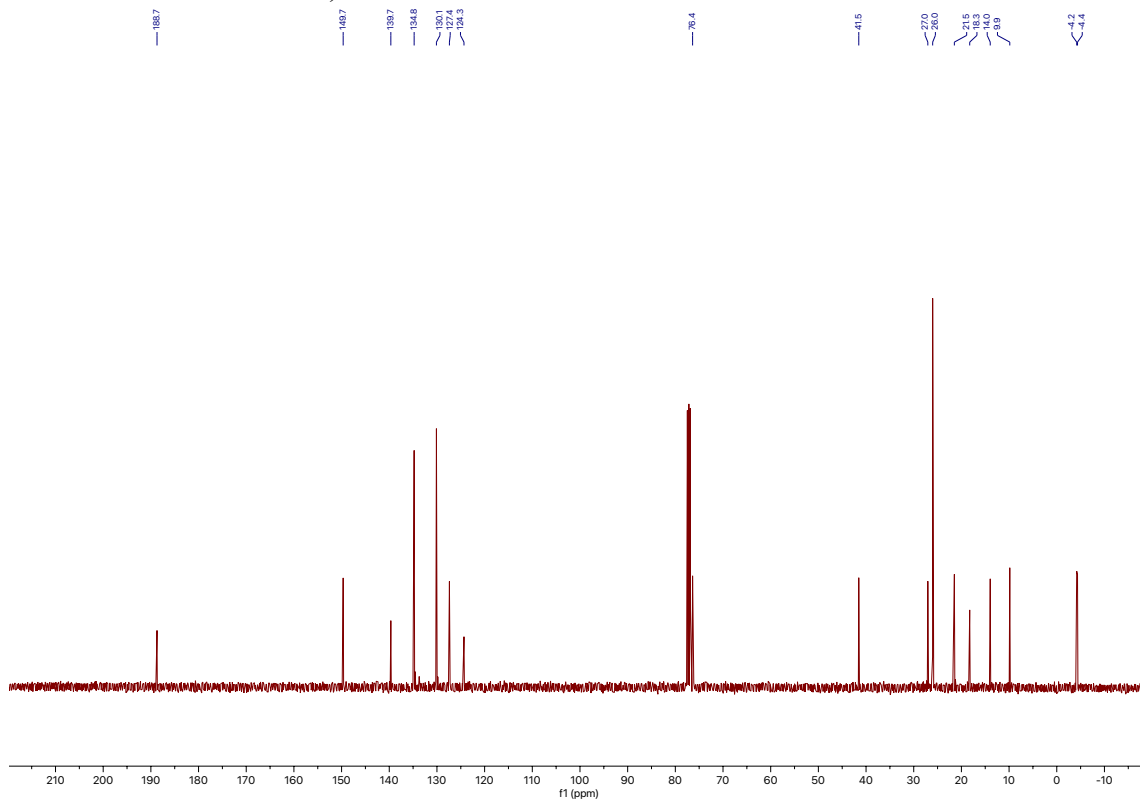
(<sup>13</sup>C NMR, CDCl<sub>3</sub>, 100 MHz)



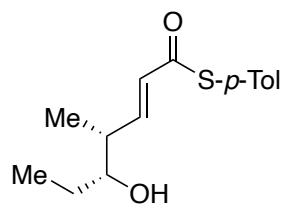
(<sup>1</sup>H NMR, CDCl<sub>3</sub>, 400 MHz)



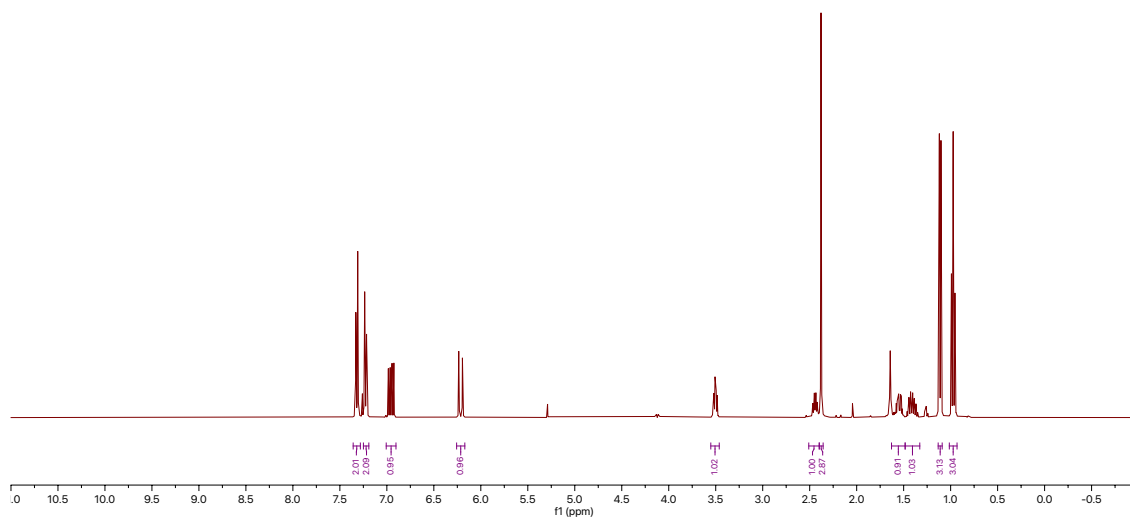
(<sup>13</sup>C NMR, CDCl<sub>3</sub>, 100 MHz)



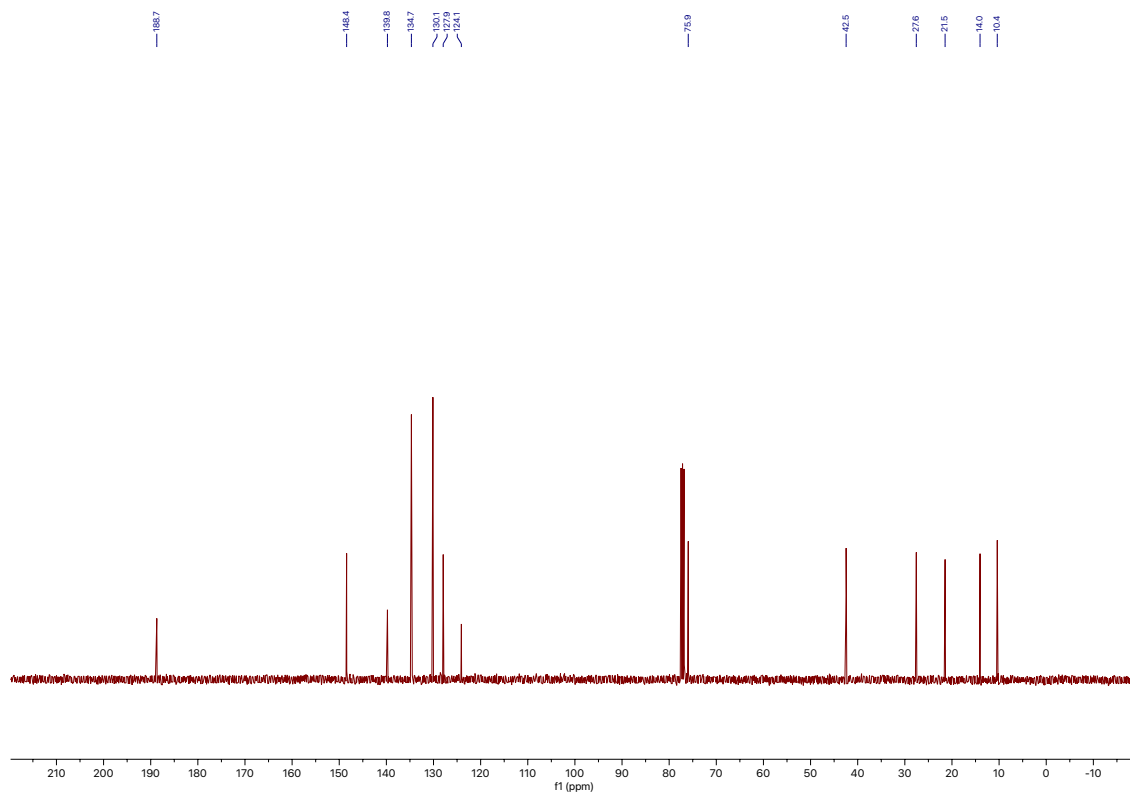
(<sup>1</sup>H NMR, CDCl<sub>3</sub>, 400 MHz)



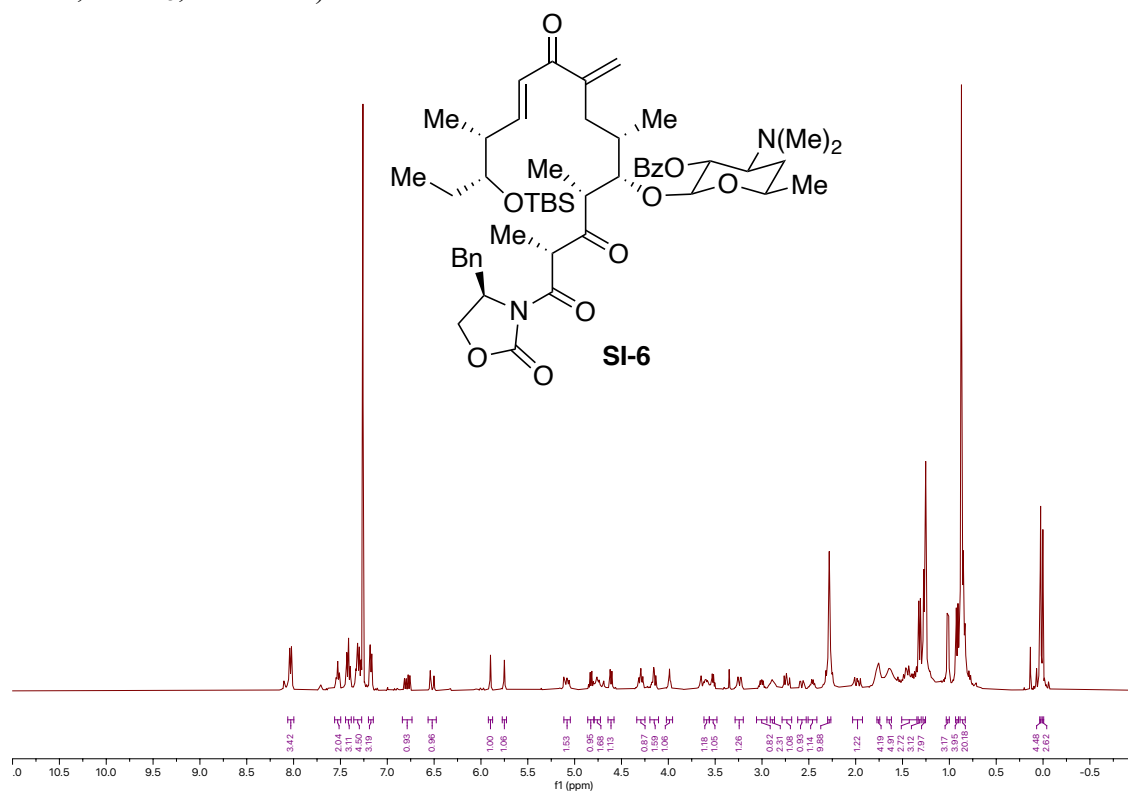
left half (19)



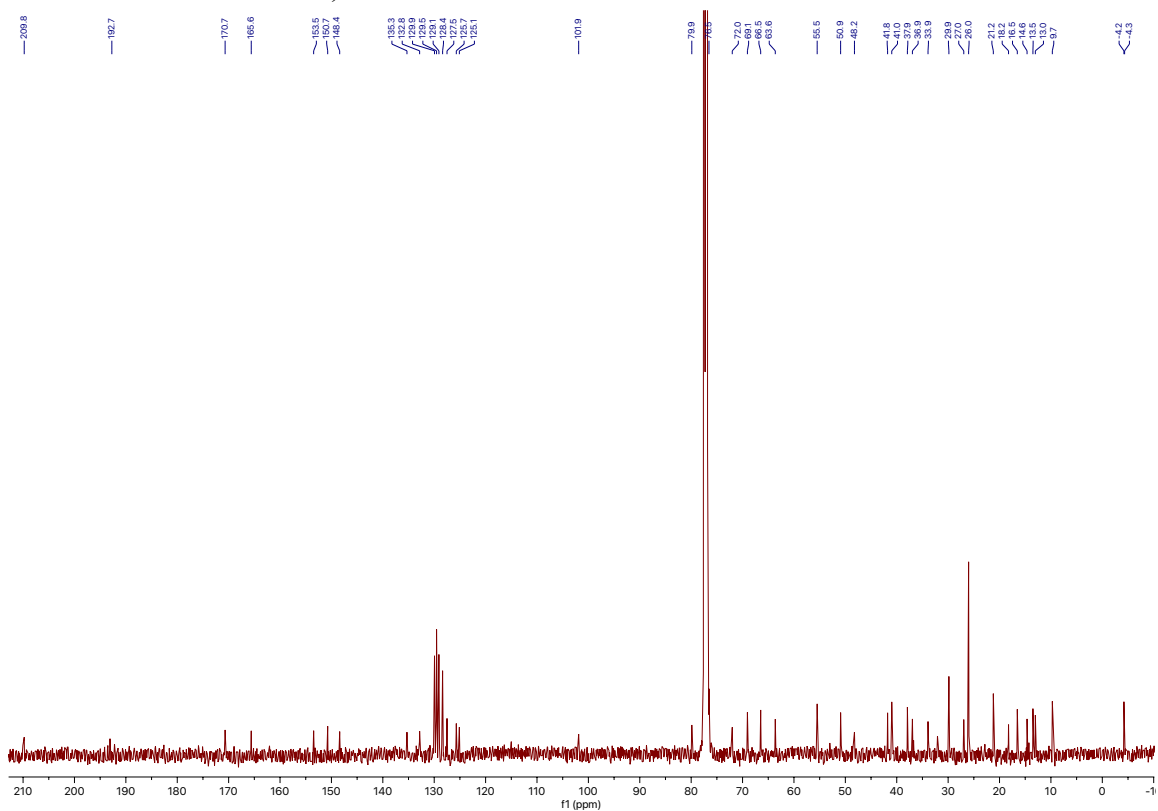
(<sup>13</sup>C NMR, CDCl<sub>3</sub>, 100 MHz)



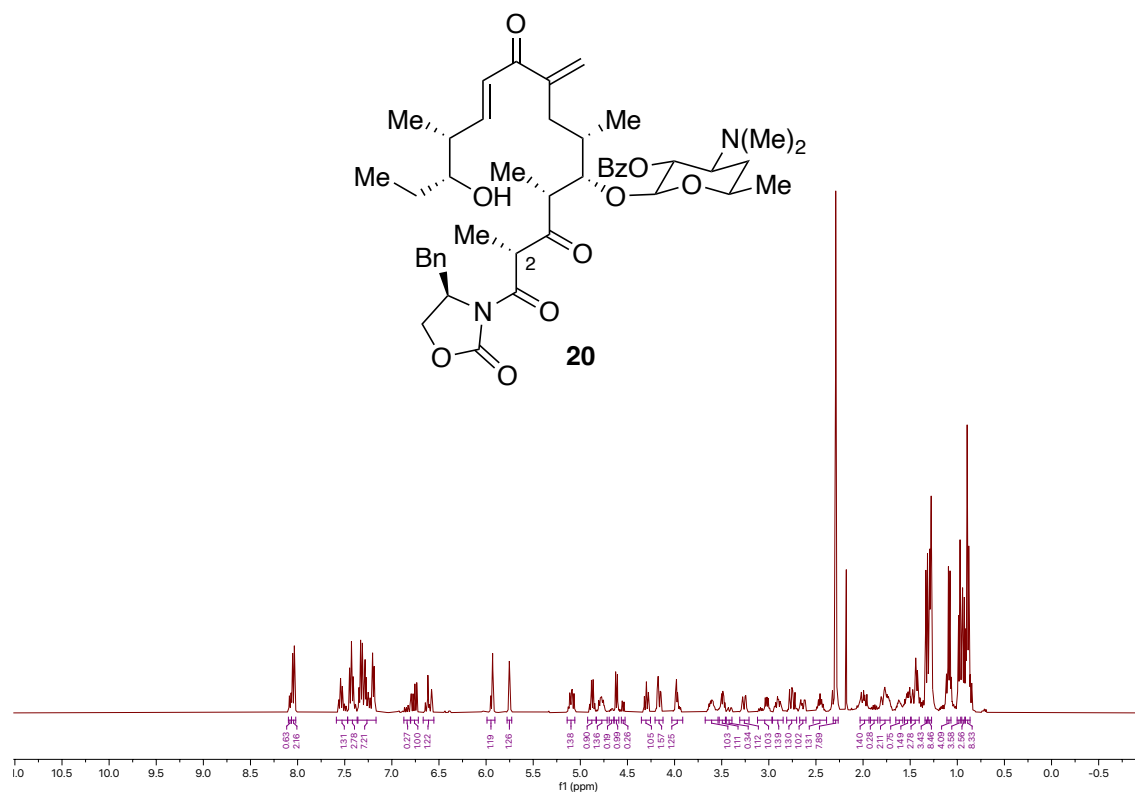
(<sup>1</sup>H NMR, CDCl<sub>3</sub>, 400 MHz)



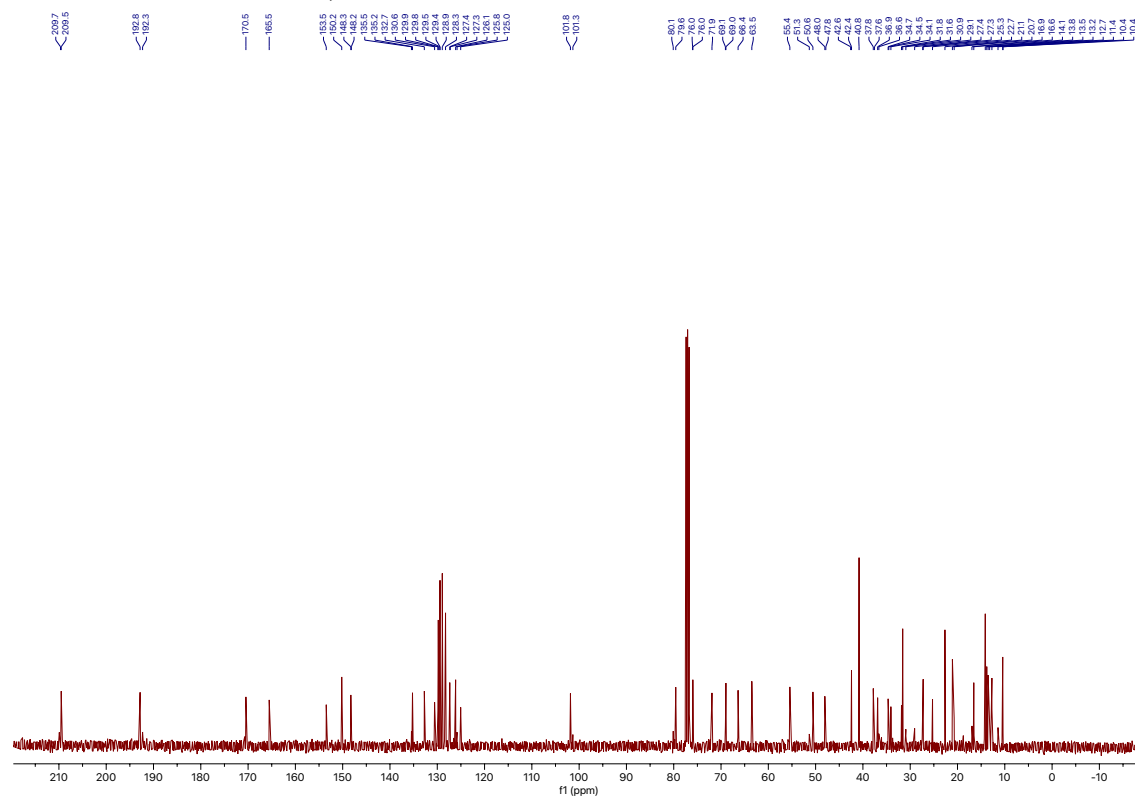
(<sup>13</sup>C NMR, CDCl<sub>3</sub>, 126 MHz)



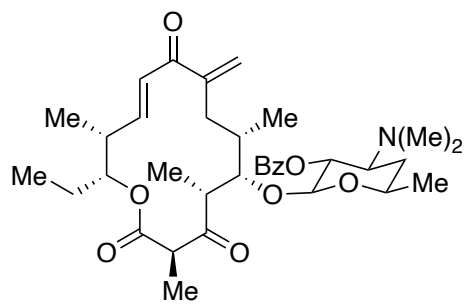
(<sup>1</sup>H NMR, CDCl<sub>3</sub>, 400 MHz)



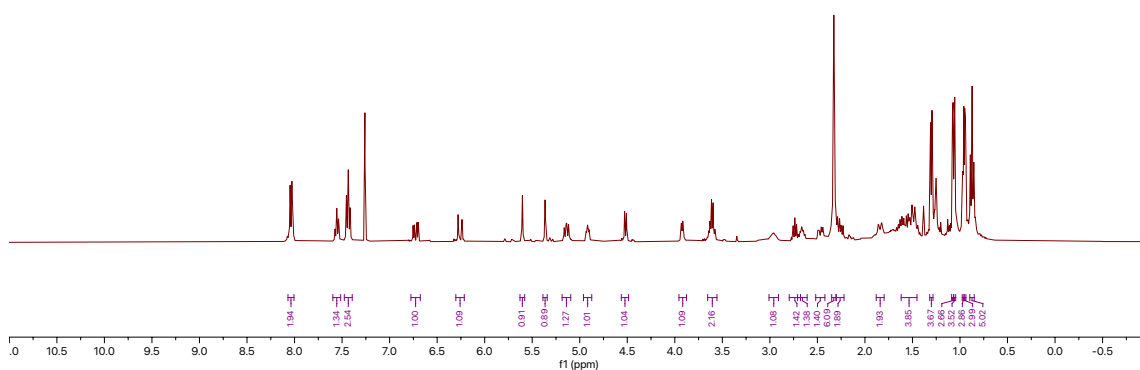
(<sup>13</sup>C NMR, CDCl<sub>3</sub>, 100 MHz)



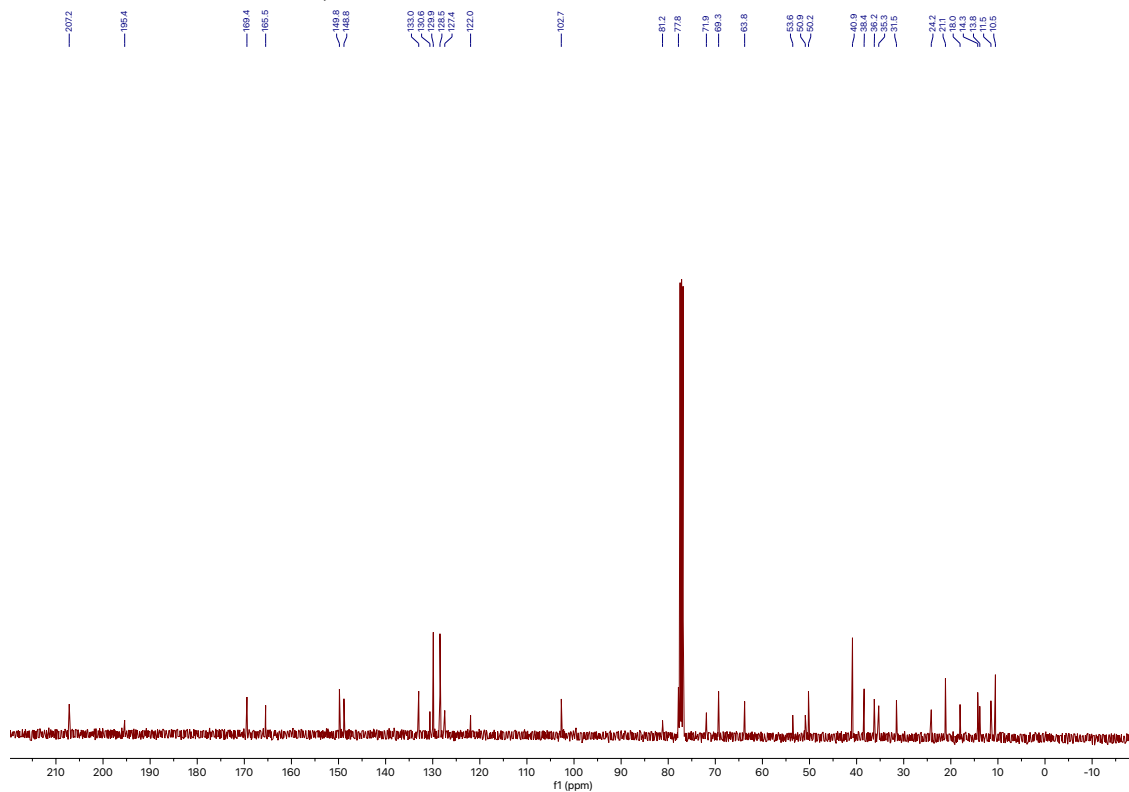
(<sup>1</sup>H NMR, CDCl<sub>3</sub>, 400 MHz)



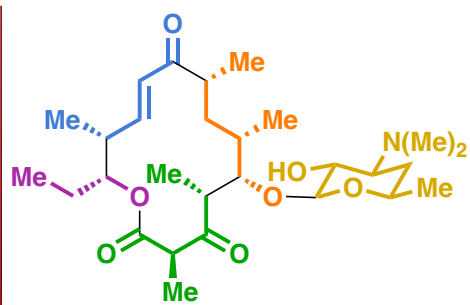
21



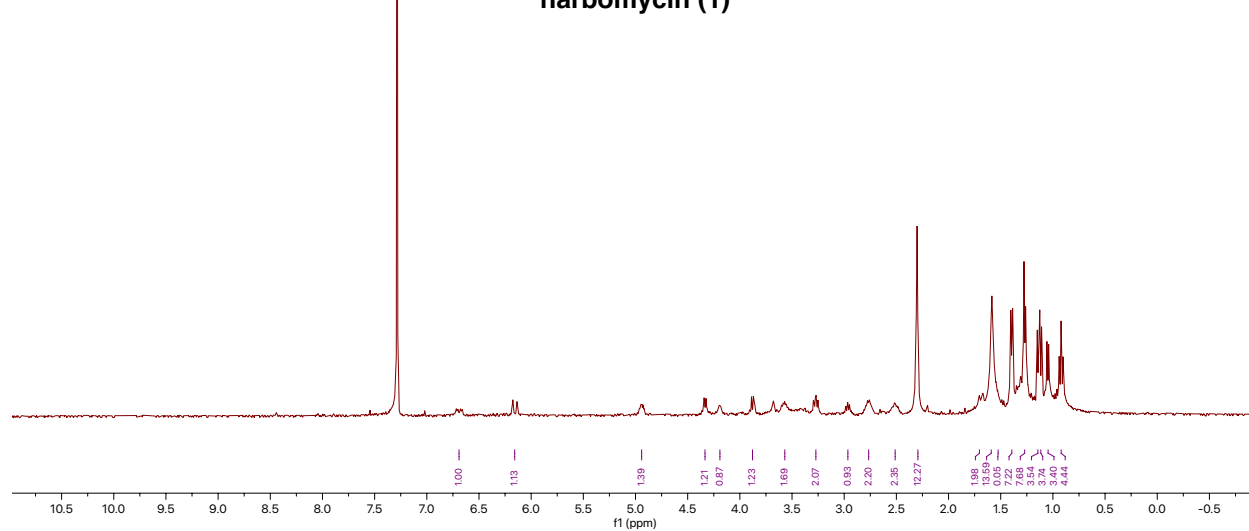
(<sup>13</sup>C NMR, CDCl<sub>3</sub>, 100 MHz)



(<sup>1</sup>H NMR, CDCl<sub>3</sub>, 400 MHz)



narbomycin (1)





## X-Ray Crystallographic Information

Compound **21**: CCDC: 2402908

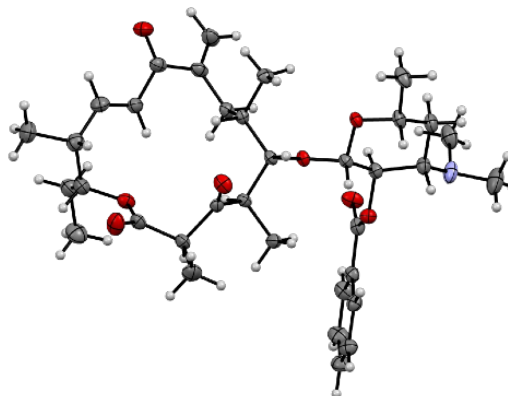
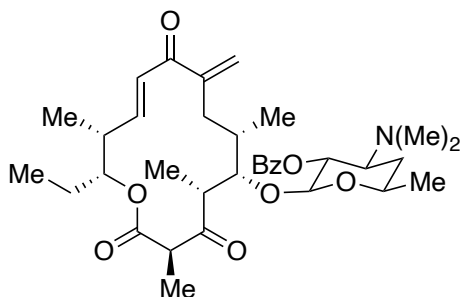


Table 2.1 Crystal data and structure refinement for QEdmondson04\_UCSF.

Identification code	QEdmondson04_UCSF	
Empirical formula	C <sub>35</sub> H <sub>49</sub> N O <sub>8</sub>	
Formula weight	611.75	
Temperature	100(2) K	
Wavelength	1.54178 Å	
Crystal system	Monoclinic	
Space group	C 2	
Unit cell dimensions	a = 29.099(4) Å	α = 90°.
	b = 9.0828(11) Å	β = 102.811(6)°.
	c = 13.6864(19) Å	γ = 90°.
Volume	3527.2(8) Å <sup>3</sup>	
Z	4	
Density (calculated)	1.152 Mg/m <sup>3</sup>	
Absorption coefficient	0.656 mm <sup>-1</sup>	
F(000)	1320	
Crystal size	0.250 x 0.100 x 0.080 mm <sup>3</sup>	
Theta range for data collection	3.311 to 68.638°.	
Index ranges	-34 ≤ h ≤ 34, -9 ≤ k ≤ 10, -16 ≤ l ≤ 16	
Reflections collected	49611	
Independent reflections	6293 [R(int) = 0.0415]	
Completeness to theta = 68.000°	99.8 %	
Absorption correction	Semi-empirical from equivalents	
Max. and min. transmission	0.7531 and 0.6947	

Refinement method	Full-matrix least-squares on F <sup>2</sup>
Data / restraints / parameters	6293 / 1 / 413
Goodness-of-fit on F <sup>2</sup>	1.029
Final R indices [I>2sigma(I)]	R1 = 0.0437, wR2 = 0.1204
R indices (all data)	R1 = 0.0442, wR2 = 0.1210
Absolute structure parameter	0.11(4)
Extinction coefficient	n/a
Largest diff. peak and hole	0.427 and -0.226 e.Å <sup>-3</sup>

Table 2.2 Atomic coordinates ( x 10<sup>4</sup>) and equivalent isotropic displacement parameters (Å<sup>2</sup>x 10<sup>3</sup>) for qedmondson04\_UCSF. U(eq) is defined as one third of the trace of the orthogonalized U<sup>ij</sup> tensor.

	x	y	z	U(eq)
O(1)	5597(1)	-675(2)	1604(2)	52(1)
O(2)	5945(1)	5156(2)	1986(2)	38(1)
O(3)	6476(1)	5989(3)	3321(2)	56(1)
O(4)	5509(1)	4689(3)	4238(2)	41(1)
O(5)	4136(1)	3781(2)	2780(1)	27(1)
O(6)	3889(1)	2535(2)	3996(1)	30(1)
O(7)	3354(1)	5742(2)	2632(1)	32(1)
O(8)	3044(1)	5117(2)	1029(2)	44(1)
N(1)	2526(1)	4295(4)	3059(2)	48(1)
C(1)	4638(1)	3765(3)	3191(2)	26(1)
C(2)	4853(1)	2368(3)	2854(2)	27(1)
C(3)	4759(1)	1013(3)	3445(2)	35(1)
C(4)	4684(1)	2090(3)	1718(2)	31(1)
C(5)	4888(1)	701(3)	1373(2)	37(1)
C(6)	4623(1)	-410(4)	940(3)	49(1)
C(7)	5414(1)	532(3)	1531(2)	38(1)
C(8)	5700(1)	1907(3)	1588(2)	38(1)
C(9)	6168(1)	1873(4)	1789(2)	42(1)
C(10)	6508(1)	3160(4)	1965(3)	44(1)
C(11)	6961(1)	2793(5)	1641(3)	58(1)
C(12)	6309(1)	4634(3)	1507(2)	41(1)
C(13)	6111(1)	4645(4)	401(3)	49(1)

Table 2.2 (continued) Atomic coordinates ( $\times 10^4$ ) and equivalent isotropic displacement parameters ( $\text{\AA}^2 \times 10^3$ ) for qedmondson04\_UCSF.  $U(\text{eq})$  is defined as one third of the trace of the orthogonalized  $U^{ij}$  tensor.

	x	y	z	$U(\text{eq})$
C(14)	5924(2)	6160(5)	7(3)	61(1)
C(15)	6075(1)	5892(3)	2855(2)	39(1)
C(16)	5654(1)	6588(3)	3155(2)	37(1)
C(17)	5817(1)	7679(4)	4017(3)	54(1)
C(18)	5353(1)	5383(3)	3480(2)	29(1)
C(19)	4853(1)	5199(3)	2884(2)	27(1)
C(20)	4578(1)	6584(3)	3063(2)	37(1)
C(21)	3864(1)	3905(3)	3495(2)	27(1)
C(22)	3627(1)	2551(4)	4768(2)	36(1)
C(23)	3756(1)	1161(4)	5358(2)	47(1)
C(24)	3107(1)	2668(4)	4260(2)	39(1)
C(25)	3014(1)	4085(4)	3639(2)	37(1)
C(26)	2209(1)	4655(7)	3701(3)	74(1)
C(27)	2337(1)	3062(5)	2412(3)	54(1)
C(28)	3359(1)	4224(3)	2953(2)	29(1)
C(29)	3183(1)	6042(3)	1657(2)	32(1)
C(30)	3196(1)	7661(3)	1465(2)	32(1)
C(31)	3000(1)	8172(4)	502(2)	42(1)
C(32)	3007(1)	9667(4)	287(3)	47(1)
C(33)	3214(1)	10656(4)	1026(2)	45(1)
C(34)	3411(1)	10160(4)	1987(2)	40(1)
C(35)	3402(1)	8666(3)	2207(2)	35(1)

Table 2.3 Bond lengths [ $\text{\AA}$ ] and angles [ $^\circ$ ] for qedmondson04\_UCSF.

O(1)-C(7)	1.212(4)
O(2)-C(15)	1.344(4)
O(2)-C(12)	1.446(4)
O(3)-C(15)	1.201(4)
O(4)-C(18)	1.213(3)

Table 2.3 (continued) Bond lengths [ $\text{\AA}$ ] and angles [ $^\circ$ ] for qedmondson04\_UCSF.

---

O(5)-C(21)	1.393(3)
O(5)-C(1)	1.445(3)
O(6)-C(21)	1.415(3)
O(6)-C(22)	1.434(3)
O(7)-C(29)	1.345(3)
O(7)-C(28)	1.446(3)
O(8)-C(29)	1.206(4)
N(1)-C(26)	1.445(4)
N(1)-C(27)	1.458(5)
N(1)-C(25)	1.477(4)
C(1)-C(2)	1.530(4)
C(1)-C(19)	1.543(3)
C(1)-H(1)	1.0000
C(2)-C(3)	1.531(4)
C(2)-C(4)	1.543(4)
C(2)-H(2)	1.0000
C(3)-H(3A)	0.9800
C(3)-H(3B)	0.9800
C(3)-H(3C)	0.9800
C(4)-C(5)	1.514(4)
C(4)-H(4A)	0.9900
C(4)-H(4B)	0.9900
C(5)-C(6)	1.328(4)
C(5)-C(7)	1.505(4)
C(6)-H(6A)	0.98(4)
C(6)-H(6B)	0.95(5)
C(7)-C(8)	1.492(4)
C(8)-C(9)	1.329(4)
C(8)-H(8)	0.9500
C(9)-C(10)	1.516(5)
C(9)-H(9)	0.9500
C(10)-C(11)	1.519(5)
C(10)-C(12)	1.536(5)
C(10)-H(10)	1.0000

Table 2.3 (continued) Bond lengths [ $\text{\AA}$ ] and angles [ $^\circ$ ] for qedmondson04\_UCSF.

---

C(11)-H(11A)	0.9800
C(11)-H(11B)	0.9800
C(11)-H(11C)	0.9800
C(12)-C(13)	1.495(5)
C(12)-H(12)	1.0000
C(13)-C(14)	1.533(6)
C(13)-H(13A)	0.9900
C(13)-H(13B)	0.9900
C(14)-H(14A)	0.9800
C(14)-H(14B)	0.9800
C(14)-H(14C)	0.9800
C(15)-C(16)	1.513(4)
C(16)-C(18)	1.530(4)
C(16)-C(17)	1.533(4)
C(16)-H(16)	1.0000
C(17)-H(17A)	0.9800
C(17)-H(17B)	0.9800
C(17)-H(17C)	0.9800
C(18)-C(19)	1.511(3)
C(19)-C(20)	1.539(4)
C(19)-H(19)	1.0000
C(20)-H(20A)	0.9800
C(20)-H(20B)	0.9800
C(20)-H(20C)	0.9800
C(21)-C(28)	1.518(3)
C(21)-H(21)	1.0000
C(22)-C(23)	1.501(4)
C(22)-C(24)	1.522(4)
C(22)-H(22)	1.0000
C(23)-H(23A)	0.9800
C(23)-H(23B)	0.9800
C(23)-H(23C)	0.9800
C(24)-C(25)	1.533(4)
C(24)-H(24A)	0.9900

Table 2.3 (continued) Bond lengths [ $\text{\AA}$ ] and angles [ $^\circ$ ] for qedmondson04\_UCSF.

---

C(24)-H(24B)	0.9900
C(25)-C(28)	1.525(4)
C(25)-H(25)	1.0000
C(26)-H(26A)	0.9800
C(26)-H(26B)	0.9800
C(26)-H(26C)	0.9800
C(27)-H(27A)	0.9800
C(27)-H(27B)	0.9800
C(27)-H(27C)	0.9800
C(28)-H(28)	1.0000
C(29)-C(30)	1.495(4)
C(30)-C(31)	1.393(4)
C(30)-C(35)	1.398(4)
C(31)-C(32)	1.391(5)
C(31)-H(31)	0.9500
C(32)-C(33)	1.386(5)
C(32)-H(32)	0.9500
C(33)-C(34)	1.389(4)
C(33)-H(33)	0.9500
C(34)-C(35)	1.391(5)
C(34)-H(34)	0.9500
C(35)-H(35)	0.9500
C(15)-O(2)-C(12)	118.2(2)
C(21)-O(5)-C(1)	114.25(17)
C(21)-O(6)-C(22)	111.7(2)
C(29)-O(7)-C(28)	118.1(2)
C(26)-N(1)-C(27)	109.8(3)
C(26)-N(1)-C(25)	111.7(3)
C(27)-N(1)-C(25)	114.5(3)
O(5)-C(1)-C(2)	109.7(2)
O(5)-C(1)-C(19)	108.7(2)
C(2)-C(1)-C(19)	113.6(2)
O(5)-C(1)-H(1)	108.2

Table 2.3 (continued) Bond lengths [ $\text{\AA}$ ] and angles [ $^\circ$ ] for qedmondson04\_UCSF.

---

C(2)-C(1)-H(1)	108.2
C(19)-C(1)-H(1)	108.2
C(1)-C(2)-C(3)	112.0(2)
C(1)-C(2)-C(4)	112.3(2)
C(3)-C(2)-C(4)	110.3(2)
C(1)-C(2)-H(2)	107.3
C(3)-C(2)-H(2)	107.3
C(4)-C(2)-H(2)	107.3
C(2)-C(3)-H(3A)	109.5
C(2)-C(3)-H(3B)	109.5
H(3A)-C(3)-H(3B)	109.5
C(2)-C(3)-H(3C)	109.5
H(3A)-C(3)-H(3C)	109.5
H(3B)-C(3)-H(3C)	109.5
C(5)-C(4)-C(2)	113.0(2)
C(5)-C(4)-H(4A)	109.0
C(2)-C(4)-H(4A)	109.0
C(5)-C(4)-H(4B)	109.0
C(2)-C(4)-H(4B)	109.0
H(4A)-C(4)-H(4B)	107.8
C(6)-C(5)-C(7)	117.4(3)
C(6)-C(5)-C(4)	122.8(3)
C(7)-C(5)-C(4)	119.8(2)
C(5)-C(6)-H(6A)	119(2)
C(5)-C(6)-H(6B)	128(3)
H(6A)-C(6)-H(6B)	112(4)
O(1)-C(7)-C(8)	121.6(3)
O(1)-C(7)-C(5)	121.1(3)
C(8)-C(7)-C(5)	117.3(3)
C(9)-C(8)-C(7)	121.6(3)
C(9)-C(8)-H(8)	119.2
C(7)-C(8)-H(8)	119.2
C(8)-C(9)-C(10)	128.2(3)
C(8)-C(9)-H(9)	115.9

Table 2.3 (continued) Bond lengths [ $\text{\AA}$ ] and angles [ $^\circ$ ] for qedmondson04\_UCSF.

---

C(10)-C(9)-H(9)	115.9
C(9)-C(10)-C(11)	111.3(3)
C(9)-C(10)-C(12)	115.7(3)
C(11)-C(10)-C(12)	110.2(3)
C(9)-C(10)-H(10)	106.4
C(11)-C(10)-H(10)	106.4
C(12)-C(10)-H(10)	106.4
C(10)-C(11)-H(11A)	109.5
C(10)-C(11)-H(11B)	109.5
H(11A)-C(11)-H(11B)	109.5
C(10)-C(11)-H(11C)	109.5
H(11A)-C(11)-H(11C)	109.5
H(11B)-C(11)-H(11C)	109.5
O(2)-C(12)-C(13)	107.5(2)
O(2)-C(12)-C(10)	110.4(2)
C(13)-C(12)-C(10)	116.4(3)
O(2)-C(12)-H(12)	107.4
C(13)-C(12)-H(12)	107.4
C(10)-C(12)-H(12)	107.4
C(12)-C(13)-C(14)	112.9(3)
C(12)-C(13)-H(13A)	109.0
C(14)-C(13)-H(13A)	109.0
C(12)-C(13)-H(13B)	109.0
C(14)-C(13)-H(13B)	109.0
H(13A)-C(13)-H(13B)	107.8
C(13)-C(14)-H(14A)	109.5
C(13)-C(14)-H(14B)	109.5
H(14A)-C(14)-H(14B)	109.5
C(13)-C(14)-H(14C)	109.5
H(14A)-C(14)-H(14C)	109.5
H(14B)-C(14)-H(14C)	109.5
O(3)-C(15)-O(2)	123.8(3)
O(3)-C(15)-C(16)	125.0(3)
O(2)-C(15)-C(16)	111.1(2)



Table 2.3 (continued) Bond lengths [ $\text{\AA}$ ] and angles [ $^\circ$ ] for qedmondson04\_UCSF.

---

C(15)-C(16)-C(18)	109.3(2)
C(15)-C(16)-C(17)	110.4(2)
C(18)-C(16)-C(17)	109.7(3)
C(15)-C(16)-H(16)	109.1
C(18)-C(16)-H(16)	109.1
C(17)-C(16)-H(16)	109.1
C(16)-C(17)-H(17A)	109.5
C(16)-C(17)-H(17B)	109.5
H(17A)-C(17)-H(17B)	109.5
C(16)-C(17)-H(17C)	109.5
H(17A)-C(17)-H(17C)	109.5
H(17B)-C(17)-H(17C)	109.5
O(4)-C(18)-C(19)	122.6(2)
O(4)-C(18)-C(16)	119.3(2)
C(19)-C(18)-C(16)	117.9(2)
C(18)-C(19)-C(20)	107.2(2)
C(18)-C(19)-C(1)	110.2(2)
C(20)-C(19)-C(1)	113.0(2)
C(18)-C(19)-H(19)	108.8
C(20)-C(19)-H(19)	108.8
C(1)-C(19)-H(19)	108.8
C(19)-C(20)-H(20A)	109.5
C(19)-C(20)-H(20B)	109.5
H(20A)-C(20)-H(20B)	109.5
C(19)-C(20)-H(20C)	109.5
H(20A)-C(20)-H(20C)	109.5
H(20B)-C(20)-H(20C)	109.5
O(5)-C(21)-O(6)	107.0(2)
O(5)-C(21)-C(28)	108.07(19)
O(6)-C(21)-C(28)	110.2(2)
O(5)-C(21)-H(21)	110.5
O(6)-C(21)-H(21)	110.5
C(28)-C(21)-H(21)	110.5
O(6)-C(22)-C(23)	106.1(2)

Table 2.3 (continued) Bond lengths [Å] and angles [°] for qedmondson04\_UCSF.

---

O(6)-C(22)-C(24)	107.6(2)
C(23)-C(22)-C(24)	114.2(2)
O(6)-C(22)-H(22)	109.6
C(23)-C(22)-H(22)	109.6
C(24)-C(22)-H(22)	109.6
C(22)-C(23)-H(23A)	109.5
C(22)-C(23)-H(23B)	109.5
H(23A)-C(23)-H(23B)	109.5
C(22)-C(23)-H(23C)	109.5
H(23A)-C(23)-H(23C)	109.5
H(23B)-C(23)-H(23C)	109.5
C(22)-C(24)-C(25)	110.3(2)
C(22)-C(24)-H(24A)	109.6
C(25)-C(24)-H(24A)	109.6
C(22)-C(24)-H(24B)	109.6
C(25)-C(24)-H(24B)	109.6
H(24A)-C(24)-H(24B)	108.1
N(1)-C(25)-C(28)	110.2(2)
N(1)-C(25)-C(24)	115.9(3)
C(28)-C(25)-C(24)	110.6(2)
N(1)-C(25)-H(25)	106.5
C(28)-C(25)-H(25)	106.5
C(24)-C(25)-H(25)	106.5
N(1)-C(26)-H(26A)	109.5
N(1)-C(26)-H(26B)	109.5
H(26A)-C(26)-H(26B)	109.5
N(1)-C(26)-H(26C)	109.5
H(26A)-C(26)-H(26C)	109.5
H(26B)-C(26)-H(26C)	109.5
N(1)-C(27)-H(27A)	109.5
N(1)-C(27)-H(27B)	109.5
H(27A)-C(27)-H(27B)	109.5
N(1)-C(27)-H(27C)	109.5
H(27A)-C(27)-H(27C)	109.5

Table 2.3 (continued) Bond lengths [Å] and angles [°] for qedmondson04\_UCSF.

---

H(27B)-C(27)-H(27C)	109.5
O(7)-C(28)-C(21)	105.9(2)
O(7)-C(28)-C(25)	107.6(2)
C(21)-C(28)-C(25)	112.4(2)
O(7)-C(28)-H(28)	110.3
C(21)-C(28)-H(28)	110.3
C(25)-C(28)-H(28)	110.3
O(8)-C(29)-O(7)	123.9(3)
O(8)-C(29)-C(30)	125.2(2)
O(7)-C(29)-C(30)	110.9(2)
C(31)-C(30)-C(35)	119.3(3)
C(31)-C(30)-C(29)	118.2(3)
C(35)-C(30)-C(29)	122.5(2)
C(32)-C(31)-C(30)	120.2(3)
C(32)-C(31)-H(31)	119.9
C(30)-C(31)-H(31)	119.9
C(33)-C(32)-C(31)	120.2(3)
C(33)-C(32)-H(32)	119.9
C(31)-C(32)-H(32)	119.9
C(32)-C(33)-C(34)	120.1(3)
C(32)-C(33)-H(33)	119.9
C(34)-C(33)-H(33)	119.9
C(33)-C(34)-C(35)	119.8(3)
C(33)-C(34)-H(34)	120.1
C(35)-C(34)-H(34)	120.1
C(34)-C(35)-C(30)	120.4(3)
C(34)-C(35)-H(35)	119.8
C(30)-C(35)-H(35)	119.8

---

Symmetry transformations used to generate equivalent atoms:

Table 2.4 Anisotropic displacement parameters ( $\text{\AA}^2 \times 10^3$ ) for qedmondson04\_UCSF. The anisotropic displacement factor exponent takes the form:  $-2\pi^2 [ h^2 a^{*2} U^{11} + \dots + 2 h k a^* b^* U^{12} ]$

	U <sup>11</sup>	U <sup>22</sup>	U <sup>33</sup>	U <sup>23</sup>	U <sup>13</sup>	U <sup>12</sup>
O(1)	63(2)	28(1)	69(2)	2(1)	22(1)	1(1)
O(2)	39(1)	33(1)	40(1)	-3(1)	6(1)	-6(1)
O(3)	33(1)	71(2)	62(1)	-20(1)	10(1)	-10(1)
O(4)	32(1)	49(1)	37(1)	4(1)	-2(1)	-7(1)
O(5)	21(1)	31(1)	27(1)	0(1)	3(1)	-3(1)
O(6)	27(1)	31(1)	34(1)	6(1)	9(1)	-2(1)
O(7)	34(1)	29(1)	31(1)	1(1)	4(1)	0(1)
O(8)	49(1)	40(1)	36(1)	-1(1)	-3(1)	-9(1)
N(1)	33(1)	63(2)	50(1)	10(1)	15(1)	17(1)
C(1)	24(1)	28(1)	26(1)	2(1)	3(1)	-4(1)
C(2)	27(1)	27(1)	28(1)	0(1)	5(1)	-2(1)
C(3)	42(1)	29(1)	35(1)	4(1)	9(1)	2(1)
C(4)	35(1)	29(1)	30(1)	0(1)	7(1)	-4(1)
C(5)	49(2)	31(1)	33(1)	-4(1)	14(1)	-10(1)
C(6)	58(2)	40(2)	52(2)	-15(1)	21(2)	-16(2)
C(7)	51(2)	30(2)	36(1)	-3(1)	18(1)	-4(1)
C(8)	44(2)	29(2)	44(2)	-1(1)	15(1)	0(1)
C(9)	43(2)	34(2)	49(2)	2(1)	10(1)	5(1)
C(10)	38(2)	44(2)	49(2)	-1(1)	9(1)	2(1)
C(11)	45(2)	60(2)	73(2)	-1(2)	21(2)	6(2)
C(12)	38(1)	34(2)	54(2)	-1(1)	15(1)	-5(1)
C(13)	54(2)	45(2)	51(2)	0(2)	18(2)	-6(2)
C(14)	65(2)	64(2)	54(2)	16(2)	13(2)	3(2)
C(15)	33(1)	34(2)	50(2)	-4(1)	10(1)	-9(1)
C(16)	32(1)	26(1)	54(2)	-1(1)	11(1)	-6(1)
C(17)	50(2)	39(2)	74(2)	-21(2)	19(2)	-11(2)
C(18)	27(1)	24(1)	36(1)	-7(1)	9(1)	-4(1)
C(19)	27(1)	24(1)	29(1)	0(1)	6(1)	-4(1)
C(20)	31(1)	26(1)	53(2)	1(1)	10(1)	0(1)
C(21)	28(1)	27(1)	28(1)	1(1)	7(1)	-3(1)
C(22)	33(1)	43(2)	34(1)	6(1)	12(1)	-6(1)

Table 2.4 (continued) Anisotropic displacement parameters ( $\text{\AA}^2 \times 10^3$ ) for qedmondson04\_UCSF. The anisotropic displacement factor exponent takes the form:  $-2\pi^2 [h^2 a^{*2} U^{11} + \dots + 2 h k a^* b^* U^{12}]$

	U <sup>11</sup>	U <sup>22</sup>	U <sup>33</sup>	U <sup>23</sup>	U <sup>13</sup>	U <sup>12</sup>
C(23)	37(2)	56(2)	47(2)	21(2)	7(1)	-2(1)
C(24)	31(1)	48(2)	41(2)	8(1)	13(1)	-1(1)
C(25)	31(1)	42(2)	40(1)	3(1)	13(1)	4(1)
C(26)	47(2)	111(4)	71(2)	16(2)	27(2)	32(2)
C(27)	27(1)	75(3)	56(2)	9(2)	2(1)	-6(2)
C(28)	28(1)	29(1)	31(1)	1(1)	5(1)	-1(1)
C(29)	23(1)	39(2)	32(1)	2(1)	2(1)	-1(1)
C(30)	24(1)	33(1)	39(1)	3(1)	4(1)	-1(1)
C(31)	35(1)	45(2)	39(2)	4(1)	-2(1)	-3(1)
C(32)	44(2)	45(2)	46(2)	14(1)	0(1)	2(1)
C(33)	40(2)	37(2)	55(2)	9(1)	4(1)	4(1)
C(34)	37(1)	34(2)	47(2)	1(1)	4(1)	2(1)
C(35)	31(1)	38(2)	34(1)	2(1)	3(1)	5(1)

Table 2.5 Hydrogen coordinates ( $\times 10^4$ ) and isotropic displacement parameters ( $\text{\AA}^2 \times 10^3$ ) for qedmondson04\_UCSF.

	x	y	z	U(eq)
H(1)	4692	3745	3938	31
H(2)	5202	2514	2994	33
H(3A)	4860	1213	4165	53
H(3B)	4936	171	3271	53
H(3C)	4422	786	3279	53
H(4A)	4336	2019	1550	38
H(4B)	4774	2941	1349	38
H(8)	5543	2830	1478	46
H(9)	6307	922	1826	50
H(10)	6597	3314	2707	52
H(11A)	6891	2604	918	88
H(11B)	7105	1915	1999	88

Table 2.5 (continued) Hydrogen coordinates ( $\times 10^4$ ) and isotropic displacement parameters ( $\text{\AA}^2 \times 10^3$ ) for qedmondson04\_UCSF.

	x	y	z	U(eq)
H(11C)	7181	3623	1796	88
H(12)	6572	5368	1649	50
H(13A)	5852	3919	239	59
H(13B)	6360	4337	54	59
H(14A)	5818	6121	-723	92
H(14B)	6176	6893	189	92
H(14C)	5659	6435	305	92
H(16)	5462	7124	2566	45
H(17A)	5541	8093	4219	80
H(17B)	5998	8474	3796	80
H(17C)	6016	7166	4587	80
H(19)	4857	5142	2156	32
H(20A)	4251	6502	2687	55
H(20B)	4724	7455	2837	55
H(20C)	4585	6675	3780	55
H(21)	3987	4711	3980	33
H(22)	3722	3423	5213	43
H(23A)	3657	309	4924	70
H(23B)	3597	1140	5919	70
H(23C)	4097	1128	5617	70
H(24A)	2915	2669	4773	47
H(24B)	3013	1806	3818	47
H(25)	3083	4922	4124	45
H(26A)	2201	3837	4165	111
H(26B)	1892	4823	3291	111
H(26C)	2320	5547	4084	111
H(27A)	2550	2834	1969	81
H(27B)	2026	3324	2007	81
H(27C)	2309	2199	2824	81
H(28)	3264	3560	2360	35
H(31)	2861	7497	-8	50

Table 2.5 (continued) Hydrogen coordinates ( $\times 10^4$ ) and isotropic displacement parameters ( $\text{\AA}^2 \times 10^3$ ) for qedmondson04\_UCSF.

	x	y	z	U(eq)
H(32)	2870	10011	-368	56
H(33)	3220	11676	875	54
H(34)	3553	10838	2493	48
H(35)	3536	8327	2865	42
H(6A)	4774(14)	-1290(50)	740(30)	51(10)
H(6B)	4293(17)	-540(50)	880(30)	64(12)

Table 2.6 Torsion angles [ $^\circ$ ] for qedmondson04\_UCSF.

C(21)-O(5)-C(1)-C(2)	123.6(2)
C(21)-O(5)-C(1)-C(19)	-111.7(2)
O(5)-C(1)-C(2)-C(3)	-77.1(2)
C(19)-C(1)-C(2)-C(3)	161.0(2)
O(5)-C(1)-C(2)-C(4)	47.7(3)
C(19)-C(1)-C(2)-C(4)	-74.2(3)
C(1)-C(2)-C(4)-C(5)	-179.2(2)
C(3)-C(2)-C(4)-C(5)	-53.5(3)
C(2)-C(4)-C(5)-C(6)	119.9(3)
C(2)-C(4)-C(5)-C(7)	-59.2(3)
C(6)-C(5)-C(7)-O(1)	-25.4(4)
C(4)-C(5)-C(7)-O(1)	153.7(3)
C(6)-C(5)-C(7)-C(8)	154.2(3)
C(4)-C(5)-C(7)-C(8)	-26.7(4)
O(1)-C(7)-C(8)-C(9)	-4.7(5)
C(5)-C(7)-C(8)-C(9)	175.7(3)
C(7)-C(8)-C(9)-C(10)	-173.9(3)
C(8)-C(9)-C(10)-C(11)	-150.4(3)
C(8)-C(9)-C(10)-C(12)	-23.7(5)
C(15)-O(2)-C(12)-C(13)	-149.0(3)
C(15)-O(2)-C(12)-C(10)	83.1(3)
C(9)-C(10)-C(12)-O(2)	65.9(3)

Table 2.6 (continued) Torsion angles [°] for qedmondson04\_UCSF.

---

C(11)-C(10)-C(12)-O(2)	-166.8(3)
C(9)-C(10)-C(12)-C(13)	-56.9(4)
C(11)-C(10)-C(12)-C(13)	70.3(4)
O(2)-C(12)-C(13)-C(14)	56.0(4)
C(10)-C(12)-C(13)-C(14)	-179.6(3)
C(12)-O(2)-C(15)-O(3)	-9.4(4)
C(12)-O(2)-C(15)-C(16)	169.8(2)
O(3)-C(15)-C(16)-C(18)	-109.7(4)
O(2)-C(15)-C(16)-C(18)	71.1(3)
O(3)-C(15)-C(16)-C(17)	11.1(5)
O(2)-C(15)-C(16)-C(17)	-168.1(3)
C(15)-C(16)-C(18)-O(4)	67.1(3)
C(17)-C(16)-C(18)-O(4)	-54.1(4)
C(15)-C(16)-C(18)-C(19)	-118.1(3)
C(17)-C(16)-C(18)-C(19)	120.7(3)
O(4)-C(18)-C(19)-C(20)	107.3(3)
C(16)-C(18)-C(19)-C(20)	-67.4(3)
O(4)-C(18)-C(19)-C(1)	-16.1(3)
C(16)-C(18)-C(19)-C(1)	169.3(2)
O(5)-C(1)-C(19)-C(18)	167.46(19)
C(2)-C(1)-C(19)-C(18)	-70.1(2)
O(5)-C(1)-C(19)-C(20)	47.6(3)
C(2)-C(1)-C(19)-C(20)	170.0(2)
C(1)-O(5)-C(21)-O(6)	-72.8(2)
C(1)-O(5)-C(21)-C(28)	168.5(2)
C(22)-O(6)-C(21)-O(5)	178.85(19)
C(22)-O(6)-C(21)-C(28)	-63.9(3)
C(21)-O(6)-C(22)-C(23)	-169.6(2)
C(21)-O(6)-C(22)-C(24)	67.9(3)
O(6)-C(22)-C(24)-C(25)	-60.0(3)
C(23)-C(22)-C(24)-C(25)	-177.4(3)
C(26)-N(1)-C(25)-C(28)	-161.0(3)
C(27)-N(1)-C(25)-C(28)	73.5(3)
C(26)-N(1)-C(25)-C(24)	72.5(4)



Table 2.6 (continued) Torsion angles [°] for qedmondson04\_UCSF.

---

C(27)-N(1)-C(25)-C(24)	-53.0(4)
C(22)-C(24)-C(25)-N(1)	176.8(2)
C(22)-C(24)-C(25)-C(28)	50.5(3)
C(29)-O(7)-C(28)-C(21)	126.1(2)
C(29)-O(7)-C(28)-C(25)	-113.5(2)
O(5)-C(21)-C(28)-O(7)	-74.0(2)
O(6)-C(21)-C(28)-O(7)	169.33(19)
O(5)-C(21)-C(28)-C(25)	168.8(2)
O(6)-C(21)-C(28)-C(25)	52.2(3)
N(1)-C(25)-C(28)-O(7)	68.1(3)
C(24)-C(25)-C(28)-O(7)	-162.5(2)
N(1)-C(25)-C(28)-C(21)	-175.7(2)
C(24)-C(25)-C(28)-C(21)	-46.3(3)
C(28)-O(7)-C(29)-O(8)	-1.9(4)
C(28)-O(7)-C(29)-C(30)	178.8(2)
O(8)-C(29)-C(30)-C(31)	5.2(4)
O(7)-C(29)-C(30)-C(31)	-175.6(2)
O(8)-C(29)-C(30)-C(35)	-173.8(3)
O(7)-C(29)-C(30)-C(35)	5.5(4)
C(35)-C(30)-C(31)-C(32)	-0.5(4)
C(29)-C(30)-C(31)-C(32)	-179.4(3)
C(30)-C(31)-C(32)-C(33)	0.7(5)
C(31)-C(32)-C(33)-C(34)	-0.4(5)
C(32)-C(33)-C(34)-C(35)	0.0(5)
C(33)-C(34)-C(35)-C(30)	0.2(4)
C(31)-C(30)-C(35)-C(34)	0.0(4)
C(29)-C(30)-C(35)-C(34)	179.0(3)

---

Symmetry transformations used to generate equivalent atoms:

## 2.6 References

1. Evans, D. A., Ennis, M. D., Le, T., Mandel, N. & Mandel, G. Asymmetric acylation reactions of chiral imide enolates. The first direct approach to the construction of chiral .beta.-dicarbonyl synthons. *J. Am. Chem. Soc.* **106**, 1154–1156 (1984).
2. Evans, D. A., Kim, A. S., Metternich, R. & Novack, V. J. General Strategies toward the Syntheses of Macrolide Antibiotics. The Total Syntheses of 6-Deoxyerythronolide B and Oleandolide. *J. Am. Chem. Soc.* **120**, 5921–5942 (1998).
3. Evans, D. A., Bender, S. L. & Morris, Joel. The total synthesis of the polyether antibiotic X-206. *J. Am. Chem. Soc.* **110**, 2506–2526 (1988).
4. Woodward, R. B. *et al.* Asymmetric total synthesis of erythromycin. 3. Total synthesis of erythromycin. *J. Am. Chem. Soc.* **103**, 3215–3217 (1981).
5. Zhang, Z., Fukuzaki, T. & Myers, A. G. Synthesis of D-Desosamine and Analogs by Rapid Assembly of 3-Amino Sugars. *Angew. Chem. Int. Ed.* **55**, 523–527 (2016).
6. Simsek, S. & Kalesse, M. Enantioselective synthesis of polyketide segments through vinylogous Mukaiyama aldol reactions. *Tetrahedron Lett.* **50**, 3485–3488 (2009).
7. Li, H., Yang, H. & Liebeskind, L. S. Synthesis of High Enantiopurity N-Protected  $\alpha$ -Amino Ketones by Thiol Ester–Organostannane Cross-Coupling Using pH-Neutral Conditions. *Org. Lett.* **10**, 4375–4378 (2008).
8. Farina, V., Kapadia, S., Krishnan, B., Wang, C. & Liebeskind, L. S. On the Nature of the ‘Copper Effect’ in the Stille Cross-Coupling. *J. Org. Chem.* **59**, 5905–5911 (1994).
9. Piemontesi, C., Wang, Q. & Zhu, J. Enantioselective Synthesis of (+)-Peganumine A. *J. Am. Chem. Soc.* **138**, 11148–11151 (2016).

10. Evans, D. A., Ennis, M. D., Le, T., Mandel, N. & Mandel, G. Asymmetric acylation reactions of chiral imide enolates. The first direct approach to the construction of chiral .beta.-dicarbonyl synthons. *J. Am. Chem. Soc.* **106**, 1154–1156 (1984).
11. Bordwell, F. G. & Fried, H. E. Acidities of the hydrogen-carbon protons in carboxylic esters, amides, and nitriles. *J. Org. Chem.* **46**, 4327–4331 (1981).
12. Celmer, W. D. Stereochemical problems in macrolide antibiotics. *Pure Appl. Chem.* **28**, 413–454 (1971).
13. Seiple, I. B. *et al.* A platform for the discovery of new macrolide antibiotics. *Nature* **533**, 338–345 (2016).
14. Guissart, C., Barros, A., Rosa Barata, L. & Evano, G. Broadly Applicable Ytterbium-Catalyzed Esterification, Hydrolysis, and Amidation of Imides. *Org. Lett.* **20**, 5098–5102 (2018).
15. Mandal, M. *et al.* Total Synthesis of Guanacastepene A: A Route to Enantiomeric Control. *J. Org. Chem.* **70**, 10619–10637 (2005).
16. Riener, K., Högerl, M. P., Gigler, P. & Kühn, F. E. Rhodium-Catalyzed Hydrosilylation of Ketones: Catalyst Development and Mechanistic Insights. *ACS Catal.* **2**, 613–621 (2012).
17. Zhao, L., Nakatani, N., Sunada, Y., Nagashima, H. & Hasegawa, J. Theoretical Study on the Rhodium-Catalyzed Hydrosilylation of C=C and C=O Double Bonds with Tertiary Silane. *J. Org. Chem.* **84**, 8552–8561 (2019).
18. Ojima, I. & Kogure, T. Selective reduction of  $\alpha,\beta$ -unsaturated terpene carbonyl compounds using hydrosilane-rhodium(I) complex combinations. *Tetrahedron Lett.* **13**, 5035–5038 (1972).

19. Belousoff, M. J. *et al.* Crystal structure of the synergistic antibiotic pair, lankamycin and lankacidin, in complex with the large ribosomal subunit. *Proc. Natl. Acad. Sci.* **108**, 2717–2722 (2011).
20. Hansen, J. L. *et al.* The Structures of Four Macrolide Antibiotics Bound to the Large Ribosomal Subunit. *Mol. Cell* **10**, 117–128 (2002).
21. Dias, L. C. & Polo, E. C. Nhatrangin A: Total Syntheses of the Proposed Structure and Six of Its Diastereoisomers. *J. Org. Chem.* **82**, 4072–4112 (2017).
22. Busch, T. *et al.* Synthesis and antiproliferative activity of new tonantzitlolone-derived diterpene derivatives. *Org. Biomol. Chem.* **14**, 9040–9045 (2016).
23. Narayan, A. R. H. *et al.* Enzymatic hydroxylation of an unactivated methylene C–H bond guided by molecular dynamics simulations. *Nat. Chem.* **7**, 653–660 (2015).

## Publishing Agreement

It is the policy of the University to encourage open access and broad distribution of all theses, dissertations, and manuscripts. The Graduate Division will facilitate the distribution of UCSF theses, dissertations, and manuscripts to the UCSF Library for open access and distribution. UCSF will make such theses, dissertations, and manuscripts accessible to the public and will take reasonable steps to preserve these works in perpetuity.

I hereby grant the non-exclusive, perpetual right to The Regents of the University of California to reproduce, publicly display, distribute, preserve, and publish copies of my thesis, dissertation, or manuscript in any form or media, now existing or later derived, including access online for teaching, research, and public service purposes.

DocuSigned by:

*Quinn Edmondson*

7F8811AB4D31406...

Author Signature

11/14/2024

Date